

---

# Temperature Predictions and Adjustment Factors for Asphalt Pavement

---

PUBLICATION NO. FHWA-RD-98-085

JUNE 2000



U.S. Department of Transportation  
**Federal Highway Administration**

Research and Development  
Turner-Fairbank Highway Research Center  
6300 Georgetown Pike  
McLean, VA 22101-2296



## **FOREWORD**

Deflection testing is an important tool for pavement evaluation. Critical for the use of this tool is the need to be able to adjust the results of the testing for the effects of the temperature of asphalt. The Seasonal Monitoring Program of the Long Term Pavement Performance program has produced the largest single source of data regarding asphalt temperature and the corresponding deflection response. These data provided an opportunity to develop methods to predict the temperature within the asphalt and to adjust the deflection results for temperature effects.

The contents of this report will be of interest to pavement researchers and to engineers involved in routine deflection testing and analysis.

T. Paul Teng, P.E.  
Director, Office of Infrastructure  
Research and Development

## **NOTICE**

This document is disseminated under the sponsorship of the Department of Transportation in the interest of information exchange. The United States Government assumes no liability for its contents or use thereof. This report does not constitute a standard, specification, or regulation.

The United States Government does not endorse products or manufacturers. Trade or manufacturers' names appear in this report only because they are considered essential to the object of the document.

**Technical Report Documentation Page**

|   |  |  |  |   |           |
|---|--|--|--|---|-----------|
| 1. Report No.<br>FHWA-RD-98-085   |  | 2. Government Accession No.  |  | 3. Recipient's Catalog No.                      |           |
| 4. Title and Subtitle<br>Temperature Predictions and Adjustment Factors for Asphalt Pavement  |  | 5. Report Date<br>06-24-2000   |  | 6. Performing Organization Code                 |           |
|   |  | 8. Performing Organization Report No.<br>DBNX94822-D   |  | 10. Work Unit No. (TRAVIS)<br>C6B               |           |
| 7. Author(s)<br>Erland O. Lukanen, Richard Stubstad, and Robert Briggs  |  | 9. Performing Organization Name and Address<br>Braun Intertec Corporation<br>6875 Washington Avenue South, P. O. Box 39108<br>Minneapolis, Minnesota 55439-0108                            |  | 11. Contract or Grant No.<br>DTFH61-94-CC-00208 |           |
| 12. Sponsoring Agency Name and Address<br>Office of Infrastructure Research and Development<br>Federal Highway Administration<br>6300 Georgetown Pike<br>McLean, Virginia 22101-2296  |  | 13. Type of Report and Period Covered<br>Final Report<br>October 1994 - June 1999  |  | 14. Sponsoring Agency Code                      |           |
|   |  | 15. Supplementary Notes<br>Contracting Officer's Technical Representative (COTR): Cheryl Richter, HRDI-13<br>Technical review provided by the TRB Expert Task Group on LTPP Data Analysis. |  |   |           |
| 16. Abstract<br>This report presents the results of an analysis of the response that deflections and backcalculated asphalt moduli have to the pavement temperature. The study used deflection and temperature data from 40 sites monitored in the Seasonal Monitoring Program of the Long Term Pavement Performance (LTPP) program.<br><br>The report presents improved methods of estimating the temperature within an asphalt pavement based on the measurement procedures used for the LTPP program. The data necessary to estimate the temperature within the asphalt included the surface temperature, time of day, depth below the surface, and the average air temperature from the previous day. Backcalculation of the asphalt modulus from the deflection data of the 40 sites was related to pavement temperature, and a method of estimating what the modulus of the asphalt would be at different temperatures is presented. Deflection and deflection basin shape factor response to temperature was also evaluated, resulting in relationships for each of the items evaluated with pavement temperature. Items evaluated include the deflection under the load plate (center sensor), center sensor minus offset sensors, center sensor divided by offset sensors, AREA factor, and the F-1 factor. The relationships were then used to develop procedures for adjusting for the effects of temperature. |  |  |  |   |           |
| 17. Key Words<br>Long Term Pavement Performance, LTPP, Seasonal Monitoring Program, SMP, temperature, temperature adjustment, backcalculated modulus, thermistor, falling-weight deflectometer, FWD.  |  |  | 18. Distribution Statement<br>No restrictions. This document is available to the public through the National Technical Information Service, Springfield, Virginia 22161. |   |           |
| 19. Security Classif. (of this report)<br>Unclassified  |  | 20. Security Classif. (of this page)<br>Unclassified   |  | 21. No. of Pages<br>77                          | 22. Price |

## SI\* (MODERN METRIC) CONVERSION FACTORS

### APPROXIMATE CONVERSIONS FROM SI UNITS

| Symbol   | When You Know              | Multiply By             | To Find                     | Symbol            | When You Know               | Multiply By | To Find                    | Symbol              |
|--|----------------------------|-------------------------|-----------------------------|-------------------|-----------------------------|-------------|----------------------------|---------------------|
| <b>LENGTH</b>  |                            |                         |                             |                   |                             |             |                            |                     |
| in   | inches                     | 25.4                    | millimeters                 | mm                | millimeters                 | 0.039       | inches                     | in                  |
| ft   | feet                       | 0.305                   | meters                      | m                 | meters                      | 3.28        | feet                       | ft                  |
| yd   | yards                      | 0.914                   | meters                      | m                 | meters                      | 1.09        | yards                      | yd                  |
| mi   | miles                      | 1.61                    | kilometers                  | km                | kilometers                  | 0.621       | miles                      | mi                  |
| <b>AREA</b>  |                            |                         |                             |                   |                             |             |                            |                     |
| in <sup>2</sup>  | square inches              | 6.452                   | square millimeters          | mm <sup>2</sup>   | square millimeters          | 0.0016      | square inches              | in <sup>2</sup>     |
| ft <sup>2</sup>  | square feet                | 0.093                   | square meters               | m <sup>2</sup>    | square meters               | 10.764      | square feet                | ft <sup>2</sup>     |
| yd <sup>2</sup>  | square yards               | 0.836                   | square meters               | m <sup>2</sup>    | square meters               | 1.195       | square yards               | yd <sup>2</sup>     |
| ac   | acres                      | 0.405                   | hectares                    | ha                | hectares                    | 2.47        | acres                      | ac                  |
| mi <sup>2</sup>  | square miles               | 2.59                    | square kilometers           | km <sup>2</sup>   | square kilometers           | 0.386       | square miles               | mi <sup>2</sup>     |
| <b>VOLUME</b>  |                            |                         |                             |                   |                             |             |                            |                     |
| fl oz  | fluid ounces               | 29.57                   | milliliters                 | mL                | milliliters                 | 0.034       | fluid ounces               | fl oz               |
| gal  | gallons                    | 3.785                   | liters                      | L                 | liters                      | 0.264       | gallons                    | gal                 |
| ft <sup>3</sup>  | cubic feet                 | 0.028                   | cubic meters                | m <sup>3</sup>    | cubic meters                | 35.71       | cubic feet                 | ft <sup>3</sup>     |
| yd <sup>3</sup>  | cubic yards                | 0.765                   | cubic meters                | m <sup>3</sup>    | cubic meters                | 1.307       | cubic yards                | yd <sup>3</sup>     |
| NOTE: Volumes greater than 1000 l shall be shown in m <sup>3</sup> . |                            |                         |                             |                   |                             |             |                            |                     |
| <b>MASS</b>  |                            |                         |                             |                   |                             |             |                            |                     |
| oz   | ounces                     | 28.35                   | grams                       | g                 | grams                       | 0.035       | ounces                     | oz                  |
| lb   | pounds                     | 0.454                   | kilograms                   | kg                | kilograms                   | 2.202       | pounds                     | lb                  |
| T  | short tons (2000 lb)       | 0.907                   | megagrams (or "metric ton") | Mg (or "t")       | megagrams (or "metric ton") | 1.103       | short tons (2000 lb)       | T                   |
| <b>TEMPERATURE (exact)</b>   |                            |                         |                             |                   |                             |             |                            |                     |
| °F   | Fahrenheit temperature     | 5(F-32)/9 or (F-32)/1.8 | Celsius temperature         | °C                | Celsius temperature         | 1.8C + 32   | Fahrenheit temperature     | °F                  |
| <b>ILLUMINATION</b>  |                            |                         |                             |                   |                             |             |                            |                     |
| fc   | foot-candles               | 10.76                   | lux                         | lx                | lux                         | 0.0929      | foot-candles               | fc                  |
| ft   | foot-Lamberts              | 3.426                   | candela/m <sup>2</sup>      | cd/m <sup>2</sup> | candela/m <sup>2</sup>      | 0.2919      | foot-Lamberts              | ft                  |
| <b>FORCE and PRESSURE or STRESS</b>                                  |                            |                         |                             |                   |                             |             |                            |                     |
| lbf  | poundforce                 | 4.45                    | newtons                     | N                 | newtons                     | 0.225       | poundforce                 | lbf                 |
| lbf/in <sup>2</sup>  | poundforce per square inch | 6.89                    | kilopascals                 | kPa               | kilopascals                 | 0.145       | poundforce per square inch | lbf/in <sup>2</sup> |

\* SI is the symbol for the International System of Units. Appropriate rounding should be made to comply with Section 4 of ASTM E380. (Revised September 1993)

# TABLE OF CONTENTS

| <u>Section</u>  | <u>Page</u> |
|---|-------------|
| CHAPTER 1. INTRODUCTION .....                                   | 1           |
| BACKGROUND .....  | 1           |
| PROJECT SCOPE .....   | 1           |
| REPORT ORGANIZATION .....                                       | 1           |
| CHAPTER 2. DATA SOURCE .....                                    | 3           |
| CHAPTER 3. DATA DEVELOPMENT FOR ANALYSIS .....                  | 7           |
| DATA COLLECTION .....   | 7           |
| Temperature Data .....  | 7           |
| Temperature Depth Data .....                                    | 10          |
| DATA PROCESSING FOR ANALYSIS .....                              | 10          |
| Thermistor Data .....   | 11          |
| Manual Temperatures .....                                       | 11          |
| Surface Temperatures .....                                      | 11          |
| Creating the Data Analysis Files .....                          | 11          |
| Comparison of Resulting Temperatures .....                      | 13          |
| Stability of the Manual Temperatures .....                      | 14          |
| Infrared Sensor Calibrations .....                              | 14          |
| CHAPTER 4. TEMPERATURE PREDICTION MODELS .....                  | 21          |
| PREDICTION MODELS .....   | 21          |
| BELLS Model .....   | 21          |
| Development of BELLS2 .....                                     | 22          |
| Shading Effect on Infrared Measurements .....                   | 25          |
| BELLS2 for Production Testing .....                             | 26          |
| Validation of the BELLS Models .....                            | 26          |
| Recommended BELLS Models, Round 1 and Round 2 Combined .....    | 27          |
| CHAPTER 5. TEMPERATURE ADJUSTMENTS FOR BACKCALCULATED           |             |
| ASPHALT MODULI .....  | 29          |
| BACKCALCULATED ASPHALT MODULI .....                             | 29          |
| Backcalculation Results .....                                   | 30          |
| Analysis Approach .....   | 30          |
| TEMPERATURE ADJUSTMENT OF BACKCALCULATED ASPHALT MODULI .....   | 37          |
| VALIDATION OF THE TEMPERATURE ADJUSTMENT MODEL .....            | 38          |
| CHAPTER 6. TEMPERATURE ADJUSTMENT FOR BASIN SHAPE FACTORS ..... | 43          |
| BASIN SHAPE FACTOR DEFINITIONS .....                            | 43          |
| AREA Shape Factor .....   | 43          |
| F-1 Shape Factor .....  | 43          |
| Deflection Basin Delta Shape Factors .....                      | 44          |
| Deflection Basin Ratio Factors .....                            | 44          |
| TEMPERATURE RELATIONSHIPS .....                                 | 44          |
| Analysis Discussion .....                                       | 44          |

## TABLE OF CONTENTS (Continued)

| <u>Section</u>   | <u>Page</u> |
|--|-------------|
| Development of the Regression Models .....                       | 45          |
| Basin Shape Models .....   | 47          |
| MODEL VALIDATION .....   | 49          |
| Comparison of Round 1 and Round 2 Data .....                     | 49          |
| TEMPERATURE ADJUSTMENTS .....                                    | 51          |
| Temperature Adjustment for Deflection Under the Load Plate ..... | 51          |
| Temperature Adjustments for Basin Shape Factors .....            | 54          |
| CHAPTER 7. CONCLUSIONS AND RECOMMENDATIONS .....                 | 57          |
| CONCLUSIONS .....  | 57          |
| RECOMMENDATIONS .....  | 57          |
| Temperature Prediction With the BELLS Models .....               | 57          |
| APPENDIX. DRAFT STANDARDS .....                                  | 59          |
| REFERENCES .....   | 71          |

## LIST OF FIGURES

| <u>Figure No.</u>  | <u>Page</u> |
|--|-------------|
| 1. Location of seasonal monitoring sites .....   | 3           |
| 2. Thermistor probe in the asphalt .....   | 8           |
| 3. Manual temperature measurement holes .....  | 9           |
| 4. Comparison of mid-depth temperatures for Site 25A .....                                       | 12          |
| 5. Comparison of the thermistor temperature and manual temperature data .....                    | 13          |
| 6. Regression coefficients for manual and thermistor data .....                                  | 14          |
| 7. Infrared sensor performance by FWD serial number .....  | 16          |
| 8. Comparison of two infrared sensors used on the same sites .....                               | 17          |
| 9. Machine differences in the default infrared temperature output .....                          | 19          |
| 10. Comparison of the BELLS model original and new coefficients .....                            | 22          |
| 11. 18-hr cycle sine functions .....   | 23          |
| 12. BELLS2 temperature predictions .....   | 24          |
| 13. Influence of shade on surface temperature .....  | 25          |
| 14. BELLS2 prediction errors .....   | 28          |
| 15. Backcalculated moduli from all stations .....  | 30          |
| 16. Backcalculated moduli from one station location .....  | 31          |
| 17. Histogram of slope coefficients for temperature versus modulus .....                         | 32          |
| 18. Slope of temperature versus modulus relationship with latitude .....                         | 33          |
| 19. Intercept of the temperature versus modulus relationship with latitude .....                 | 34          |
| 20. The influence of asphalt condition and thickness on the modulus-temperature relationships .. | 35          |
| 21. Relationship between slope and intercept for Site 08SA .....                                 | 36          |
| 22. Relationship between slope and intercept for all sites .....                                 | 37          |
| 23. Distribution of temperature versus modulus regression slopes .....                           | 39          |
| 24. Temperature versus deflection coefficients .....   | 52          |
| 25. Intercept of temperature versus deflection regressions .....                                 | 53          |
| 26. FWD temperature adjustment factors for defl36 = 100 $\mu$ m and 40° latitude .....           | 54          |

## LIST OF TABLES

| <u>Table No.</u>   | <u>Page</u> |
|--|-------------|
| 1. Seasonal monitoring study sections .....  | 4           |
| 2. Layer thickness information .....   | 5           |
| 3. Regression comparison of infrared sensors .....   | 15          |
| 4. Comparison of infrared sensor default output .....  | 18          |
| 5. Intercepts, slopes, and R-squared regression coefficients of the median-based<br>representative station ..... | 41          |
| 6. Regression and validation data set .....  | 46          |
| 7. Regression and validation statistics .....  | 49          |
| 8. Illustration of Round 1 and Round 2 differences using AREA regression statistics .....                        | 50          |

## LIST OF ABBREVIATIONS/TERMS

|         |  |
|---------|--|
| AASHO   | American Association of State Highway Officials                            |
| AASHTO  | American Association of State Highway and Transportation Officials         |
| AC      | asphalt concrete   |
| AREA    | deflection basin shape characteristic                                      |
| BELLS   | asphalt temperature prediction equation described in reference 7           |
| BELLS2  | modified asphalt temperature prediction equation presented in this report  |
| defl0   | deflection sensor at center of FWD load plate                              |
| defl8   | deflection sensor 203 mm from center of FWD load plate                     |
| defl12  | deflection sensor 305 mm from center of FWD load plate                     |
| defl18  | deflection sensor 457 mm from center of FWD load plate                     |
| defl24  | deflection sensor 610 mm from center of FWD load plate                     |
| defl36  | deflection sensor 914 mm from center of FWD load plate                     |
| defl60  | deflection sensor 1524 mm from center of FWD load plate                    |
| delta8  | d(0)-d(8)  |
| delta12 | d(0)-d(12)   |
| delta18 | d(0)-d(18)   |
| delta24 | d(0)-d(24)   |
| delta36 | d(0)-d(36)   |
| delta60 | d(0)-d(60)   |
| D.IR    | infrared temperature sensor output at factory default calibration settings |
| F-1     | deflection basin shape characteristic                                      |
| FHWA    | Federal Highway Administration   |
| FWD     | falling-weight deflectometer   |
| IR      | infrared temperature   |
| LTPP    | Long Term Pavement Performance   |
| ratio8  | r(0)/r(8)  |
| ratio12 | r(0)/r(12)   |
| ratio18 | r(0)/r(18)   |
| ratio24 | r(0)/r(24)   |
| ratio36 | r(0)/r(36)   |
| ratio60 | r(0)/r(60)   |
| SCR     | Surface Condition Rating   |
| SMP     | Seasonal Monitoring Program  |



# CHAPTER 1. INTRODUCTION

## BACKGROUND

The use of surface deflection measurements on pavements has steadily increased in popularity with highway agencies since the American Association of State Highway Officials (AASHO) Road Test was conducted. Deflection testing is used to evaluate a variety of pavement characteristics, including axle or vehicle load capacity, structural life, and uniformity. Deflection results of all pavements are dependent on seasonal variations that affect the underlying aggregate and subgrade. The results from asphalt pavements are also dependent on the temperature of the asphalt. In order to meaningfully analyze the deflection results, the deflections, or deflection analysis results, must be adjusted to account for the seasonal and temperature effects. Over the years, a number of methods have been developed to measure the asphalt temperature and to adjust the deflection results for the effects of temperature.

Deflection equipment and analysis methodologies have continued to improve over the years, but the study of the effects of temperature on the deflections of asphalt pavements have generally been limited in scope or location. The Seasonal Monitoring Program (SMP)<sup>(1)</sup> of the Long Term Pavement Performance (LTPP) program<sup>(2)</sup> provides the most comprehensive temperature and deflection data set ever to be assembled. The LTPP program provides both the need and the opportunity to:

- Develop a means of determining the temperature of the asphalt pavement at depth from surface infrared temperature measurements.
- Develop methods or factors to adjust deflections, or deflection analysis results, for the effects of temperature.

## PROJECT SCOPE

The project has two primary objectives that follow the opportunities described above:

- Develop a model that can be used to predict the temperature within an asphalt layer from surface temperature data collected during routine deflection testing.
- Develop relationships between asphalt temperature, pavement deflections, deflection basin shape factors, and backcalculated asphalt modulus. The models are to provide the basis for adjusting the moduli, deflection basin shape factors, and deflections for temperature.

## REPORT ORGANIZATION

This report briefly describes the SMP data and the method used to process the data for analysis. The two objectives of the project are covered in separate chapters: Chapter 4 deals with estimating the temperature within an asphalt pavement layer and Chapter 5 deals with the relationship between backcalculated asphalt modulus values and temperature. Chapter 6 discusses the relationships that were developed between deflection basin shape factor responses and temperature. A process for adjusting for the effects of temperature is given for each of the temperature-sensitive responses evaluated.



## CHAPTER 2. DATA SOURCE

The LTPP's SMP (SMP) provided the data necessary to accomplish the objectives. Specific program data used included temperature measurements from within the asphalt pavement, falling-weight deflectometer (FWD) deflection data<sup>(3)</sup>, and layer type and thickness data. The initial analysis was with data from 25 LTPP flexible seasonal monitoring sections tested during Round 1 of the SMP, which ran from March 1994 to May of 1995. Upon completion of the analysis and a review of the results, it was decided to use the data from Round 2 of the SMP, which ran from July 1995 to October 1996, for a validation check. As described later, the Round 2 sections were significantly different than the Round 1 sections. The data from Rounds 1 and 2 were combined and subsequently divided into two sets, one for the development of the models and one for validation of the models.

Figure 1 shows the general location of each SMP site. Information regarding each of the SMP sections included in this study is contained in Tables 1 and 2. Table 1 contains a section location description and table 2 lists the section pavement composition.

As shown by the dots in Figure 1, the site locations represent a wide range of geographical and climatic locations, ranging from dry-no freeze to wet-freeze. The sites also provided a reasonably wide range of asphalt thicknesses, ranging from 46 mm to 305 mm.

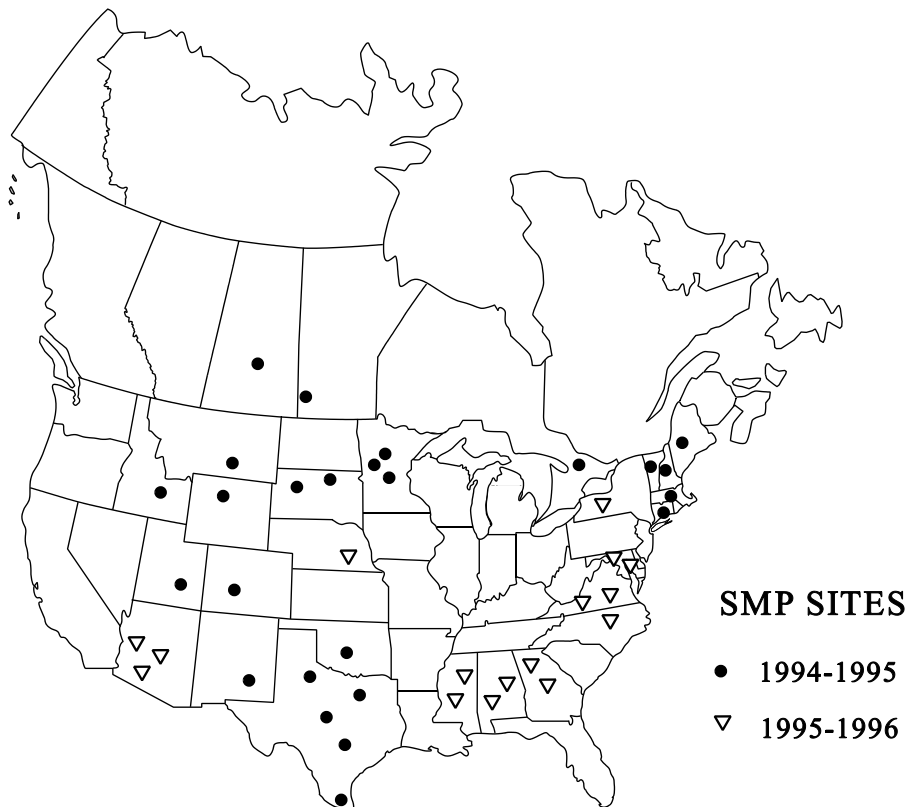


**Figure 1. Location of seasonal monitoring sites.**

**Table 1. Seasonal monitoring study sections.**

| <b>SMP ID</b> | <b>Round</b> | <b>Section ID</b> | <b>State or Province</b> | <b>Location</b>                                   |
|---------------|--------------|-------------------|--------------------------|---|
| 01SA          | 2            | 010101            | Alabama                  | U.S. 280, 2.9 km W of CR 183                      |
| 01SB          | 2            | 010102            | Alabama                  | U.S. 280, 4.51 km W of CR 183                     |
| 04SA          | 2            | 040113            | Arizona                  | U.S. 93 NB, MP 52.62, Kingman                     |
| 04SB          | 2            | 040114            | Arizona                  | U.S. 93 NB, MP 58.61, Kingman                     |
| 04SC          | 2            | 041024            | Arizona                  | I-40 EB, MP 106.9, approx. 63 km W of U.S. 89     |
| 08SA          | 1            | 081053            | Colorado                 | U.S. 50 NB, MP 75.3, near Delta                   |
| 09SA          | 1            | 091803            | Connecticut              | SH 117 NB, MP 3.47, near New London               |
| 10SA          | 2            | 100102            | Delaware                 | U.S. 113, 2.0 km S of SR 16                       |
| 13SB          | 2            | 131031            | Georgia                  | U.S. 19, 5.64 km N of GA 53                       |
| 13SC          | 2            | 131005            | Georgia                  | SH 247, 1.77 km E of Peach/Houston Co. Line       |
| 16SB          | 1            | 161010            | Idaho                    | I-15 SB, MP 132 near Idaho Falls                  |
| 23SA          | 1            | 231026            | Maine                    | U.S. 2 WB, near Wilton                            |
| 24SA          | 2            | 241634            | Maryland                 | SH 90, 1.0 km E of US 50                          |
| 25SA          | 1            | 251002            | Massachusetts            | I-391 WB, MP 1.95, near Springfield               |
| 27SA          | 1            | 271018            | Minnesota                | U.S. 10 EB, MP 140, W of Little Falls             |
| 27SB          | 1            | 271028            | Minnesota                | U.S. 10 EB, MP 58, E of Detroit Lakes             |
| 27SC          | 1            | 276251            | Minnesota                | U.S. 2 WB, MP 113 on Bemidji Bypass               |
| 28SA          | 2            | 281802            | Mississippi              | U.S. 84, 2.41 km W of Covington/Jones Co. Line    |
| 28SB          | 2            | 281016            | Mississippi              | SH 35, 2.25 km N of Natchez Trail                 |
| 30SA          | 1            | 308129            | Montana                  | U.S. 12 EB, MP 137, near Ryegate                  |
| 31SA          | 2            | 310114            | Nebraska                 | U.S. 81, 10.8 km S of Hebron                      |
| 33SA          | 1            | 331001            | New Hampshire            | I-393 EB, Concord                                 |
| 35SA          | 1            | 351112            | New Mexico               | U.S. 62 EB, MP 81.3, W of Hobbs                   |
| 36SB          | 2            | 360801            | New York                 | Lake Ontario State Pkwy, Near Hamilton Beach Park |
| 37SE          | 2            | 371028            | North Carolina           | SH 17, 2.6 km S of the Virginia State Line        |
| 40SA          | 1            | 404165            | Oklahoma                 | U.S. 60 WB, MP 8.4, E of Junction SH 58           |
| 46SA          | 1            | 460804            | South Dakota             | SH 1804 EB, 14.5 km NW of Pollock                 |
| 46SB          | 1            | 469187            | South Dakota             | SH 73 SB, MP 156, 29.0 km S of Faith              |
| 48SA          | 1            | 481077            | Texas                    | U.S. 287 SB, near Estelline                       |
| 48SB          | 1            | 481068            | Texas                    | SH 19 NB, near Paris                              |
| 48SE          | 1            | 481122            | Texas                    | U.S. 181 NB, near Floresville                     |
| 48SF          | 1            | 481060            | Texas                    | U.S. 77 NB, near Victoria                         |
| 48SG          | 1            | 483739            | Texas                    | U.S. 77 NB, near Raymondville                     |
| 49SB          | 1            | 491001            | Utah                     | U.S. 191 SB, MP 23.74, near Bluff                 |
| 50SA          | 1            | 501002            | Vermont                  | U.S. - 7 NB, near New Haven                       |
| 51SA          | 2            | 510113            | Virginia                 | SR 265, 4.1 km S of SR 695                        |
| 51SB          | 2            | 510114            | Virginia                 | SR 265, 137 m S of SR 695                         |
| 56SA          | 1            | 561007            | Wyoming                  | U.S. 16 EB, MP 60.06, near Cody                   |
| 83SA          | 1            | 831801            | Manitoba                 | PTH 1 WB, 46 km W of Brandon                      |
| 87SA          | 1            | 871622            | Ontario                  | Hwy 11 NB, near Bracebridge                       |
| 90SA          | 1            | 906405            | Saskatchewan             | PTH 16 EB, E of Plunkett                          |

**Table 2. Layer thickness information.**

| SMP ID | AC (mm) | Base (mm) | Type       | Sub-Base (mm) | Type          | Subgrade Type | Comments          |
|--------|---------|-----------|------------|---------------|---------------|---------------|-------------------|
| 01SA   | 178     | 203       | Cr. Stone  | ----          | ----          | CL            |                   |
| 01SB   | 102     | 305       | Cr. Stone  | ----          | ----          | CL            |                   |
| 04SA   | 114     | 191       | Agg.       | ----          | ----          | SW            |                   |
| 04SB   | 173     | 305       | Agg.       | ----          | ----          | SW            |                   |
| 04SC   | 274     | 160       | Agg.       | ----          | ----          | SW            |                   |
| 08SA   | 117     | 114       | Cr. Gravel | 597           | Soil Agg.     | CL            |                   |
| 09SA   | 189     | 305       | Gravel     | ----          | ----          | ML w/G        |                   |
| 10SA   | 114     | 336       | Agg.       | 870           | Silty Sand    | SC            | Section not used  |
| 13SB   | 305     | 254       | Cr. Stone  | ----          | ----          | MH            |                   |
| 13SC   | 178     | 253       | Cr. Stone  | ----          | ----          | SM            |                   |
| 16SB   | 277     | 137       | Cr. Gravel | ----          | ----          | SM            |                   |
| 23SA   | 147*    | 447       | Gravel     | ----          | ----          | SM w/G        | *L05 is 163 mm AC |
| 24SA   | 211     | 246       | F. Sand    | 1117          | Sand & Silt   | ML            |                   |
| 25SA   | 193*    | 102       | Cr. Gravel | 213           | Soil Agg.     | SP w/M        | *L05 is 163 mm AC |
| 27SA   | 112     | 132       | Gravel     | ----          | ----          | SP w/M        |                   |
| 27SB   | 244     | ----      | ----       | ----          | ----          | SP w/M        |                   |
| 27SC   | 180     | 267       | Gravel     | ----          | ----          | SP w/M        |                   |
| 28SA   | 220     | 51        | Silty Sand | ----          | ----          | SC            |                   |
| 28SB   | 195     | 525       | Granular   | ----          | ----          | SM            |                   |
| 30SA   | 76      | 579       | Cr. Gravel | ----          | ----          | CL            |                   |
| 31SA   | 178     | 305       | Agg.       | ----          | ----          | CL            |                   |
| 33SA   | 212     | 490       | Gravel     | 366           | Cr. Slag      | SP w/M        |                   |
| 35SA   | 160     | 152       | Soil Agg.  | ----          | ----          | SP            |                   |
| 36SB   | 132     | 238       | Agg.       | ----          | ----          | SC            |                   |
| 37SE   | 264     | 136       | Silty Sand | ----          | ----          | SM            |                   |
| 40SA   | 64      | 137       | HMAC       | ----          | ----          | SM            |                   |
| 46SA   | 178     | 305       | Gravel     | ----          | ----          | ML            |                   |
| 46SB   | 140     | 152       | Gravel     | 76            | Gravel w/Silt | CH            |                   |
| 48SA   | 147*    | 264       | Cr. Stone  | ----          | ----          | ML            | *L05 is 130 mm AC |
| 48SB   | 254*    | 152       | Cr. Stone  | 203           | Lime-Tr. Soil | CL            | *L05 is 276 mm AC |
| 48SE   | 81      | 396       | Soil Agg.  | 213           | F. Gr. Soil   | SP            |                   |
| 48SF   | 191     | 312       | Cr. Stone  | 152           | Lime-Tr. Soil | SM            |                   |
| 48SG   | 46      | 290       | Soil Agg.  | 188           | Lime-Tr. Soil | SP            |                   |
| 49SB   | 140     | 147       | Soil Agg.  | ----          | ----          | SM            |                   |
| 50SA   | 211     | 655       | Cr. Gravel | ----          | ----          | GP w/M        |                   |
| 51SA   | 102     | 203       | Agg.       | 152           | Cmt. Tr. Soil | ML            |                   |
| 51SB   | 178     | 302       | Agg.       | 150           | Cmt. Tr. Soil | ML            |                   |
| 56SA   | 76      | 157       | Cr. Gravel | ----          | ----          | SM            |                   |
| 83SA   | 114     | 152       | Cr. Gravel | 305           | Gravel        | SM            |                   |
| 87SA   | 135     | 168       | Cr. Gravel | 668           | Sand          | MH            |                   |
| 90SA   | 71      | 279       | Cr. Gravel | ----          | ----          | SP w/M        |                   |

<sup>1</sup>Unified Soil Classification



## CHAPTER 3. DATA DEVELOPMENT FOR ANALYSIS

The LTPP program's SMP is the source of all of the data used in this study. The SMP was designed to study the effect that seasonal variations have on pavement performance. Some of the environmental factors include temperature and seasonal effects on pavement deflection response to load. The SMP requires much more intensive monitoring than the rest of the LTPP program. The expectation is that the SMP will be used to establish relationships between pavement performance response measures, such as deflection and profile, and temperature and season, as appropriate. The purpose of the study is to:

- Establish methods of predicting asphalt temperatures from surface temperature measurements.
- Develop a method of adjusting deflection response of asphalt pavements and backcalculated asphalt moduli for the effects of temperature.

The seasonal effects are being evaluated in separate studies.

### DATA COLLECTION

Two specific categories of SMP monitoring data from the sites were used;

- Temperature data for the asphalt pavement, both surface and internal, and air temperatures.
- FWD deflection data.

In addition, data describing the section layer type and thicknesses, plus latitude, longitude, and elevation data were obtained.

### Temperature Data

Four separate forms of temperature data were obtained for this study:

- Air temperature from SMP instrumentation.
- Asphalt temperature from instrumentation.
- Asphalt temperatures manually recorded during FWD testing.
- Surface temperature recorded by the FWD device.

#### *Air Temperature Instrumentation Data*

Each of the SMP sites includes a miniature weather station. The station records air temperature and precipitation on an hourly basis. The air temperatures are recorded once per minute by an on-site data logger. The hourly average is stored in memory at the end of each hour.

#### *Asphalt Temperature Instrumentation Data*

The instrumentation includes temperature sensors in the asphalt, as well as in the underlying base and subgrade. The temperature sensors in the asphalt are contained in a 300-mm temperature probe. The probe contains a thermistor at each end and one at the center of the probe as shown in figure 2. The probes were installed in a slot cut in the asphalt; they were positioned so that the ends of the probe were 25 mm from the surface and bottom of the asphalt. The on-site data logger in the weather station reads

the temperature from the thermistors once a minute. The readings are stored internally and at the end of every hour, the average temperature for each probe is stored in the data logger memory. This method of monitoring and recording the average hourly asphalt temperature results in a temperature that, for this study, was associated with the half-hour. This method of data recording became statistically important in the analysis as discussed later.

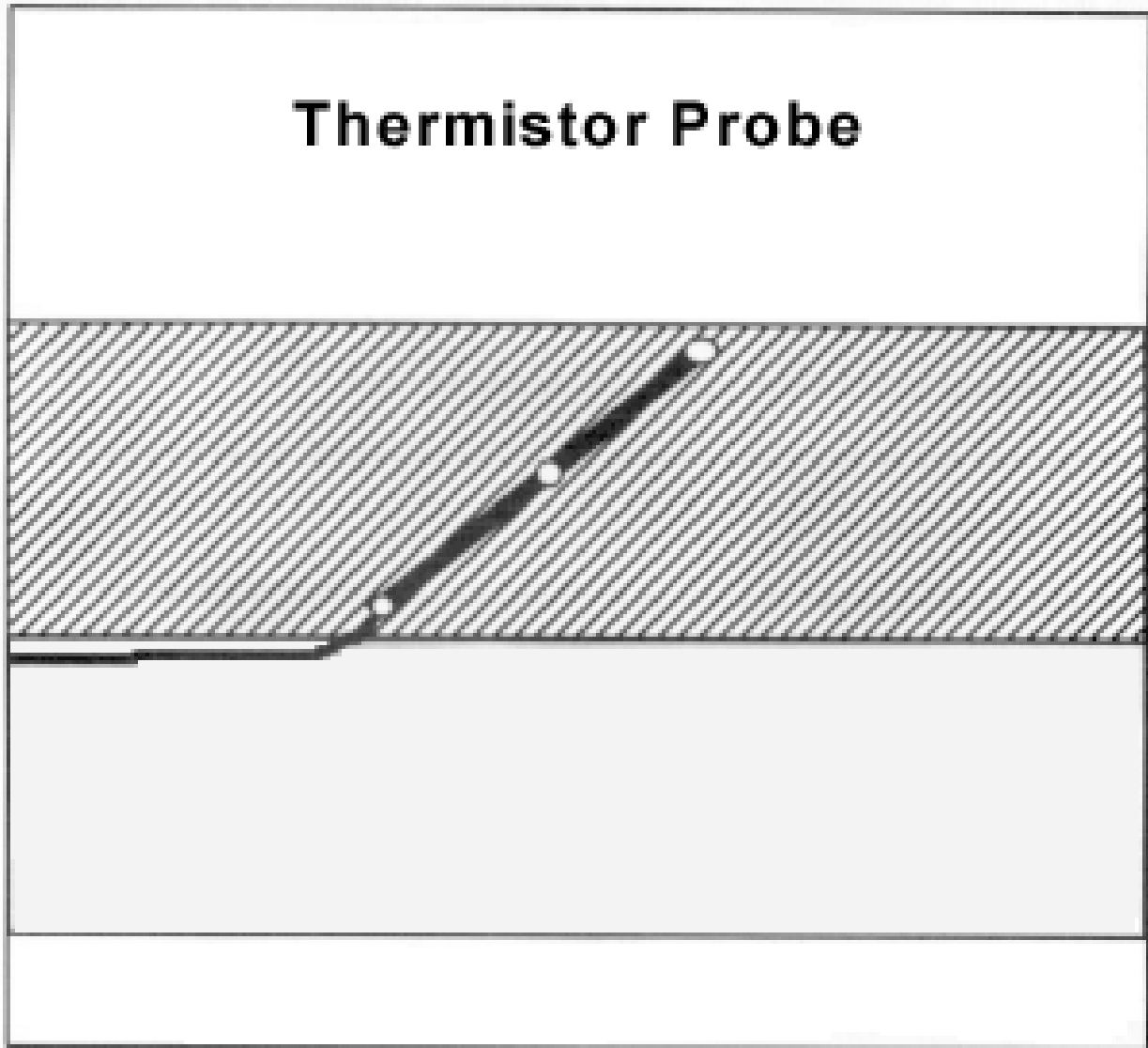


**Figure 2. Thermistor probe in the asphalt.**



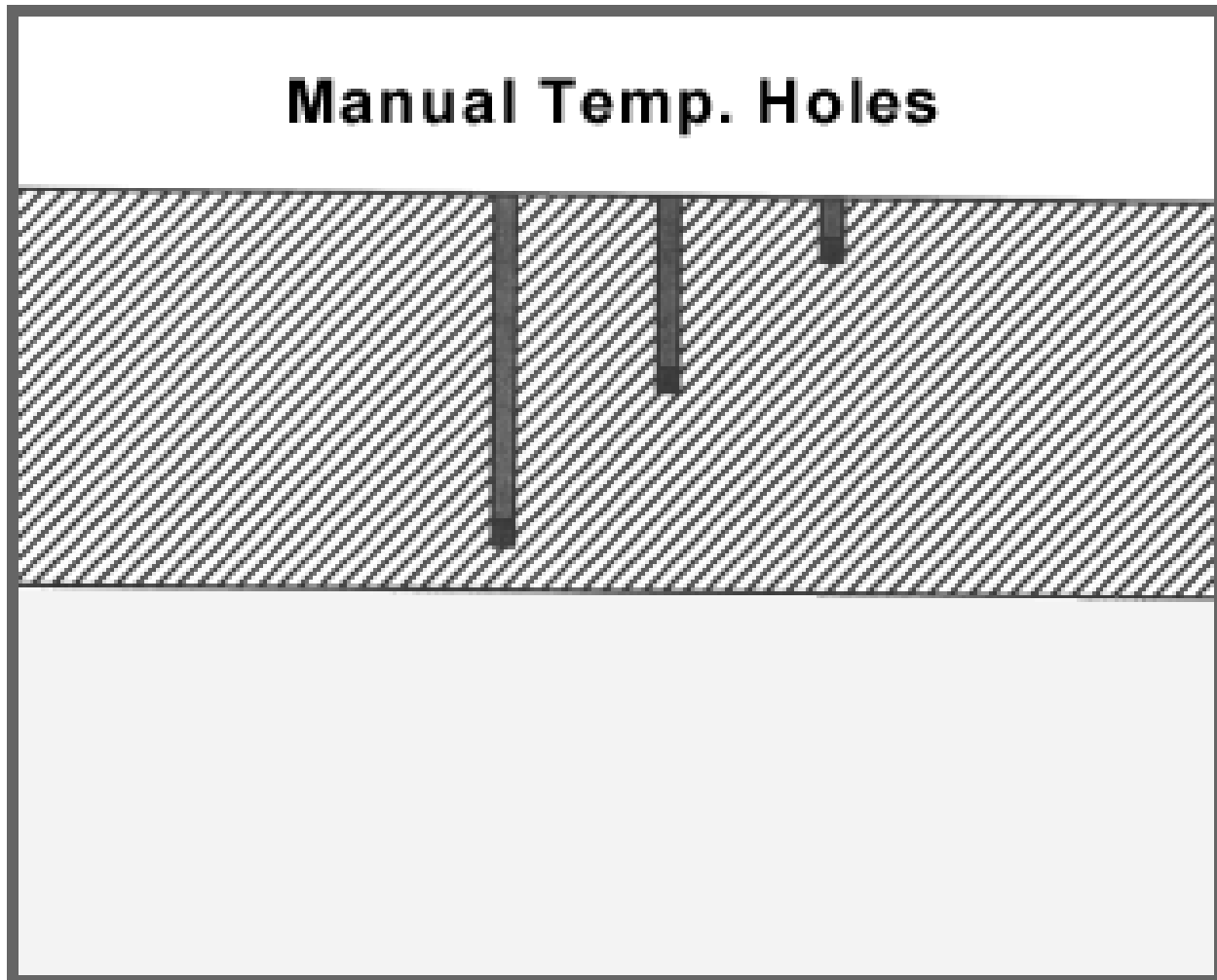


**Figure 3. Manual temperature measurement holes.**

Data collected in the North Central Region (NCR) for the LTPP program was collected initially to develop a process to assemble the data into a suitable format for analysis. A small filter program was developed to extract data from the environmental monitoring instrumentation files to develop flat files of the hourly temperatures of the three thermistors in the asphalt at each seasonal site.

### ***Manually Recorded Temperatures***

During deflection testing, the asphalt temperature was manually measured at approximate half-hour intervals at holes drilled to about 25 mm from the surface, mid-depth, and 25 mm from the bottom of the asphalt as shown in figure 3. A small amount of mineral oil or glycol (about 12-mm deep) is placed at the bottom of each hole for heat transfer. A tip-sensitive probe, attached to a hand-held device that displays the temperature to the nearest tenth degree Fahrenheit, is placed in the liquid at the bottom of the hole. The time, temperature, and depth is manually recorded for each set of manual readings. These data are referred to as the manual temperatures in this report.

The association of the manual temperature measurement with a specific time resulted in a better statistical relationship with the surface temperatures as described later in this report.

### *Surface Temperature*

For each deflection test, an infrared sensor mounted on the FWD measured the surface temperature of the asphalt. The surface temperature readings were recorded in the deflection data file. It should be noted that the test locations are about 7.6 meters apart, but the FWD and tow vehicle is about 10 meters long. Thus, the tow vehicle shades two test locations at the same time — the location tested and next test location. The typical time test at each location is about 3 minutes. Since the temperature is recorded at the end of the test cycle, the pavement surface has been in shade for about 6 min. before the infrared temperature measurement is made.

### *Time of Temperature Measurements*

The times for the surface temperature measurements and manual temperature measurements are specifically recorded at the time of measurement. The time of the instrumentation temperature is the time that the data are recorded into the data logger. Because the data logger measures the temperature every minute and records the average temperature for the hour, the temperature is not associated with any specific time. Since the temperature recorded represents the average temperatures for the previous hour, for this study, the instrumentation temperatures were assigned to be the temperature of the pavement at the half-hour.

### **Temperature Depth Data**

The temperatures measured within the asphalt, by thermistors or manually, have a specific depth associated with each measurement. The depth data is used in an interpolation process to estimate the temperature at the mid-depth and third-depth locations.

### *Thermistor Depths*

The depth of each thermistor below the surface of the asphalt was recorded at the time of installation. These depths are considered to remain constant over the course of this study. If a pavement was overlaid during the study, the depths need to be adjusted.

### *Temperature Hole Depths*

The temperature hole depths were measured at each monitoring cycle. The hole depths were not constant over the duration; they occasionally changed if the holes were cleaned or were redrilled. Details regarding the temperature measurement process are in the FWD operators field manual<sup>(3)</sup>.

## **DATA PROCESSING FOR ANALYSIS**

The data processing for analysis included a number of specific steps to associate an asphalt temperature within the pavement with the surface temperature measured by the FWD. Since the surface temperature measurements did not occur at the same time as the in-depth measurements, interpolation methods were used to estimate the manual and thermistor temperatures at the times of the surface temperature measurements. Also, since the depths associated with the temperatures measured within the pavements

varied, interpolation methods were used to estimate the temperatures at the third- and the half-depth positions.

### **Thermistor Data**

The thermistor data was obtained in its raw field file format from the on-site data logger files. One file was generated each time the section was visited for monitoring which was approximately once per month. These files contain a variety of records, of which only specific record containing the time, the air temperature, precipitation, and thermistor temperature data for the top five thermistors were of interest. A QuickBASIC<sup>1</sup> program was written that would extract the data from the field (onsite) files and write the instrumentation data of interest into one comma-delimited flat file for each section. The times in the field files that covered the beginning and ending of daylight savings time were adjusted based on information provided by each region. Each region handled daylight savings time in a different way, so even with the time-change adjustment, there may be a few data records that have incorrect times. This is important since the surface temperature data were only obtained during the warming time of the day and an hour difference may result in temperature change of several degrees.

### **Manual Temperatures**

Manual temperatures for the SMP sections were extracted by each of the regions from the Regional Information Management System (RIMS) and furnished in an ASCII flat file format. The flat file contained the date, time, depth, and temperature of each manual temperature measurement. No additional intermediate processing of the manual temperature data was necessary.

### **Surface Temperatures**

The surface temperatures measured during FWD testing was the primary independent variable used in the asphalt temperatures analysis predictions. These temperatures were extracted from the FWD files and placed into a single flat file for each site that included the section identification, date, time, station, lane, surface temperature (called the infrared (IR) temperature), and normalized 40.5 kN (9,000-lbf) deflections.

### **Creating the Data Analysis Files**

A QuickBASIC program was written that would first read the IR data file to get the date and time of the IR temperature. The program would then search the thermistor data file for the daily high and low air temperature for each of the 5 days preceding the day of testing, the previous night's low temperature, and all of the thermistor data for the day of testing. The thermistor data for each sensor was then fitted to a cubic spline routine<sup>(4)</sup> to interpolate the thermistor temperatures to the time of the IR temperature readings. Once the thermistor temperatures were interpolated for time, a second interpolation was used to interpolate the thermistor temperatures to third-depth and mid-depth temperatures using a second-order polynomial.<sup>(5)</sup> The resulting time- and depth-interpolated thermistor data was written to a flat file. Interpolated manual data were written to the same file; however, the manual data was treated differently. The manual data were first interpolated for the third-depth and mid-depth using the polynomial interpolation; the cubic spline procedure was then used to interpolate third-depth and mid-depth temperatures for each FWD test time. The reason for proceeding with depth first and time second was that the depth of measurement sometimes changed during the day if the hole was re-drilled or cleaned. If

---

<sup>1</sup> QuickBASIC is a trade mark of Microsoft.

the time of the FWD test occurred before or after the time the manual temperatures were measured, no extrapolation was made and a missing data filler was written to the file instead. Therefore, the resulting flat file consisted of:

- Site ID.
- Date and time.
- IR and air temperatures measured by the FWD.
- Last night's low air temperature.
- Daily high and low temperatures for each of the preceding 5 days.
- Time-interpolated individual thermistor data.
- Corresponding thermistor depths.
- Time- and depth-interpolated thermistor temperatures for third and mid-depth.
- Depth- and time-interpolated manual temperatures.
- Sky cover recorded during the manual temperature measurement that was the closest, timewise, to the IR test time.

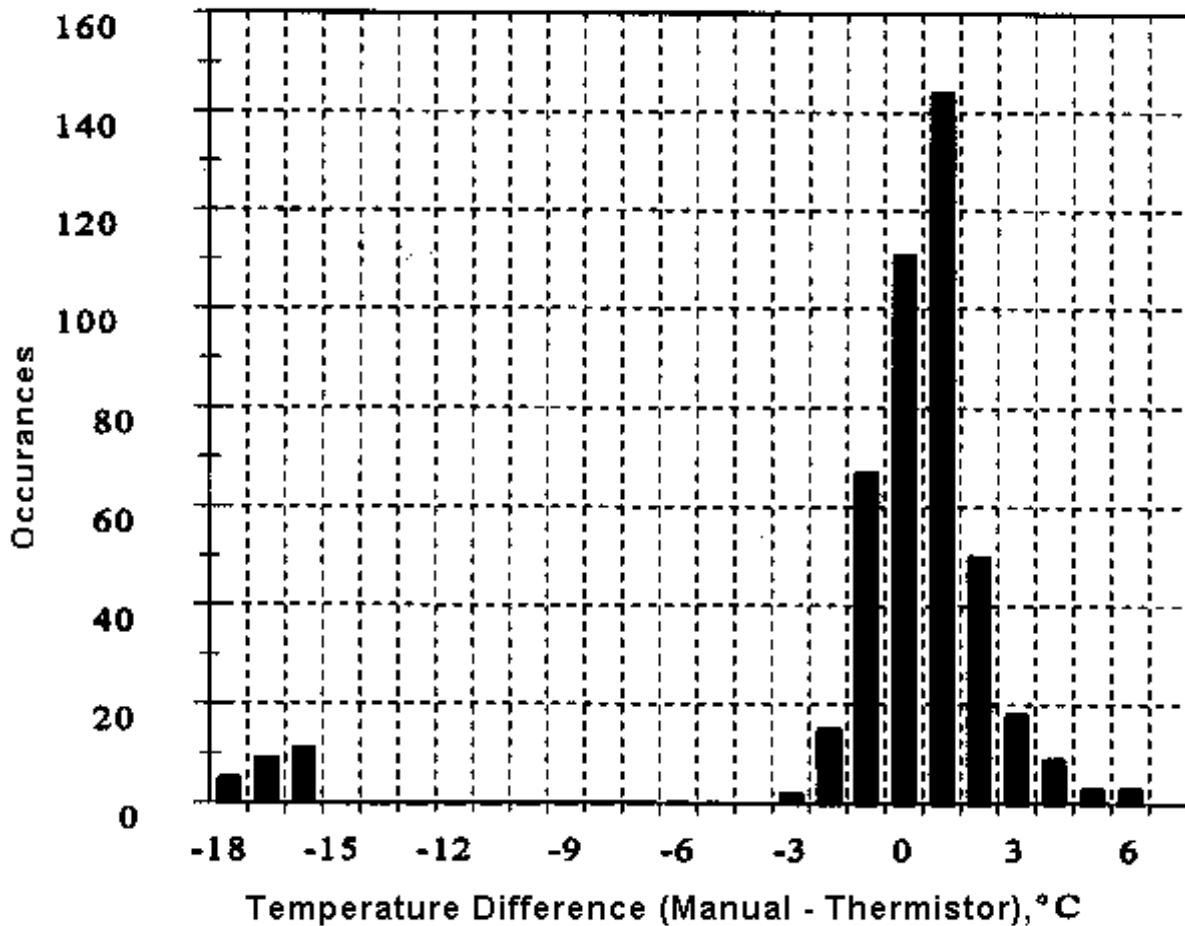


Figure 4. Comparison of mid-depth temperatures for Site 25A.

## Comparison of Resulting Temperatures

The above filtering and interpolations required numerous calculations. Since the thermistor and manual interpolations underwent separate calculation processes, a comparison of the third-depth and mid-depth thermistor and manual temperatures were made. In addition, the third-depth manual temperatures were compared with the IR temperatures as an independent check.

### *Manual Versus Thermistor Comparisons*

The thermistor and manual comparisons identified three forms of discrepancies — those caused by programming and processing errors, those caused by errors made when the manual data was recorded in the field or entered into RIMS, and discrepancies that could not be explained with the information available. Fortunately, after the programming errors were corrected, the remaining discrepancies made up only a small amount of the overall data set. The final data set used to develop the models for predicting temperatures within the asphalt had good agreement between the thermistor and manual mid-depth temperatures. A linear regression correlation between the manual and thermistor values had a standard error of estimate of  $1.27^{\circ}\text{C}$ , an intercept of  $0.37^{\circ}\text{C}$ , and a slope of 0.977.

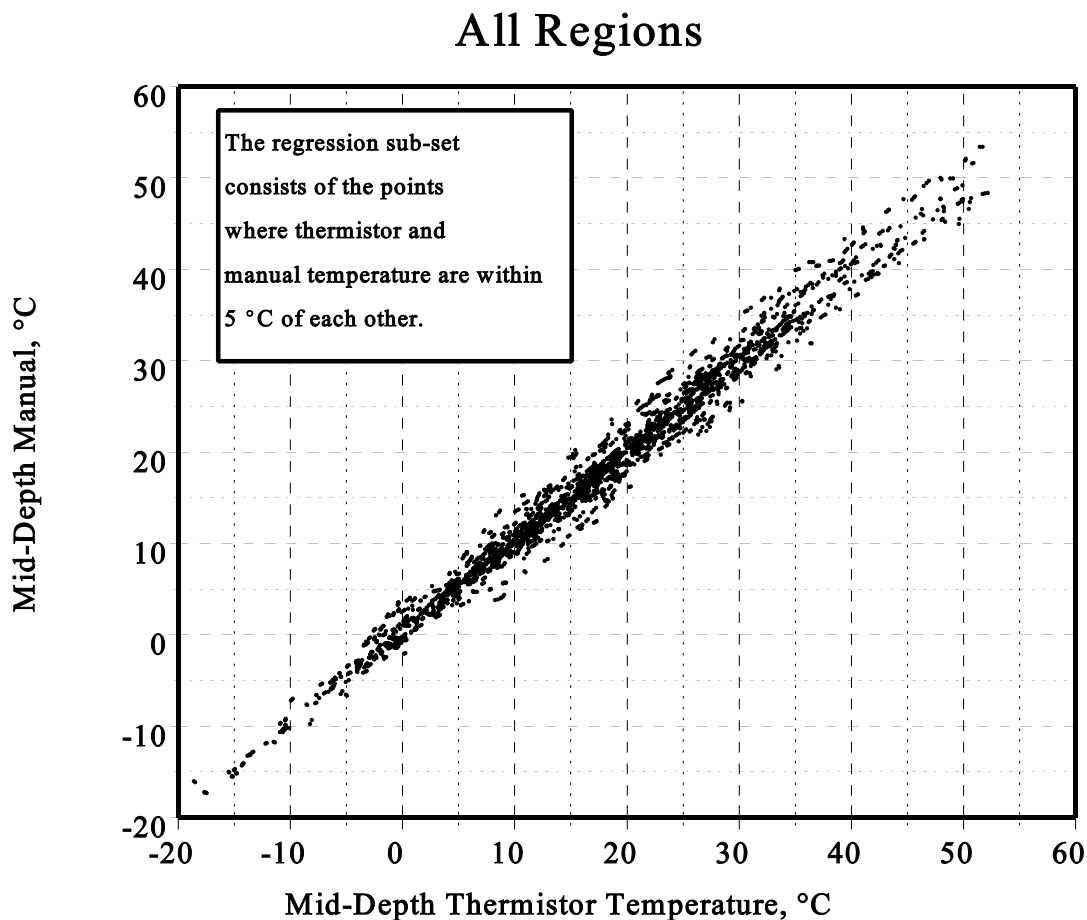


Figure 5. Comparison of the thermistor temperature and manual temperature data.

During the development of the final data set used for developing the prediction models with the Round 1 data, only IR data from within 10 m of the instrumentation were used, and only the records where the absolute value of the difference between the mid-depth thermistor and manual temperatures was less than 5° C. The 5° C value was selected as a reasonable value to use based on the distribution of differences to cull out problem data records. Figure 4, developed from site 25SA, show the frequency distribution of the difference between the manual and thermistor temperatures at mid-depth. The plot shows a bi-modal shape with a grouping at about -15 to -18° C, which was considered to be data errors or misreadings. Without checking all 25 sections, the value of 5 was selected as a query screening criteria for all of the temperature data.

**Stability of the Manual Temperatures**

Figure 5 shows the comparison of the mid-depth manual temperatures and thermistor temperatures representing a data set with the manual and thermistor mid-points are within 5° C of each other as described above. The 5° C criteria only eliminated about 5 percent of the data. From a regression standpoint, the biggest impact of removing the records with more than 5° C difference between the manual and thermistor temperatures was the improvement of the correlation coefficient and standard error of estimate; the constant and x coefficients remain about the same, implying that the data errors did not contain a significant bias.

Figure 5 also shows that the temperatures agree quite well at the lower temperatures and spread out as the temperature increases. This is more evident when evaluating the plots of manual and thermistor data at a site on a specific day. The thermistors seem to stay more consistent. The thermistor data is actually an average of the last 60 readings taken at 1-min. intervals, so any of the short-term fluctuations are averaged out of the thermistor data. The averaging process filters the short-term temperature variations out of the data before it is recorded.

The regression results for the mid-depth manual and thermistor temperatures are shown below in figure 6. This shows encouraging results with an intercept (constant) that is less than 1 and a slope that is less than 2 percent off of unity. The regression line crosses the line of equality at about 29 °C.

**Surface Versus Manual Third-Depth Comparisons**

The comparison of the IR data to the third-depth temperatures revealed a problem of a different nature. It was discovered that there were distinct differences in IR measurements, depending on the FWD used. This problem was traced to the IR calibration process. As a final result, only data from the Raytec brand of sensor, adjusted to restore the IR readings to the default manufacturer calibration factors, were used to develop the temperature prediction models.

| <b>M.mid=Const.+Slope*T.mid</b> |       |
|---------------------------------|-------|
| <b>Regression Output:</b>       |       |
| Constant                        | 0.37  |
| Std. Error of Y Estimate        | 1.27  |
| R-Squared                       | 0.989 |
| No. Of Observations             | 3658  |
| Degrees of Freedom              | 3656  |
| X Coefficient(s)                | 0.977 |

**Figure 6. Regression coefficients for manual and thermistor data.**

**Infrared Sensor Calibrations**

The initial attempt at developing a pavement temperature prediction model was with all of the data from the Round 1 sites. During this process, it was discovered that there were characteristic differences between FWD units. To evaluate the extent of this difference, a simple regression of the IR temperatures to manually measured temperatures, interpolated to

the third-depth, was made for each individual unit. The results of the regressions are shown in table 3. (Unit 060W is Unit 060 with a Williams sensor, and 060R is with a Raytec sensor.) All the units show reasonably good correlation coefficients, but there was significant differences in the slopes and constants.

There could be a variety of reasons for the differences if the comparisons were made on a site-by-site basis. Factors such as the surface color of the pavement and depth to the third-depth would be expected to result in different slopes and constants. However, these results are from a number of sites so it is unlikely that the differences in the constants and slopes were site dependent.

**Table 3. Regression comparison of infrared sensors.**

| <b>Simple Linear Regression: M.third = Const. + Slope * IR</b> |               |               |              |                  |                      |            |
|--|---------------|---------------|--------------|------------------|----------------------|------------|
| <b>Region</b>  | <b>FWD SN</b> | <b>Const.</b> | <b>Slope</b> | <b>Std. Err.</b> | <b>R<sup>2</sup></b> | <b>No.</b> |
| <b>North Atlantic</b>  | 058 (a)       | 2.43          | 0.6307       | 2.93             | 0.861                | 191        |
|  | 129 (b)       | 1.01          | 0.8474       | 2.31             | 0.938                | 874        |
| <b>N.Central</b>   | 060W (c)      | 4.24          | 0.8141       | 4.14             | 0.929                | 43         |
|  | 060R (d)      | 3.95          | 0.7579       | 3.17             | 0.934                | 886        |
| <b>South</b>   | 059 (e)       | -1.65         | 0.9301       | 2.60             | 0.952                | 258        |
|  | 132 (f)       | 1.52          | 1.1350       | 2.20             | 0.974                | 293        |
| <b>West</b>  | 061 (g)       | 0.90          | 0.7925       | 2.14             | 0.870                | 192        |
|  | 131 (h)       | 1.23          | 1.0932       | 2.79             | 0.964                | 318        |
| <b>Average</b>   |               | 1.70          | 0.8751       | 2.79             | 0.928                |            |
| <b>Standard Dev.</b>   |               | 1.88          | 0.1703       | 0.66             | 0.041                |            |

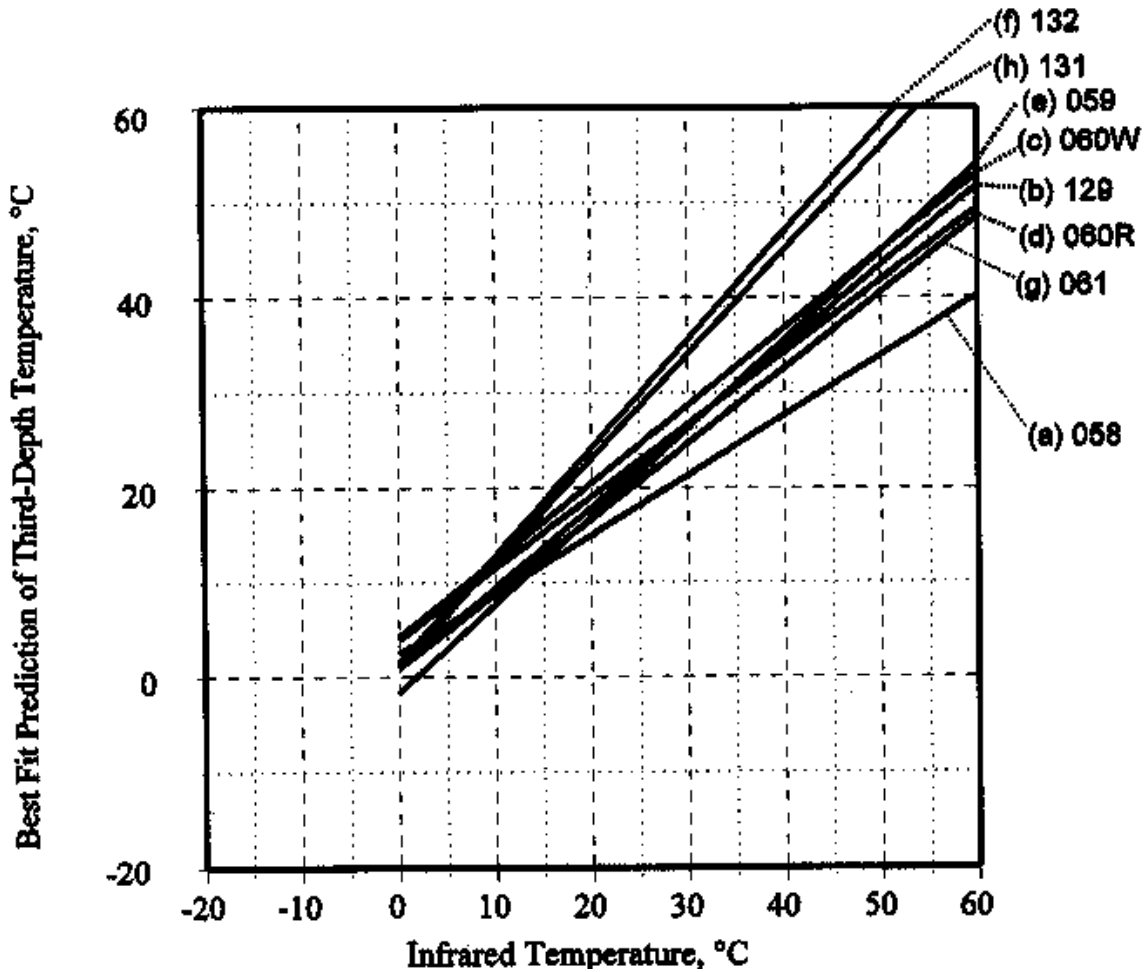


**Figure 7. Infrared sensor performance by FWD serial number.**

Figure 7 shows of each of the regression lines keyed to the letters in the left column of table 3. The graph shows that five of the units are grouped reasonably close together, and at high temperatures, Units 131 (h) and 132 (f) are reading high and Unit 58 (a) is reading low. Of the units that are grouped together, Unit 59 (e) has a higher slope. It is apparent that a combination of data from all of the infrared sensors may not be a good predictor of the internal temperatures of the pavement. If the data used in the analysis was to be restricted to the four units with similar coefficients — Units 058, 060R, 060W, and 061 — the result would be a much smaller data set, but still representing a wide geographical area, but not all of the units.

Figure 8 is a more detailed plot the differences between the two units in the Southern Region. The data points show that the relationship between the IR temperature measurements and the manually measured temperatures, interpolated to the third-depth, have similar scatter, but significantly different slopes and intercepts. This shows that the sensors are equally stable, but indicates that they may not have been calibrated to the same temperatures. (Calibration of the IR sensors was done by calibrating the sensor output to the temperature of an ice bath and to a container of hot water.)





**Table 4. Comparison of infrared sensor default output.**

| <b>Comparison of IR sensors by correlating the default IR to the interpolated manual temperature at third-depth.</b> |   |                                 |                  |                            |                           |                      |                                  |
|--|---|---------------------------------|------------------|----------------------------|---------------------------|----------------------|----------------------------------|
| <b>FWD by IR Sensor</b>  | <b>Regression Coefficients</b>  |                                 |                  |                            |                           |                      |                                  |
|  | <b><math>T_{\frac{1}{3}} = \text{Constant} + x \text{ Coef.} * \text{IR}</math></b> |                                 |                  |                            |                           |                      |                                  |
|  | <b>Constant</b>   | <b>Std. Error of Y Estimate</b> | <b>R-Squared</b> | <b>No. of Observations</b> | <b>Degrees of Freedom</b> | <b>x Coefficient</b> | <b>Std. Error of Coefficient</b> |
| 058  | -0.41458  | 1.77483                         | 0.94942          | 189                        | 187                       | 0.76953              | 0.01299                          |
| 059  | -0.69662  | 2.87543                         | 0.93959          | 343                        | 341                       | 0.90952              | 0.01249                          |
| 060W   | 6.93162   | 2.24609                         | 0.96227          | 621                        | 619                       | 0.77404              | 0.00616                          |
| 060R   | 1.75579   | 2.09092                         | 0.95475          | 499                        | 497                       | 0.88203              | 0.00861                          |
| 061  | 3.75686   | 3.77776                         | 0.82738          | 407                        | 405                       | 0.67594              | 0.01534                          |
| 129  | 2.07866   | 2.58846                         | 0.93056          | 893                        | 891                       | 0.82774              | 0.00757                          |
| 131  | 1.91422   | 2.72482                         | 0.96992          | 390                        | 388                       | 0.88756              | 0.00794                          |
| 132  | 2.53508   | 2.03758                         | 0.97845          | 373                        | 371                       | 0.89156              | 0.00687                          |
| <b>ALL UNITS</b>   | <b>3.29893</b>  | <b>3.38347</b>                  | <b>0.93098</b>   | <b>3734</b>                | <b>3732</b>               | <b>0.81298</b>       | <b>0.00362</b>                   |

Table 4 shows the differences that still existed in the data set for developing temperature prediction models. The serial number of the FWD identifies the specific IR sensor manufacturer. All of the older units have Williamson sensors except unit 060R which has a Raytec sensor. Of the sensors used in the above units, the default IR results of three units do not conform with the group: Unit 058 and Unit 061 both tend to read higher pavement surface temperatures at the upper range as indicated by the low x coefficient; unit 060W reads lower pavement surface temperatures as indicated by the high constant as shown in figure 9.

Unfortunately, Unit 060W is the sensor the BELLS<sup>(6)</sup> equation was based on as reported at the fourth International Conference on the Bearing Capacity of Roads and Airfields. Therefore, the BELLS equation overpredicts the asphalt temperatures in the low temperature range and underpredicts in the high temperature range. It is also apparent that the results from Unit 060W was suspect based on the work done by Dr. Richard Kim at North Carolina State University<sup>(7)</sup>.

Further evaluations found the Raytec factory calibrations to be reasonably good, leading to the process of doing periodic field checks with an independent sensor to confirm the sensor was working properly. On that basis, the development of a temperature prediction model was based on the IR readings from the Raytec sensors, adjusted to the factory calibration settings.

## IR Sensors Used in SMP Study

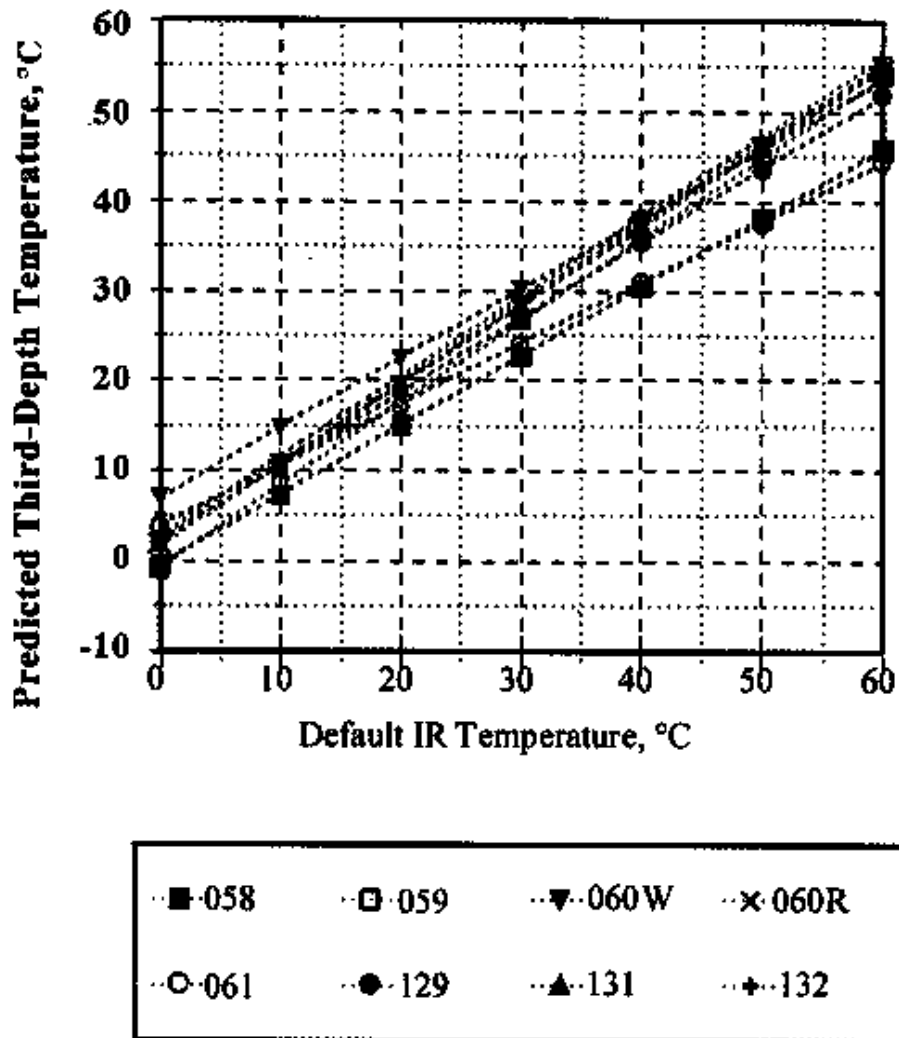


Figure 9. Machine difference in the default infrared temperature output.



## CHAPTER 4. TEMPERATURE PREDICTION MODELS

There are two objectives for the development of methods to predict temperature within an asphalt pavement.

- Develop new coefficients for the BELLS temperature prediction model. The equation was developed to predict temperature within asphalt pavements at the third-depth. Independent variables used in the equation include surface temperature, time of test, the previous 5-day average air temperature, and the depth to the third-point.
- Determine if improvements could be made in the BELLS model and whether previous 5-day average air temperature, which is difficult to obtain, could be replaced by a more easily obtained air temperature.

### PREDICTION MODELS

#### BELLS Model

A regression analysis was run to develop a new set of BELLS model coefficients using the Round 1 Raytec data. Remarkably, the R-squared and standard error of estimate were very close to that of the original BELLS model, particularly when considering that the data now represented 25 sites rather than 9, and that the temperature at both the mid-depth and third-depth are included in the same data set. The R-squared using 0.975 and the standard error of estimate is 1.91°C, which is close to the original model R-squared of 0.97 and standard error of estimate of 1.8°C. However, the new coefficients were very different. A malfunctioning IR sensor was used to collect much of the data used to develop the original BELLS model, as discussed above, and was thought to be the reason for the difference in the coefficients.

The new coefficients for the BELLS equation are:

$$T_d = 2.8 + 0.894 * IR + \{\log(d) - 1.5\} \{-0.540 * IR + 0.770 * (5\text{-day}) + 3.763 * \sin(hr - 18) + \{\sin(hr - 14)\} \{0.474 + 0.031 * IR\} \quad (1)$$

where:

|       |   |   |
|-------|---|---|
| $T_d$ | = | Pavement temperature at depth d, °C   |
| IR    | = | Infrared surface temperature, °C  |
| log   | = | Base 10 logarithm   |
| d     | = | Depth at which mat temperature is to be predicted, mm                                 |
| 5-day | = | Previous mean 5-day air temperature, °C   |
| sin   | = | Sine function on a 24-hr clock system, with $2\pi$ radians equal to one 24-hour cycle |
| hr    | = | Time of day in 24-hr system   |

Note: To use the time-hour function correctly, divide the number of hours (after subtracting the appropriate shift of 14 or 18) by 24, multiply by  $2\pi$ , and apply the sine function in radians.

A reason for such a large change in the coefficients is the IR sensors used to measure this data are more accurate over the range of data collected, and the model, therefore, is less dependent on the 5-day air temperature.

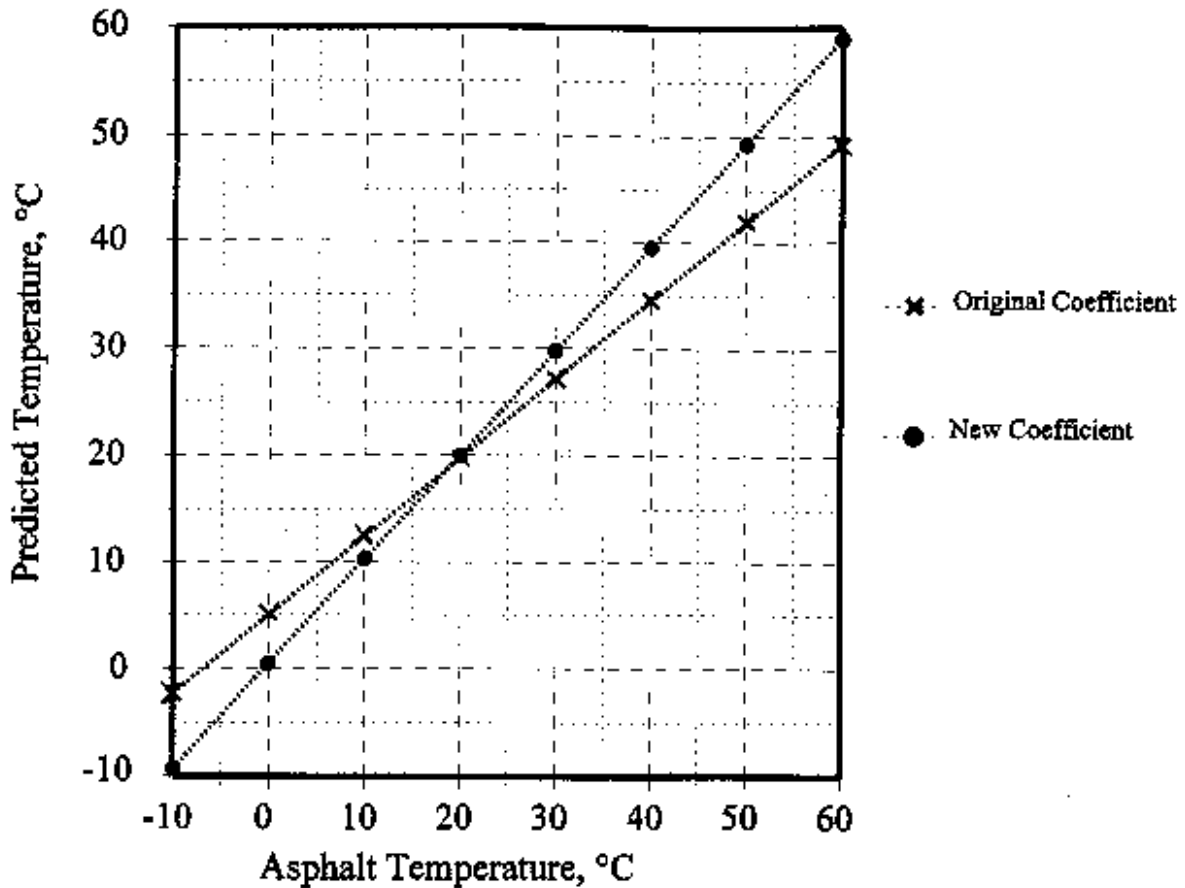


Figure 10. Comparison of the BELLS model original and new coefficients.

Figure 10 shows the prediction trend of the original BELLS coefficients compared to the updated coefficients. It shows that the original coefficients resulted in an overprediction of temperature when it was cold, the same at about 20 °C, and under prediction of temperatures when it was hot.

### Development of BELLS2

The 5-day air temperature has proven to be difficult to obtain for routine testing; the previous day's air temperature is more easily obtained by the FWD operator. Sources, such as local radio or newspapers, can provide a recent temperature history. For LTPP data analysis, the 5-day air temperature can be obtained from the climatic database that is associated with LTPP; however, agencies performing routine testing have no easy source for such information.

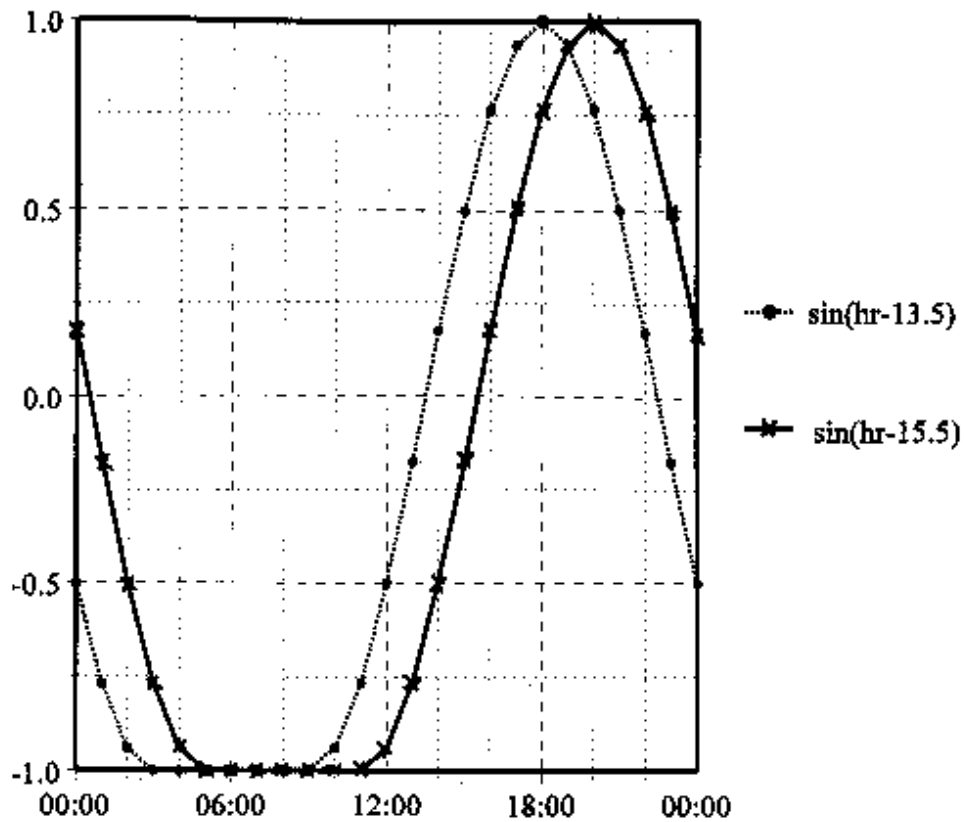


Figure 11. 18-hr cycle sine functions.

The BELLS model was patterned after the original Herb Southgate work, and in keeping with the basic parameters of the Southgate method, several modifications were made to the BELLS model that resulted in an improved model called BELLS2. The daily temperature variation does not follow a uniform sine wave, but instead is skewed to a shorter warming time and a longer cooling time. To approximate the shape of the warming and cooling trends, the sine functions of the BELLS model were replaced by two sine functions based on an 18-hr cycle as shown in figure 11. The form of the resulting equation is:

$$T_d = 2.9 + 0.935 * IR + \{\log(d) - 1.25\} \{-0.487 * IR + 0.626 * (1\text{-day}) + 3.29 * \sin(hr_{18} - 15.5)\} + 0.037 * IR * \sin(hr_{18} - 13.5) \quad (2)$$

where:

- $T_d$  = Pavement temperature at depth d, °C
- IR = Infrared surface temperature, °C
- log = Base 10 logarithm
- d = Depth at which mat temperature is to be predicted, mm
- 1-day = Average air temperature the day before testing
- sin = Sine function on an 18-hr clock system, with  $2\pi$  radians equal to one 18-hr cycle
- $hr_{18}$  = Time of day, in 24-hr clock system, but calculated using an 18-hr asphalt concrete (AC) temperature rise- and fall-time cycle, as indicated by the notes below

Notes: BELLS2 has been verified at both mid-depth and third-depth temperature points. Almost no difference exists in the regressions derived from the data at either depth; thus, they were combined.

When using the  $\sin(\text{hr}_{18} - 15.5)$  (decimal) function, only use times from 11:00 to 05:00 hrs. If the actual time is not within this time range, then calculate the sine as if the time was 11:00 hrs (where the sine = -1). If the time is between midnight and 05:00 hrs, add 24 to the actual (decimal) time. Then calculate as follows: If the time is 13:15, then in decimal form,  $13.25 - 15.50 = -2.25$ ;  $-2.25/18 = -0.125$ ;  $-0.125 \times 2\pi = -0.785$  radians;  $\sin(-0.785) = -0.707$ . [Note that an *18-hr* sine function is assumed, with “flat” negative 1 segment between 05:00 and 11:00 hrs as shown by the solid line in figure 11.]

When using the  $\sin(\text{hr}_{18} - 13.5)$  (decimal) function, only use times from 09:00 to 03:00 hrs. If the actual time is not within this time range, then calculate the sine as if the time is 09:00 hrs (where the sine = -1). If the time is between midnight and 03:00 hrs, add 24 to the actual (decimal) time. Then calculate as follows: If the time is 15:08, then in decimal form,  $15.13 - 13.50 = 1.63$ ;  $1.63/18 = 0.091$ ;  $0.091 \times 2\pi = 0.569$  radians;  $\sin(0.569) = 0.539$ . [Note that an *18-hr* sine function is assumed, with “flat” negative 1 segment between 03:00 and 09:00 hrs as shown by the dotted line in figure 11.]

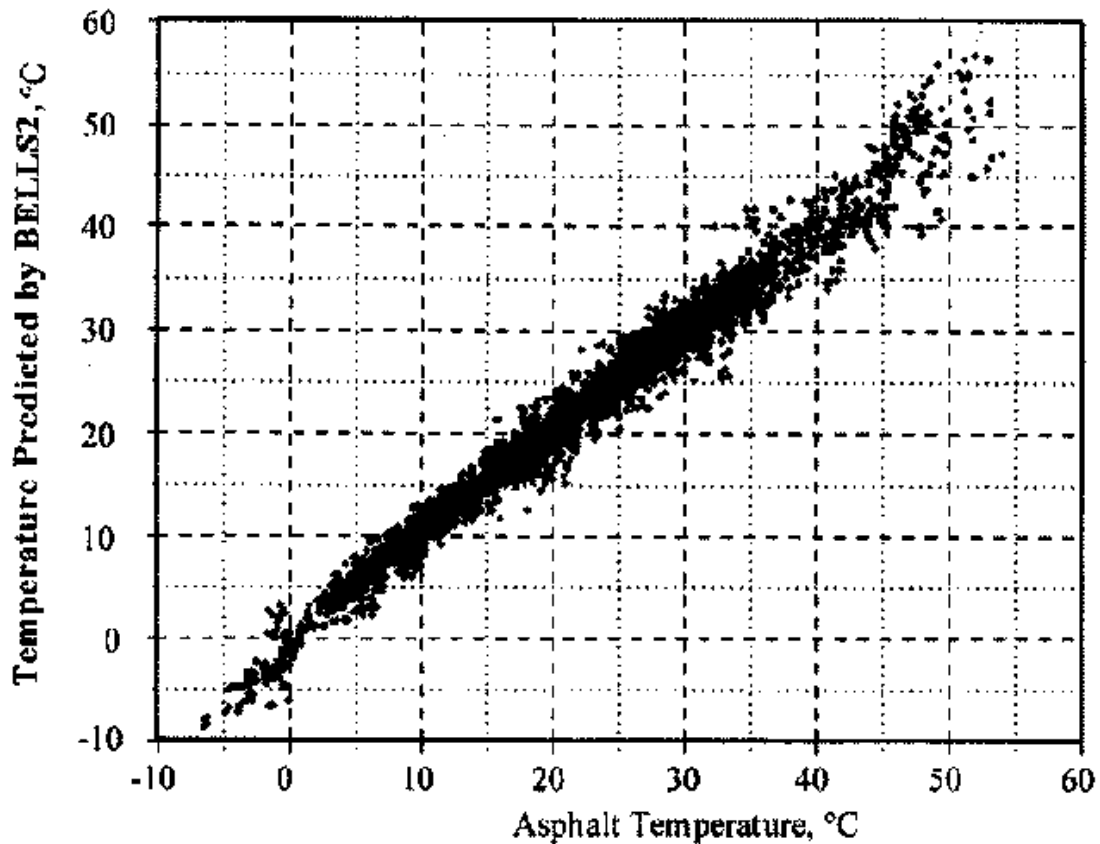


Figure 12. BELLS2 temperature predictions.



The data set was restricted to a temperature range of 0 to 40 °C, resulting in a data set of 3335 records, as compared to the full data set of 3,722 records.. The coefficients were very similar to the coefficients obtained using the full data set, but the standard error was improved. There was more scatter in the data at temperatures greater than 40 °C, as shown in figure 12. The statistics for the above regression are an R-squared of 0.973 and a standard error of estimate of 1.60 °C, which is an improvement over the original BELLS model. The regression R-squared using all the data points is 0.978 and the standard error of estimate is 1.78. (The higher number of observations in the reason that both the R-squared and standard error of estimate increase.)

### Shading Effect on Infrared Measurements

One factor that relates to the results of all of the temperature prediction models presented here is the LTPP method of testing and its effect on the surface temperature measurement. The testing is at 7.6-m intervals. The distance from the IR sensor to the front bumper of the tow vehicle is about 9 m; therefore, the tow vehicle is shading the next test point while the FWD is testing. Each test takes approximately 3 min; therefore, each test location is shaded for about 6 min. Since the FWD records the surface temperature at the end of the test cycle, the pavement surface is shaded for about 6 min before the reading is taken.

Since routine testing by highway agencies does not follow the LTPP protocols, shading during routine testing is typically 15 to 30 s. To determine what impact the shading has on the surface temperature, surface measurements were made periodically at several locations and under different sky

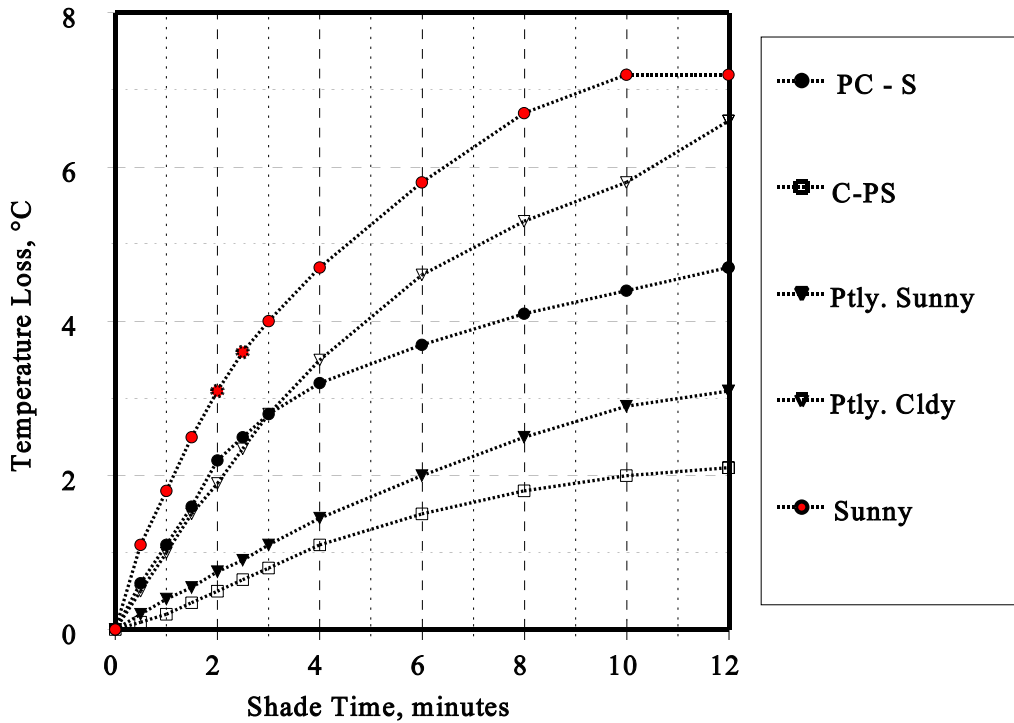


Figure 13. Influence of shade on surface temperature.

covers. Figure 13 shows the effects of shading that were measured on several pavement surfaces near Ojai, California and Starke, Florida. It shows that a shaded surface temperature can drop by about 1.5 to 5°C between 30 s and 6 min of shading, depending on the sky cover at the time.

One positive effect from the extended shading is that the rapid changes that can occur in surface temperature due to transient sunshine is minimized. The shading allows the surface temperature to moderate to a temperature much more representative of the temperature near the surface than it would be if the measurement was made when the sun was shining on the surface. The comparison of regression residuals to sky cover shows almost no significant effect; whereas, if the surface temperature was measured before any shading occurred, or very shortly after the surface was shaded, a more significant relationship would be expected.

### **BELLS2 for Production Testing**

To provide a version of BELLS2 that can be used for production testing, the infrared temperatures were adjusted according to sky cover data recorded at the site. The adjustment consisted of adding the following amounts to the infrared readings, based on sky cover:

| <u>Sky Cover</u>     | <u>Temperature Added to Infrared Measurements, °C</u> |
|----------------------|---|
| <b>Sunny</b>         | 4   |
| <b>Partly Cloudy</b> | 3   |
| <b>Cloudy</b>        | 1.5   |

These amounts were the estimated amount of surface cooling based on the limited measurements made.

The BELLS2 model was used and new regression coefficients were developed to produce a prediction model that will be of better use for production testing. The resulting equation is:

$$T_d = 1.38 + 0.907 * IR + \{\log(d) - 1.25\} \{-0.540 * IR + 0.764 * (1\text{-day}) + 2.39 * \sin(hr_{18} - 15.5)\} + 0.060 * IR * \sin(hr_{18} - 13.5) \quad (3)$$

### **Validation of the BELLS Models**

A temperature data set was developed with the Round 2 SMP test data. The only difference between the makeup of the Round 1 and Round 2 data sets was Round 2 included all of the infrared data, whereas the Round 1 was limited to those test locations within 10 m of the manual temperature test holes. Round 2 data were used to check the regression models.

The BELLS model from the Round 1 data set was used to predict the temperatures at the third- and mid-depths using the Round 2 data. The predicted values were subtracted from the measured values to produce a set of residuals. The average of the residuals was 0.16 °C and the standard deviation (S.D.) of the residuals was 1.85, which compares favorably to the standard error of estimate of 1.78 for the Round 1 BELLS regression. The regression for the shade-adjusted BELLS also compared favorably to the Round 2 data (an average residual of -0.13 and S.D. of the residuals of 1.97). Figure 14 shows the performance of the BELLS model on Round 1, Round 2 validation, and for the model with new coefficients from the combined Rounds 1 and Round 2 data.

## Recommended BELLS Models Rounds 1 and 2 Combined

Combining the Rounds 1 and 2 data provides an opportunity for a slight improvement in the regression models. New regression models were developed for both the LTPP testing protocols (BELLS2) and for the shade-adjusted surface temperatures (BELLS3). Equations 4 and 5 are the recommended models for predicting the temperatures within asphalt pavements.

### *BELLS2 (LTPP testing Protocol)*

$$T_d = 2.78 + 0.912 * IR + \{\log(d) - 1.25\} \{-0.428 * IR + 0.553 * (1\text{-day}) + 2.63 * \sin(\text{hr}_{18} - 15.5)\} + 0.027 * IR * \sin(\text{hr}_{18} - 13.5) \quad (4)$$

Observations = 10,304

Adjusted R-Squared = 0.977

Standard Error = 1.8 °C

### *BELLS3 (Routine Testing Methods)*

$$T_d = 0.95 + 0.892 * IR + \{\log(d) - 1.25\} \{-0.448 * IR + 0.621 * (1\text{-day}) + 1.83 * \sin(\text{hr}_{18} - 15.5)\} + 0.042 * IR * \sin(\text{hr}_{18} - 13.5) \quad (5)$$

Observations = 10,304

Adjusted R-Squared = 0.975

Standard Error = 1.9 °C

Figure 14 shows the frequency of the absolute error for equations 2 and 4. Figure 14 is the cumulative frequency of absolute errors for equations 2 and 4 from the regression data set and as applied to Round 2 data. From a practical standpoint, it can be seen that equation 2 gave valid results when tested with the Round 2 data. The difference, however, was significant because of the size of the data sets. The model developed from the combined data set (equation 4) shows just slightly less error than the model from Round 1 (equation 2) when applied to the Round 2 data.

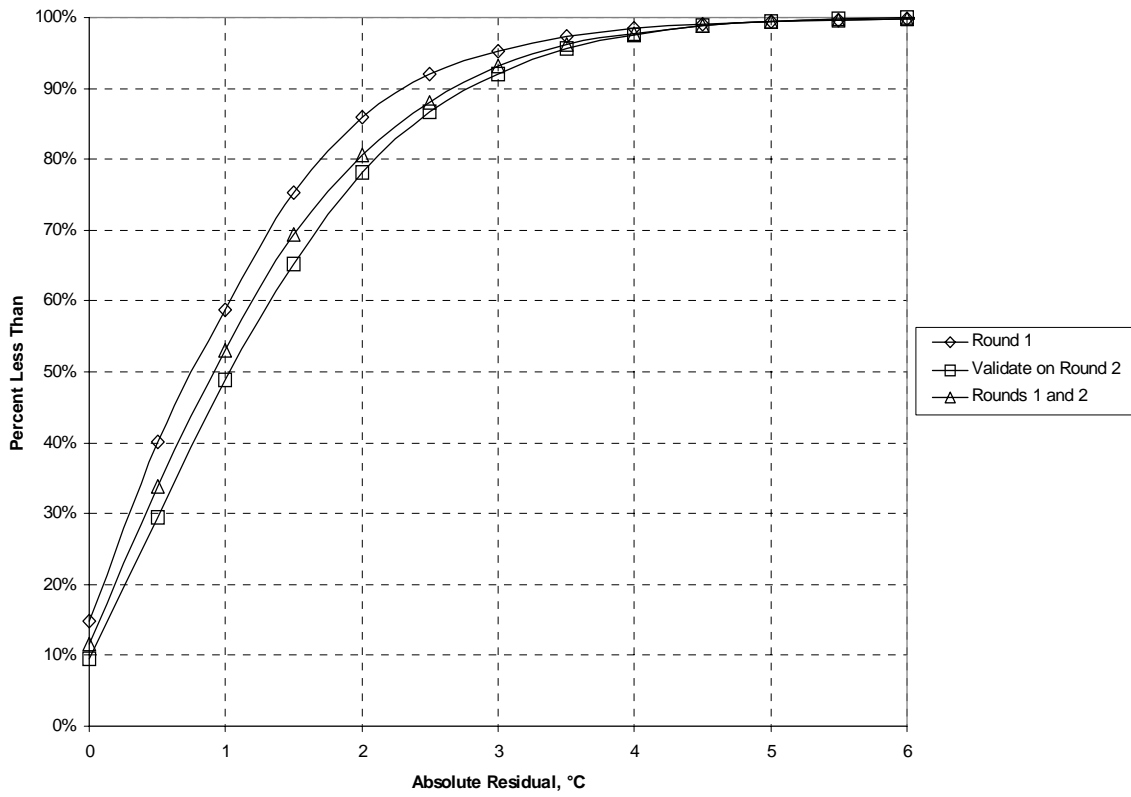


**Figure 14. BELLs2 prediction errors.**

## **CHAPTER 5. TEMPERATURE ADJUSTMENTS FOR BACKCALCULATED ASPHALT MODULI**

The stiffness, or modulus, of asphaltic concrete (AC) is very temperature-sensitive. Routine deflection test results must nearly always be adjusted to represent the deflection at a standard temperature or some other reference temperature that is needed for analysis. Also, the backcalculated modulus must be adjusted to the modulus expected at some selected reference or characteristic temperature for the section being analyzed. A number of procedures have been developed to adjust the deflections under the load plate and backcalculated asphalt moduli for temperature; however, most are based on limited data or for earlier deflection equipment, such as the Benkelman beam.

The temperature and deflection data from the LTPP's SMP provide a large data source from a broad geographical area and from a variety of pavement structures. The data from the 25 asphalt sections from Round 1 of the SMP were initially used to develop relationships and 15 sections from Round 2 were used to validate the results. As described later, the sections in Round 2 were significantly different from Round 1 sections. Models were developed to relate the temperature at the mid-depth of the asphalt layer to the backcalculated asphalt moduli. The temperature within the asphalt, as described in the section dealing with temperature prediction, was interpolated for each FWD test. The relationship between the asphalt temperature and the corresponding asphalt moduli was developed. This provided a basis for moduli adjustment procedures.

### **BACKCALCULATED ASPHALT MODULI**

The backcalculated asphalt moduli and deflection basin factors analyzed include:

- Asphalt Moduli obtained by backcalculation using the following three programs:
  - WESDEF.
  - MODULUS 5.1.
  - ELMOD4.

The three backcalculation programs used were chosen to represent three different backcalculation approaches. WESDEF is a classical backcalculation program that minimizes the difference between a calculated basin and the measured basin by adjusting the modulus of the various layers through a series of iterations. MODULUS is a database matching program that calculates a number of deflection basins representing the range of allowable elastic moduli for each of the layers, and then using an interpolation matching scheme, calculates the layer moduli that results in the best match. ELMOD4 uses the Odemark equivalent thickness approach rather than the WESLEA elastic layer routine used in WESDEF and MODULUS.

The normalized 40-kN (drop height 2) deflections were used to backcalculate the layer moduli. Each of the three backcalculation programs described above were used for the Round 1 deflection data and only WESDEF was used for the Round 2 data. The sections were modeled according to the layer configurations listed in table 2. There were a total of 26,697 Round 1 deflection tests that were available for analysis by each of the 3 programs, for a total of 80,091 backcalculations. There were 12,018 Round 2 deflection tests backcalculated with WESDEF.

## Backcalculation Results

All of the Round 1 drop height 2 deflection data was analyzed by each of the three backcalculation programs. The backcalculated results were imported into spreadsheets so the backcalculated results could be re-associated with the correct station, time, date, and pavement temperature.

## Analysis Approach

The analysis of the Round 1 backcalculated moduli data was approached on a test station basis. Pavement deflection response varies with distance (spacial variation). This also holds true for backcalculated asphalt moduli and its relationship with pavement temperature. Regressions run on all the data from a site would result in lower correlation coefficients (R-squared) and higher standard error of estimates than from specific locations.

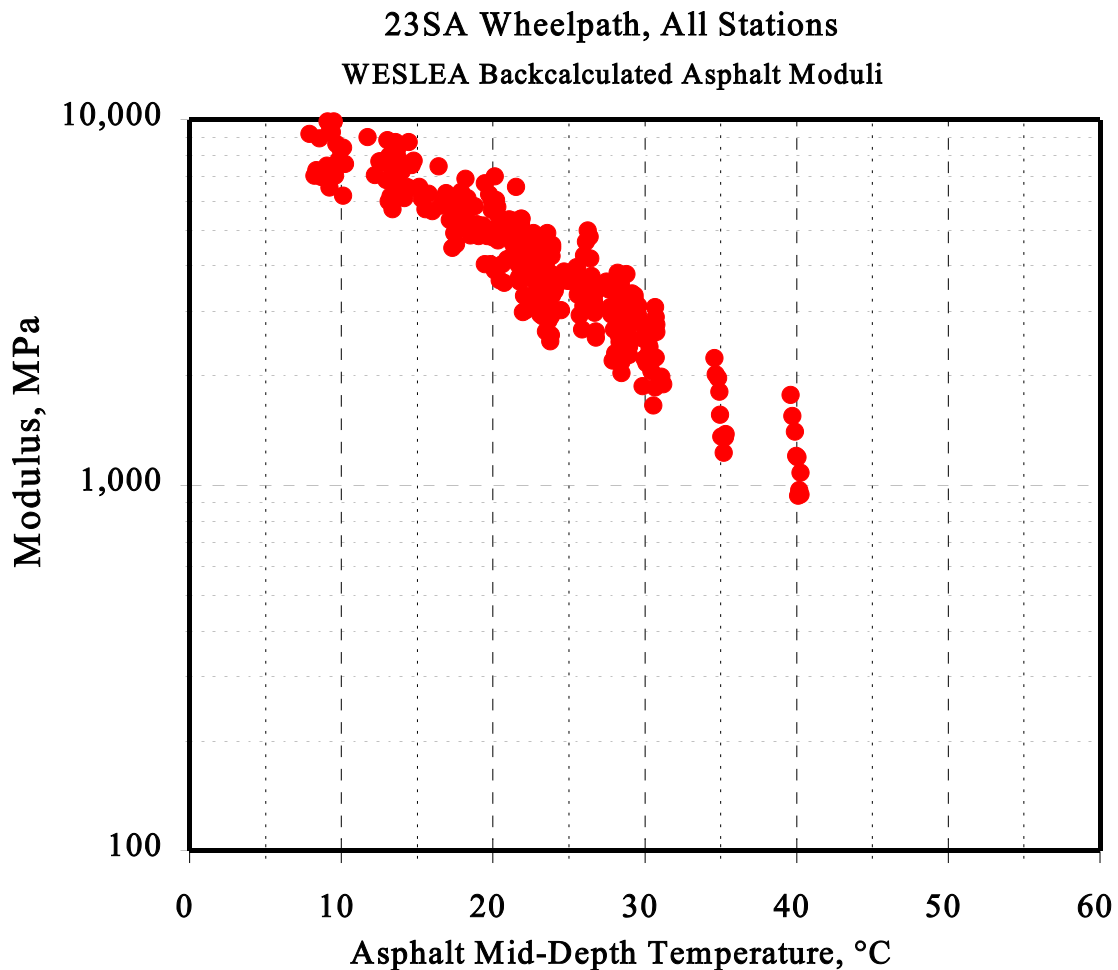


**Figure 15. Backcalculated moduli from all stations**

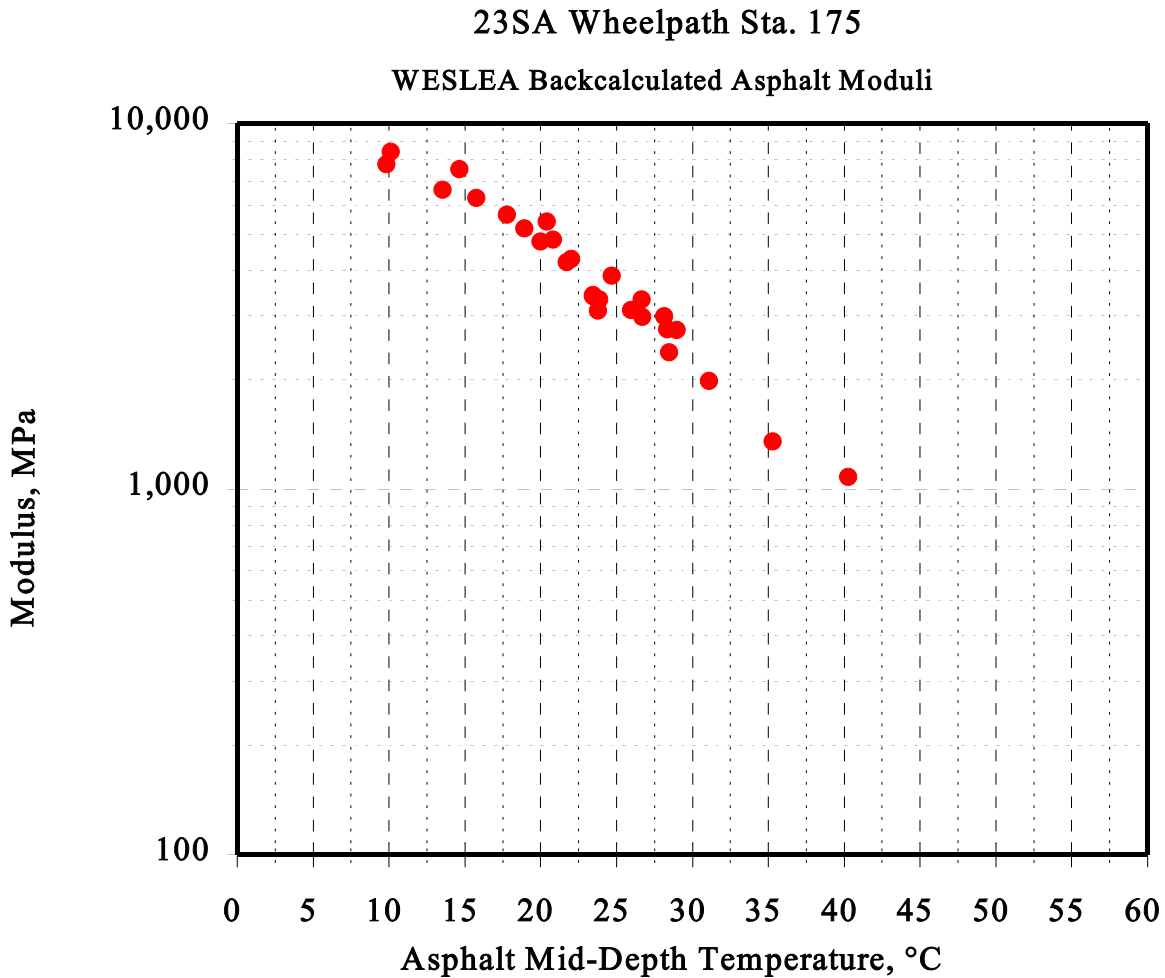


**Figure 16. Backcalculated moduli from one station location**

Figures 15 and 16 show a comparison of the WESDEF results from all of the stations in the wheelpath of Site 23SA and from a single test location (Station 175) respectively. Figure 16 is an example of a good fit between temperature and backcalculated asphalt modulus. Figure 15 shows the additional scatter due to the variation in pavement response from station to station. This spacial variation may be caused by changes in the thickness, mix properties, and condition of the asphalt and other pavement layers; there are no data available that represent a measure of thickness or material properties on a station-by-station basis. The surface condition is available and does relate to how the modulus responds to temperature, but was not characterized on a station-by-station basis for this study. The regression correlation coefficient (R-squared) for the data in figure 15 is 0.87 and is 0.96 for the data in figure 16. Site 23SA is one of the more consistent sites in Round 1; however, there still is a notable difference in the correlation for the two data sets. The regression for Station 175 indicates that the temperature explains 96 percent of the variation in the log of the moduli; however, for all stations, the temperature explains only 87 percent of the variation in the log of the moduli. For other sites, spacial variations generally resulted in larger differences.

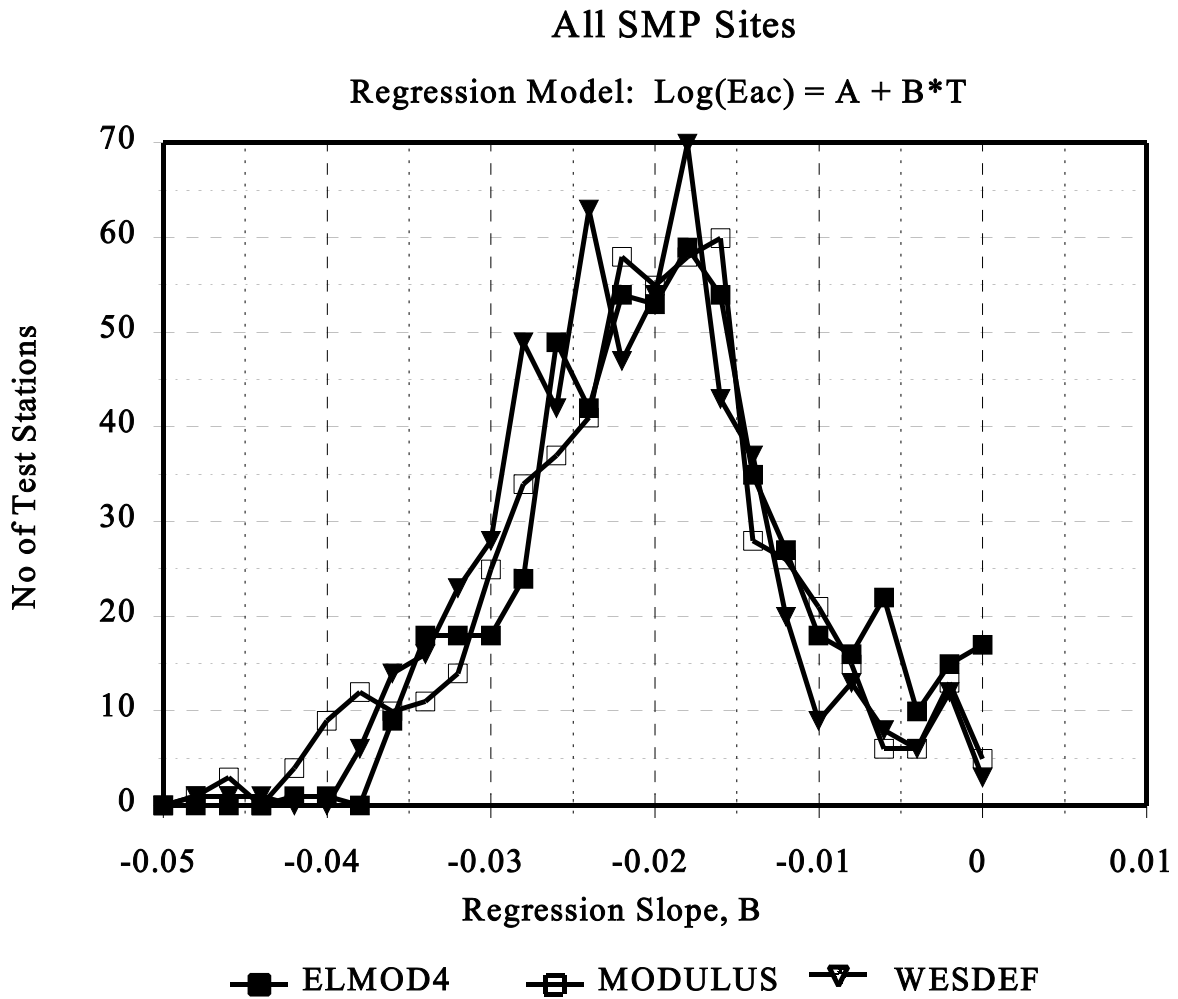


**Figure 17. Histogram of slope coefficients for temperature versus modulus.**

The best-fitting model for relating the backcalculated asphalt moduli to the mid-depth temperatures is semi-logarithmic, as shown in Figures 15 and 16. An expectation is that the moduli values would tend toward asymptotic behavior at the extreme cold and hot temperatures. However, data from SMP showed very little tendency toward such behavior.

Regression analysis, with the base 10 logarithms of the moduli as the dependent (y) variable and the mid-depth temperature as the independent (x) variable, was done on a station-by-station basis. Data during the frozen time of the year was excluded. The regression results for each of the test stations at a site were placed in a table for analysis.



A station was selected to represent the temperature versus backcalculated asphalt modulus relationship for each test lane of each section. The test station that had a slope and intercept that was the closest to the median rankings of the slope and intercept values was selected for each lane at each SMP site. The results for the Round 1 sites are shown in table 5. A histogram of the slopes from all of the regressions from Round 1, station by station, is shown in figure 17. The distribution is slightly skewed toward the left (steeper slopes) due to several sites, for example, 46SA and 50SA. The asphalt moduli of these sections are more sensitive to temperature than the rest of the sites, which have slopes that typically range from -0.016 to -0.025.

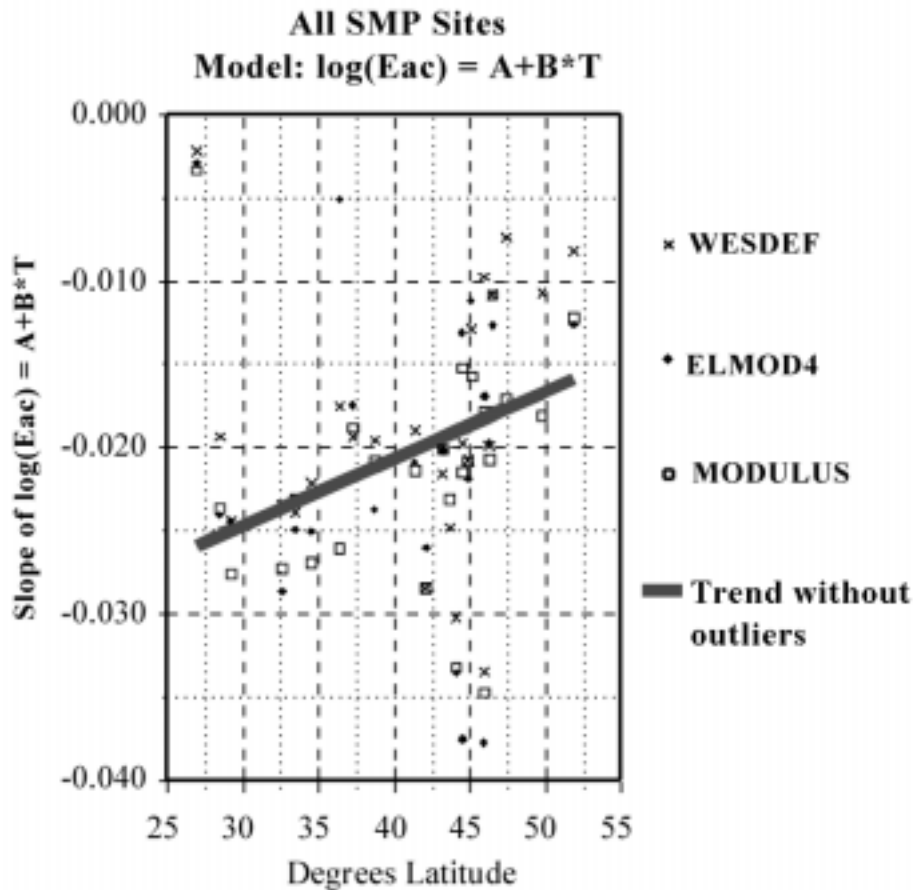


**Figure 18. Slope of temperature versus modulus relationship with latitude.**

The variation in intercept and slope from test station to test station is due to a variety of factors that are not a part of the LTPP database. A few of the items that could influence the slope and intercept of the regressions include:

**Asphalt Binder and Mix Characteristics:** The asphalt binder and mix characteristics are known to have a significant influence on the stiffness of the mix. Part of the variation in both the intercept and slope is expected to be due to mix and binder characteristics. Binder tests were not part of the LTPP program for General Pavement Studies (GPS). SMP sites that are on GPS sections will not have binder data without additional testing. *It is recommended that the binder and mix characteristics be determined to establish a relationship between the backcalculated moduli and mix characteristics.* Asphalt binders used in hot climates are generally stiffer or harder than the asphalt binders used in cold climates. Figures 18 and 19

show that the latitude of the site is related to both the regression slopes and intercepts. The latitude could be thought of as a crude predictor of binder stiffness.

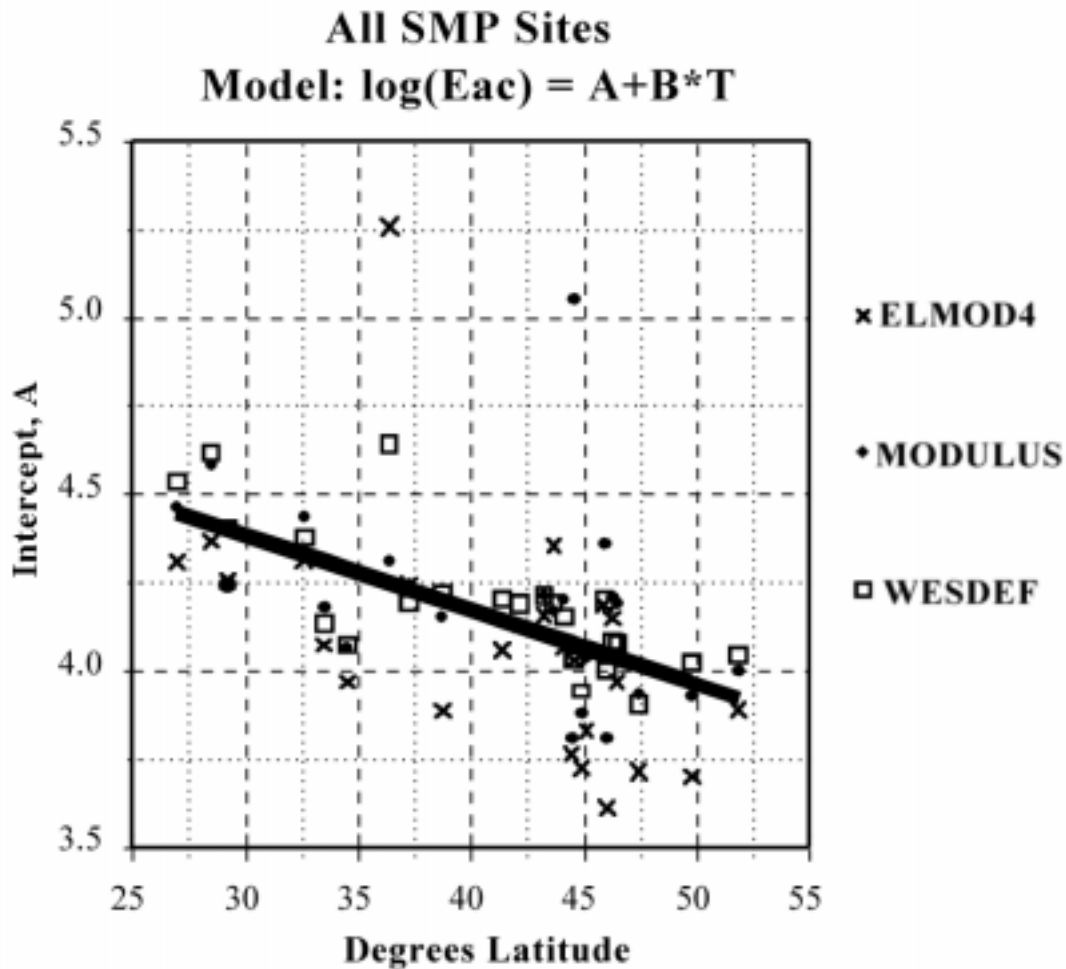


**Figure 19. Intercept of the temperature versus modulus relationship with latitude.**

**Pavement Structural Variation:** Variations in pavement structure, particularly layer thicknesses, can have a significant effect on the backcalculation results. If the asphalt layer thickness at a particular station is greater than the thickness used in the analysis, the intercept will decrease, or conversely, a thinner layer would cause the intercept to increase. Other mix properties, such as density, may also have an effect.

**Surface Condition and Asphalt Thickness:** During the analysis, a relationship between the average R-squared for each section and the thickness and condition of the asphalt was observed. The combination of asphalt thickness and condition seemed to have an effect on the regression R-squared and the error. As the asphalt thickness decreased, and/or the condition decreased, the correlation R-squared tended to decrease. Since there was no composite pavement condition scoring method available within LTPP, a Surface Condition Rating (SCR) was estimated for each of the sections based on the distress surveys. The SCR values assigned ranged from 5.0 for a new pavement to 2.0 for the sites with the most cracking. Figure 20 shows the general relationship between SCR, asphalt thickness, and R-squared. A similar type of relationship may also exist for the backcalculation error.

### WESDEF Regression Results R-Squared, f(thickness and condition)

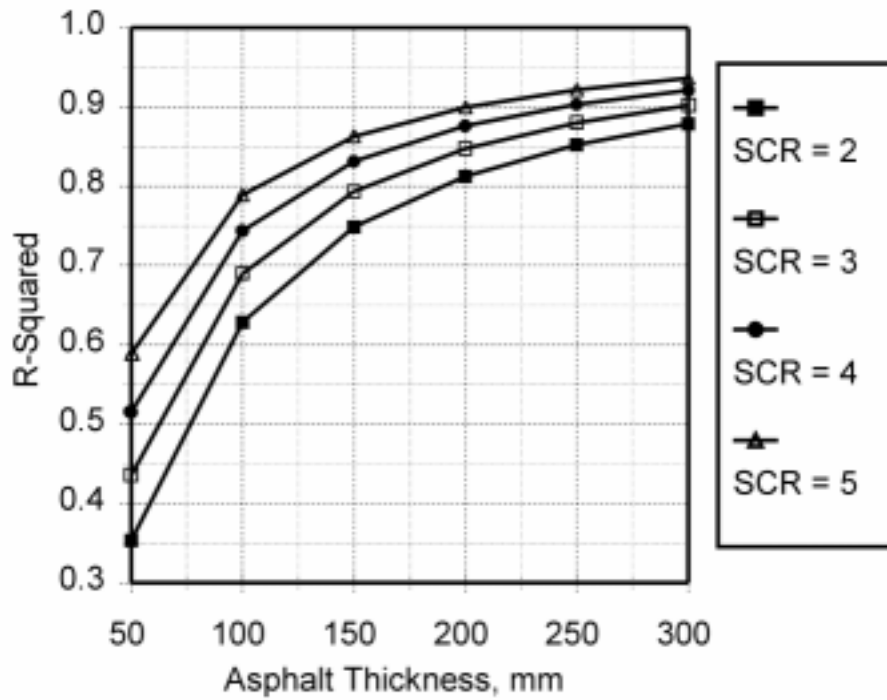
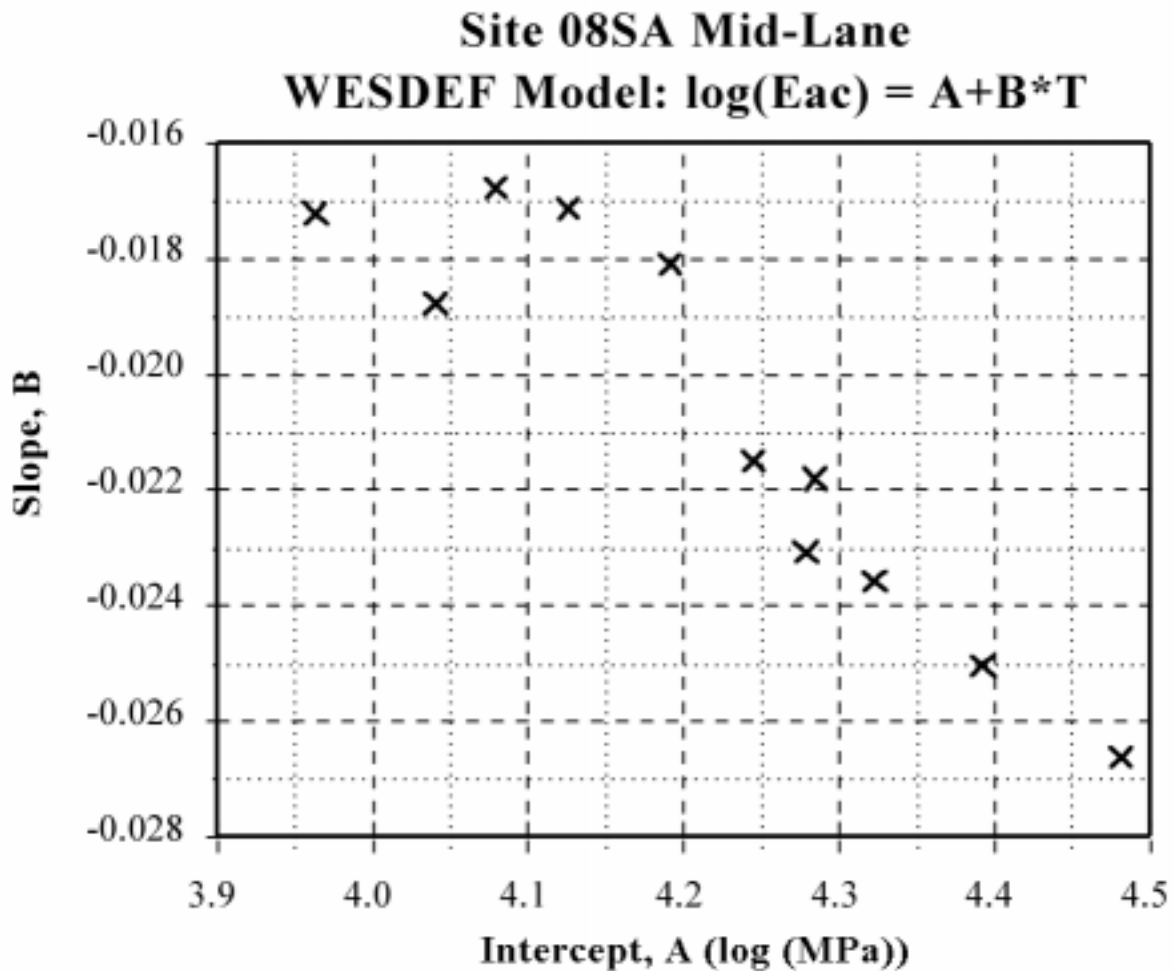


Figure 20. The influence of asphalt condition and thickness on the modulus-temperature relationships.



**Figure 21. Relationship between slope and intercept for Site 08SA.**

**Slope-Intercept Interaction:** There is a distinct inverse relationship between the intercept and the slope that would imply that the stiffer asphalts are more sensitive to changes in temperature. (The higher the backcalculated modulus values at low temperatures, the steeper the slope.) Figure 21 shows a general trend for the mid-lane of Site 08SA and figure 22 shows that the trend exists for all of the Round 1 sites in the study.

**Outliers:** The slopes and intercepts for some of the sites do not follow the trends for the rest of the sites and could be considered outliers for several reasons. Sites 46SA and 50SA have significantly higher slopes than the other sections. Site 40SA has higher intercepts than any of the other sites. Site 46SB has abnormal results for the wheelpath tests. Site 48SG has a thin asphalt layer over a cement-stabilized base and shows very little response to temperature. Site 90SA, which has a thin asphalt surface, is in poor to fair condition, and is on a strong subgrade; it also does not show as much response to temperature.

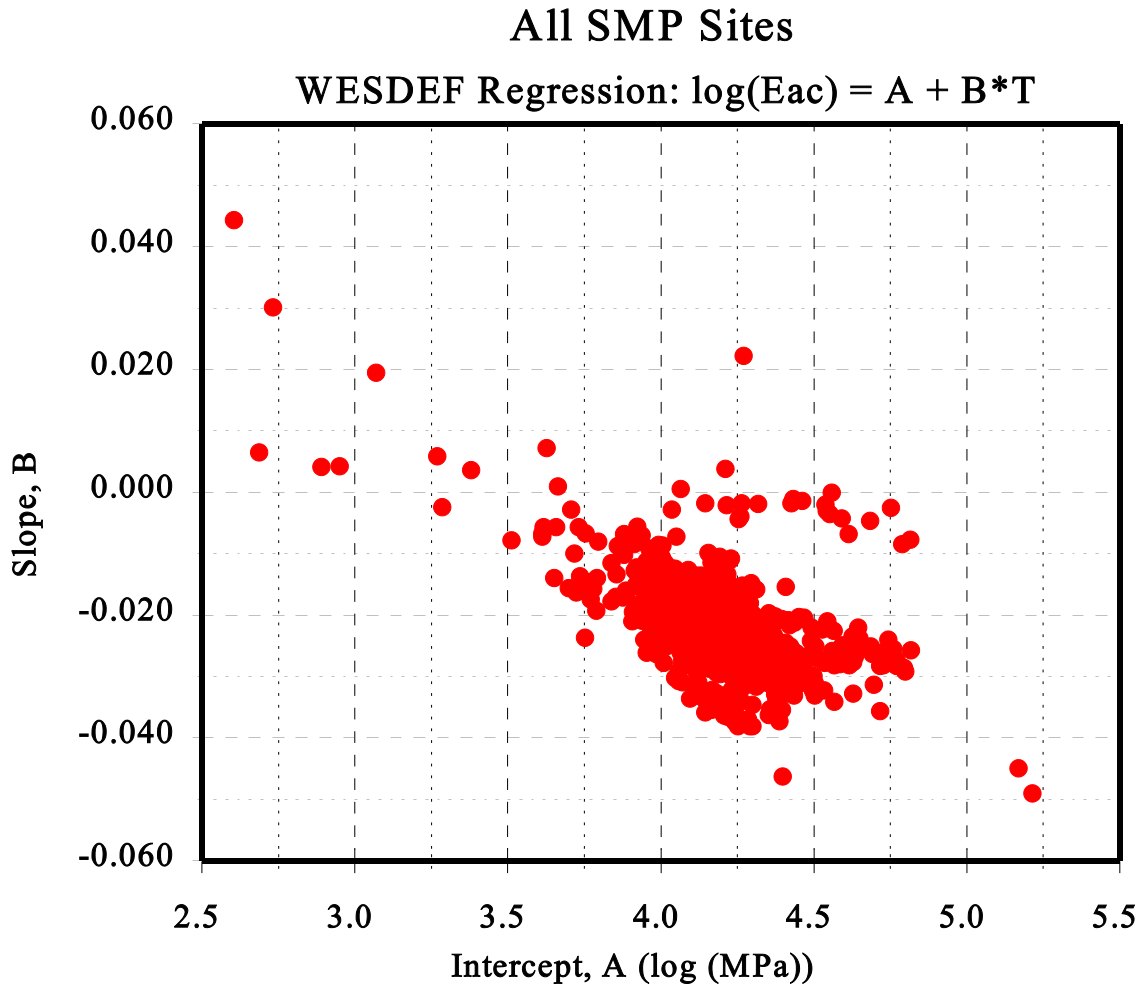


**Figure 22. Relationship between slope and intercept for all sites.**

#### **TEMPERATURE ADJUSTMENT OF BACKCALCULATED ASPHALT MODULI**

The semi-logarithmic format of the equation relating the asphalt modulus to the mid-depth asphalt temperature allows for a simple means of adjusting the backcalculated asphalt modulus for the effects of temperature. The approach is to calculate a modulus temperature adjustment factor using the following equation:

$$ATAF = 10^{\text{slope} \cdot (T_r - T_m)} \quad (6)$$

where:

|       |   |   |
|-------|---|---|
| ATAF  | = | Asphalt temperature adjustment factor   |
| slope | = | Slope of the log modulus versus temperature equation<br>(-0.0195 for the wheelpath and -0.021 for mid-lane are recommended) |
| $T_r$ | = | Reference mid-depth hot-mix asphalt (HMA) temperature   |
| $T_m$ | = | Mid-depth HMA temperature at time of measurement  |

Most of the slopes range between -0.010 and -0.027 (a reasonably broad range). The most common occurring slopes are -0.0195 for tests taken in the wheelpaths and -0.021 for tests taken mid-lane. Without a means of further defining the characteristics of the asphalt mix, these are the recommended slopes to use for the temperature adjustment model.

It should be noted, however, that the slope does have a correlation with the latitude of the site, which is expected to relate to the grading of the asphaltic cement used. The data from Round 1 showed that the slopes are generally steeper in the south than they are in the north, and since the mean slope from Round 2 is steeper than the one from Round 1, it remains consistent with the location of the sites.

## **VALIDATION OF THE TEMPERATURE ADJUSTMENT MODEL**

In Round 1, 577 specific test points on 25 different sites in the United States and Canada were tested as part of the LTPP program's SMP. Each of these test locations were typically tested 1 to 4 times each visit, and were visited 12 to 15 different times over the course of a year. Within Round 1, 14,672 tests were used (more than 25 tests per station) to develop 577 regression relationships between the temperature at the mid-depth of the asphalt and the backcalculated asphalt modulus.

The item of particular interest in this project is the slope of the regression equation. The 25 sites in Round 1 produced an array of 577 slopes, which can be characterized by a mean and a standard deviation. The mean slope – one for mid-lane and one for the wheelpath – was recommended for use in adjusting the backcalculated modulus for the effects of temperature. The distribution of the slopes is shown in figure 23.

At the end of the project, Round 2 SMP data were available and it was decided to use Round 2 data to verify the results obtained from Round 1. Round 2 consisted of 321 specific test points on 15 different sites in the United States. Round 2 sites differed from Round 1 sites in that they tended to be newer; were generally located farther south; and there were no Round 2 sites with less than 100 mm of asphalt, whereas there were three sites in Round 1 with less than 100 mm of asphalt. The same analysis was repeated with Round 2 data, resulting in an array of regression slopes. The distribution of the Round 2 slopes are also shown in figure 23.

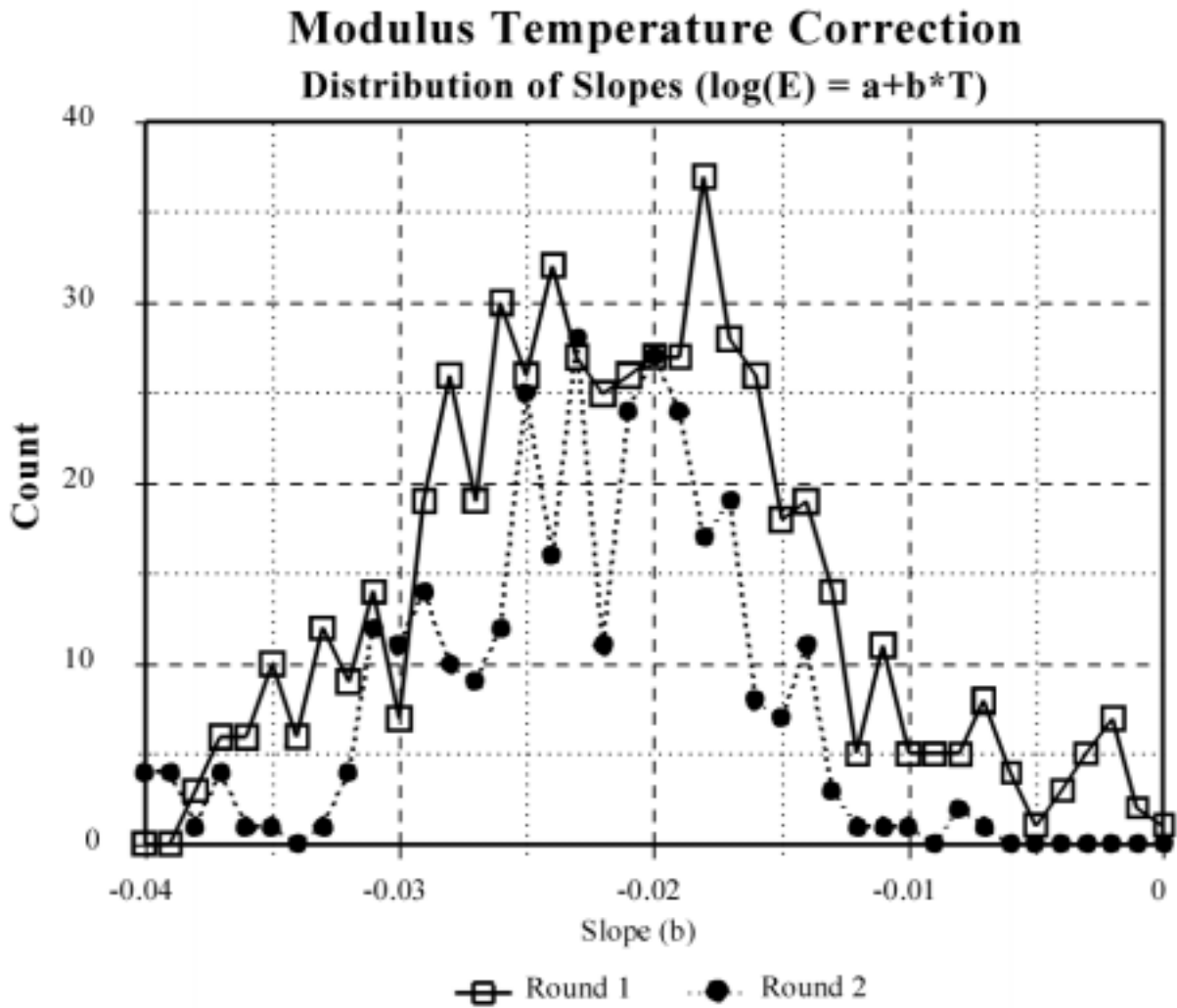


**Figure 23. Distribution of temperature versus modulus regression slopes.**

The appearance of the two distribution plots indicates that they appear to be of the same population. Statistical tests, however, show that the difference between the two populations is significant. The standard error of difference between the mean values of the two averages is 0.000541 and the difference between the mean value of the two averages is 0.00283, which is 5.23 times the standard error of the differences, indicating that the two data sets are different with nearly 100-percent certainty.

|                           | <u>Round 1</u> | <u>Round 2</u> |
|---------------------------|----------------|----------------|
| <b>Mean Slope</b>         | -0.0206        | -0.0234        |
| <b>S.D. of Slope</b>      | 0.00941        | 0.00669        |
| <b>No. of Data Points</b> | 577            | 321            |

The two populations of representative slopes, however, are not significantly different. The process of selecting the most representative test location changes the results of the statistical test, primarily because of the smaller number of data points as illustrated below:

|  | <u>Round 1</u> | <u>Round 2</u> |
|--|----------------|----------------|
| <b>Mean Representative Slope</b>         | -0.02148       | -0.02349       |
| <b>S.D. of Representative Slopes</b>     | 0.007234       | 0.006356       |
| <b>No. of Representative Data Points</b> | 50             | 30             |

The standard error of difference between the mean values of the two averages is 0.00155 and the difference between the mean value of the two averages is 0.00201, which is 1.32 times the standard error of estimate of the difference in the means. The t-statistic of 1.32 is less than the 1.96 ratio required to say the populations are different with 95-percent confidence.



**Table 5. Intercepts, slopes, and R-squared regression coefficients of the median-based representative station.**

| Sect.   | Location and Elevation |        |      | AC<br>(mm) | Intercepts |       |         |       |        |       | Slopes |        |         |        |        |        | R-squared |       |         |       |        |       |
|---------|------------------------|--------|------|------------|------------|-------|---------|-------|--------|-------|--------|--------|---------|--------|--------|--------|-----------|-------|---------|-------|--------|-------|
|         | Lat.                   | Long.  | Elev |            | ELMOD4     |       | MODULUS |       | WESDEF |       | ELMOD4 |        | MODULUS |        | WESDEF |        | ELMOD4    |       | MODULUS |       | WESDEF |       |
|         |                        |        |      |            | F1         | F3    | F1      | F3    | F1     | F3    | F1     | F3     | F1      | F3     | F1     | F3     | F1        | F3    | F1      | F3    | F1     | F3    |
| 08SA    | 38.70                  | 108.03 | 2428 | 117        | 3.907      | 3.758 | 4.173   | 3.990 | 4.245  | 4.110 | -0.020 | -0.017 | -0.024  | -0.018 | -0.022 | -0.018 | 0.765     | 0.736 | 0.867   | 0.815 | 0.751  | 0.799 |
| 09SA    | 41.40                  | 72.03  | 78   | 189        | 4.108      | 4.065 | 4.197   | 4.129 | 4.231  | 4.199 | -0.017 | -0.018 | -0.020  | -0.020 | -0.020 | -0.019 | 0.764     | 0.856 | 0.778   | 0.851 | 0.818  | 0.828 |
| 16SB    | 43.68                  | 112.12 | 2256 | 277        | 4.486      | 4.493 | 4.318   | 4.346 | 4.329  | 4.391 | -0.027 | -0.027 | -0.023  | -0.024 | -0.027 | -0.031 | 0.848     | 0.860 | 0.886   | 0.920 | 0.888  | 0.938 |
| 23SA    | 44.57                  | 70.29  | 230  | 147        | 4.138      | 4.189 | 5.241   | 4.307 | 4.157  | 4.267 | -0.025 | -0.025 | -0.042  | -0.028 | -0.026 | -0.029 | 0.795     | 0.952 | 0.779   | 0.929 | 0.924  | 0.949 |
| 25SA    | 42.14                  | 72.61  | 42   | 193        | 4.046      | 3.972 | 4.072   | 4.176 | 4.118  | 4.236 | -0.028 | -0.018 | -0.026  | -0.026 | -0.029 | -0.027 | 0.867     | 0.839 | 0.870   | 0.901 | 0.849  | 0.935 |
| 27SA    | 46.02                  | 94.45  | 340  | 112        | 3.515      | 3.467 | 3.679   | 3.819 | 3.993  | 3.989 | -0.008 | -0.001 | -0.015  | -0.012 | -0.018 | -0.013 | 0.130     | 0.001 | 0.525   | 0.282 | 0.777  | 0.514 |
| 27SB    | 46.50                  | 95.57  | 417  | 244        | 4.100      | 4.068 | 4.318   | 4.286 | 4.209  | 4.238 | -0.013 | -0.013 | -0.015  | -0.016 | -0.014 | -0.016 | 0.968     | 0.920 | 0.972   | 0.975 | 0.941  | 0.944 |
| 27SC    | 47.42                  | 94.90  | 430  | 180        | 3.808      | 3.864 | 4.117   | 4.105 | 4.058  | 4.064 | -0.012 | -0.011 | -0.022  | -0.016 | -0.022 | -0.016 | 0.130     | 0.251 | 0.921   | 0.688 | 0.861  | 0.794 |
| 30SA    | 46.31                  | 109.13 | 2098 | 76         | 4.131      | 4.200 | 4.204   | 4.310 | 4.103  | 4.362 | -0.021 | -0.017 | -0.021  | -0.018 | -0.020 | -0.024 | 0.696     | 0.579 | 0.732   | 0.607 | 0.858  | 0.981 |
| 33SA    | 43.23                  | 71.47  | 119  | 212        | 4.120      | 4.064 | 4.198   | 4.153 | 4.193  | 4.115 | -0.019 | -0.018 | -0.019  | -0.017 | -0.020 | -0.016 | 0.915     | 0.856 | 0.928   | 0.932 | 0.935  | 0.928 |
| 35SA    | 32.64                  | 103.53 | 1776 | 160        | 4.351      | 4.234 | 4.474   | 4.378 | 4.403  | 4.397 | -0.023 | -0.021 | -0.028  | -0.026 | -0.029 | -0.026 | 0.986     | 0.765 | 0.950   | 0.823 | 0.964  | 0.933 |
| 40SA    | 36.38                  | 98.23  | 623  | 194        | 5.236      | 5.332 | 4.400   | 4.095 | 4.692  | 4.629 | -0.015 | -0.022 | -0.011  | -0.003 | -0.026 | -0.028 | 0.774     | 0.766 | 0.079   | 0.004 | 0.948  | 0.918 |
| 46SA    | 45.95                  | 100.29 | 520  | 178        | 4.164      | 4.200 | 4.347   | 4.382 | 4.243  | 4.219 | -0.034 | -0.035 | -0.038  | -0.039 | -0.035 | -0.037 | 0.974     | 0.966 | 0.973   | 0.971 | 0.962  | 0.962 |
| 46SB    | 44.92                  | 102.00 | 760  | 140        | 3.789      | 3.814 | 3.916   | 3.967 | 4.008  | 4.005 | -0.023 | -0.022 | -0.023  | -0.027 | -0.021 | -0.023 | 0.880     | 0.943 | 0.884   | 0.767 | 0.959  | 0.872 |
| 48SA    | 34.53                  | 100.43 | 867  | 147        | 4.021      | 3.921 | 4.122   | 4.043 | 4.131  | 4.030 | -0.022 | -0.017 | -0.025  | -0.020 | -0.027 | -0.021 | 0.931     | 0.956 | 0.940   | 0.967 | 0.947  | 0.962 |
| 48SB    | 33.51                  | 95.59  | 210  | 254        | 4.102      | 4.015 | 4.244   | 4.096 | 4.190  | 4.156 | -0.024 | -0.022 | -0.027  | -0.023 | -0.026 | -0.023 | 0.965     | 0.969 | 0.983   | 0.966 | 0.972  | 0.968 |
| 48SE    | 29.23                  | 98.25  | 216  | 81         | 4.146      | 4.113 | 4.187   | 4.271 | 4.395  | 4.332 | -0.024 | -0.024 | -0.024  | -0.028 | -0.029 | -0.028 | 0.912     | 0.893 | 0.894   | 0.928 | 0.872  | 0.891 |
| 48SF    | 28.50                  | 97.05  | 37   | 191        | 4.314      | 4.295 | 4.625   | 4.503 | 4.651  | 4.494 | -0.018 | -0.018 | -0.023  | -0.023 | -0.024 | -0.022 | 0.955     | 0.957 | 0.985   | 0.916 | 0.943  | 0.904 |
| 48SC    | 26.98                  | 97.80  | 17   | 46         | 4.287      | 4.155 | 4.469   | 4.328 | 4.593  | 4.427 | -0.003 | -0.001 | -0.003  | -0.001 | -0.004 | -0.002 | 0.170     | 0.041 | 0.463   | 0.065 | 0.356  | 0.086 |
| 49SB    | 37.28                  | 109.58 | 2071 | 140        | 4.361      | 4.252 | 4.313   | 4.323 | 4.155  | 4.138 | -0.022 | -0.022 | -0.018  | -0.020 | -0.019 | -0.020 | 0.937     | 0.943 | 0.924   | 0.867 | 0.802  | 0.957 |
| 50SA    | 44.12                  | 73.18  | 134  | 211        | 4.058      | 4.159 | 4.190   | 4.346 | 4.128  | 4.238 | -0.033 | -0.031 | -0.033  | -0.035 | -0.032 | -0.033 | 0.953     | 0.911 | 0.973   | 0.902 | 0.975  | 0.917 |
| 56SA    | 44.50                  | 108.92 | 2459 | 76         | 3.953      | 3.351 | 3.866   | 3.438 | 4.157  | 3.878 | -0.019 | -0.015 | -0.016  | -0.013 | -0.014 | -0.017 | 0.478     | 0.501 | 0.711   | 0.804 | 0.640  | 0.948 |
| 83SA    | 49.80                  | 100.67 | 460  | 114        | 3.690      | 3.722 | 3.877   | 3.953 | 4.062  | 4.099 | -0.010 | -0.008 | -0.017  | -0.015 | -0.018 | -0.016 | 0.155     | 0.204 | 0.893   | 0.815 | 0.787  | 0.641 |
| 87SA    | 45.11                  | 79.31  | 467  | 135        | 3.871      | 3.860 | 4.053   | 4.099 | 4.107  | 4.075 | -0.012 | -0.015 | -0.011  | -0.018 | -0.017 | -0.018 | 0.517     | 0.760 | 0.341   | 0.774 | 0.653  | 0.801 |
| 90SA    | 51.89                  | 105.45 | 800  | 71         | 4.040      | 3.856 | 4.038   | 3.824 | 4.168  | 3.964 | -0.008 | -0.006 | -0.015  | -0.009 | -0.011 | -0.009 | 0.345     | 0.269 | 0.753   | 0.619 | 0.664  | 0.681 |
| AVERAGE |                        |        |      |            | 4.110      | 4.057 | 4.226   | 4.147 | 4.229  | 4.202 | -0.019 | -0.018 | -0.022  | -0.020 | -0.022 | -0.021 | 0.712     | 0.682 | 0.800   | 0.763 | 0.842  | 0.842 |



## CHAPTER 6. TEMPERATURE ADJUSTMENT FOR BASIN SHAPE FACTORS

### BASIN SHAPE FACTOR DEFINITIONS

The stiffness, or modulus, of asphalt concrete (AC) is very sensitive to changes in the temperature of the asphalt. The stiffness of the asphalt, in turn, affects the shape of the deflection basin. If basin shape factors are to be used in the structural analysis of flexible pavements, they need to be adjusted for temperature.

Deflection basin shape factors that are temperature-dependent that are evaluated in this study include:

- AREA.
- F-1 factor.
- Deflection deltas (deflection under load plate minus deflection some distance from the load plate), including Surface Curvature Index.
- Deflection ratios (deflection under load plate divided by the deflection some distance from the load plate).

### AREA Shape Factor

The AREA basin factor is a calculation of the normalized (or non-dimensional) area of a deflection basin. The AREA factor is proportional to the ratio of the pavement stiffness to the subgrade stiffness. In this case, the pavement stiffness is a function of both thickness and material strength. The AREA factor was developed by Professor Marshall Thompson at the University of Illinois at Champaign. The formula to calculate the AREA factor is:

$$AREA = 6 \left( \frac{defl0}{defl0} + \frac{2defl12}{defl0} + \frac{2defl24}{defl0} + \frac{defl36}{defl0} \right) \quad (7)$$

where the terms are as defined on page vi in the front of this report.

As shown in equation 7, the deflections from sensors defl12, defl24, and defl36 are normalized by dividing the deflection by defl0. The AREA is the sum of the *normalized* areas between each of these sensors.

### F-1 Shape Factor

The F-1 basin factor is a calculation of a normalized (or non-dimensional) representation of the amount of curvature in the deflection basin and is inversely proportional to the ratio of the pavement stiffness to the subgrade stiffness. In this case, the pavement stiffness is a function of both thickness and material strength. The F-1 factor was developed by Professor Thompson at the University of Illinois. The formula for calculating the F-1 factor is:

$$F-1 = \frac{defl0 - defl24}{defl12} \quad (8)$$

As shown in equation 8, the F-1 factor is normalized by dividing the difference in the defl0 and defl24 deflections by defl12.

## **Deflection Basin Delta Shape Factors**

Delta deflection is the difference between the deflection measured under the load plate and the deflection at some offset distance. For the purpose of this report, the names assigned for the various offsets are:

delta8: defl0 - defl8  
delta12: defl0 - defl12  
delta18: defl0 - defl18  
delta24: defl0 - defl24  
delta36: defl0 - defl36  
delta60: defl0 - defl60

The delta# terms will be used as nouns.

A common example of this type of basin shape factor is the Surface Curvature Index (SCI), which is similar to delta12 (the difference between the center sensor and the deflection at 305 mm). This basin characteristic for asphalt pavements is very dependent on the temperature of the asphalt.

Delta deflection is influenced by a variety of factors. Some of the factors are:

- Temperature of the asphalt.
- Thickness of the asphalt.
- Overall stiffness and thickness of the pavement section.
- Stiffness of the subgrade.
- Depth to the apparent stiff layer (i.e., bedrock).
- Offset distance.

## **Deflection Basin Ratio Factors**

The ratio of the deflection at the center of the load plate to the deflection at some offset distance is not commonly used in deflection analysis. The ratios, however, are basin shape characteristics that are affected by the same conditions that affect the delta basin factors as described above.

## **TEMPERATURE RELATIONSHIPS**

### **Analysis Discussion**

One of the primary goals in this study was to develop relationships between the various deflection characteristics of asphalt pavements and the temperature of the asphalt. Compared to any previous study, the SMP provides a remarkably large and diverse database. Data were collected from 40 sites across the United States and Canada – 25 from Round 1 and 15 from Round 2. At each of these sites, tests were taken at nominal 7.62-m intervals. Special care was taken to ensure that the FWD was placed on exactly the same spot (~25 mm) every time the location was tested. This resulted in data that were very consistent for any particular test location. Natural spatial variation in the pavement structure, however, resulted in different deflection behavior from station to station. Since the purpose of the study was to evaluate the temperature response, the approach taken was to minimize the spatial effects. To minimize spatial effects, a method was devised to select one representative test location for each pass (wheelpath and mid-lane) for each site. The selection of a single representative test location from each lane of each site minimizes the spatial scatter within the data.

The representative stations were selected through a multi-step process. The first step was to conduct eight regressions, one for the AREA factor, one for the F-1 factor, and six for the delta8 through delta60 factors. This resulted in 8 regressions for each of the 22 test locations or 176 regressions per site. Simple two-variable models were used for these initial regressions. The basin shape factor, or a log transform of the basin shape factor, was the dependent variable, and the temperature at the mid-depth position in the asphalt was the independent variable. These models were found to provide the best fit overall for individual test locations. This resulted in an intercept and slope for the eight basin shape factors at each test location. The regression coefficients were tabulated, one for each basin characteristic evaluated. The intercept and slope values for each site pass were ranked for each basin characteristic. The intercepts and slopes were highly correlated and the rankings were done so that the rankings would go in the same order for both the intercept and the slope. That is, if the intercept and slope values were inversely correlated and the intercept was ranked in ascending order, the slope was ranked in descending order. The rankings were summed and the median rank sum value was selected. The next step was to sum the square of the deviation of the individual rankings from the median value for each basin shape factor. For each pass, the station with the lowest summed square deviation was selected as the representative station. In case of a tie, the best correlation (R-squared) was used as a tie breaker. The results for each of the basin characteristics were brought together in one table. The location that was representative for the majority of the basin characteristics was the location selected to be in the analysis data set (one for mid-lane and one for the wheelpath). In most cases, it was noted that the same test location was the representative basin for each basin characteristic.

Once all of the representative test locations were identified, all of the data from those locations were assembled into a single file. This was the data set used to develop the temperature response models for each of the basin shape factors.

A less rigorous version of this process was used for the original analysis of the Round 1 data and resulted in a different set of representative stations for each basin characteristic. This process was used for Round 2 data to ensure greater consistency between models. The process was then applied to all of the Round 1 data, resulting in a different data set from Round 1 than was used for the original.

Once the process was completed, it resulted in a data set consisting of 2,254 records. The fields for each record consisted of the round, lane pass, station, normalized 40.5-kN load deflections for all seven sensors, backcalculated asphalt modulus, asphalt thickness, mid-depth temperature, date and time of test, and latitude of the site.

The resulting data set was split in two – one for model development and the other for validation. A modeling data set and a validation data set were used to prevent overfitting of the regression model to the data.

### **Development of the Regression Models**

The deflection tests from the representative stations provided 2,254 records for the development of the models. This data set was divided into two equal-sized subsets on an odd/even record number basis, resulting in 1,127 records in each data set. The first data set was used to develop the regression models and the second data set was used to check the models. During the analysis, the regression residuals were checked against the independent variables. The regression checks revealed that the data from the wheelpath on Site 56SA were showing unique behavior; the deflections near the load plate were much higher than for similar sections and much higher than in the mid-lane. It was concluded that the high deflections were a symptom of degradation of the asphalt layer, possibly from fatigue, stripping, or both. The wheelpath data were subsequently removed from both the model data set and the validation data set.

This left 2,237 total records, of which 1,118 records were used for the regression analysis work.

The resulting data records consisted of 17 fields. The fields are described in table 6. The data set only included the backcalculated modulus and deflections. The deflection basin shape factors were calculated from the deflections and were not included as individual fields.

**Table 6. Regression and validation data set.**

| <b>GENERAL SITE VARIABLES</b>  |  |
|--|--|
| <b>Round</b>   | First or second round of the SMP testing (1 or 2)                        |
| <b>Site</b>  | SMP Site ID  |
| <b>Lat.</b>  | Latitude of the site (degrees)   |
| <b>Lane</b>  | F1 for mid-lane and F3 for wheelpath                                     |
| <b>Station</b>   | Station where the test was taken   |
| <b>Date</b>  | Date of test in spreadsheet code values                                  |
| <b>AC</b>  | Thickness of the asphalt layer (mm)                                      |
| <b>d.day</b>   | Time of test in decimal day form   |
| <b>Deflections in <math>\mu\text{m}</math>, normalized to a 40.5-kN plate load</b> |  |
| <b>defl0</b>   | Deflection at the center of the load plate                               |
| <b>defl8</b>   | Deflection at 203 mm from the center of the load plate                   |
| <b>defl12</b>  | Deflection at 305 mm from the center of the load plate                   |
| <b>defl18</b>  | Deflection at 457 mm from the center of the load plate                   |
| <b>defl24</b>  | Deflection at 610 mm from the center of the load plate                   |
| <b>defl36</b>  | Deflection at 914 mm from the center of the load plate                   |
| <b>defl60</b>  | Deflection at 152 mm from the center of the load plate                   |
| <b>Variables corresponding to individual tests</b>                                 |  |
| <b>E-1</b>   | Backcalculated modulus of the asphalt layer (MPa) (not used in models)   |
| <b>T</b>   | Temperature at the mid-depth of the asphalt layer ( $^{\circ}\text{C}$ ) |

The basic form of the models was examined during the analysis of the Round 1 data. These were all basic two-variable models. The base 10 logarithmic transformation of the deflection basin shape characteristic was the dependent variable (in all cases except for the AREA basin shape factor), and the asphalt temperature at mid-depth was the independent variable. The general form was as follows:

$$\text{Basin Shape Factor} = \text{Intercept} + \text{Slope} * \text{Temperature}$$

Analysis indicated that the intercept and slope values correlated to other site variables. It was found that the base 10 logarithmic transformation of the thickness of the asphalt, the latitude of the site, the defl36 deflection, and their interactions were significant factors for the intercept and the slope. The asphalt thickness was expected to be significant in all of these relationships since the factors were sensitive to the thickness of the asphalt. The sensitivity to defl36 was because all basin shape factors were related (directly or inversely) to the ratio of the stiffness of the pavement structure to the stiffness of the underlying subgrade. In this case, the base 10 log of defl36 was selected to be a simple indicator of the stiffness of the subgrade because it was slightly more sensitive to the relationships than the other offset sensors. The expected reason the latitude was a significant factor was the practice of using softer asphalt binders in cold climates (the higher latitudes) and harder asphalt binders in warm climates (lower latitudes). Binder stiffness was not available for the SMP sections, so the base 10 log of the latitude was a rough substitute for binder stiffness. The use of binder stiffness, or asphalt grading, as a variable would make the models much more universal and the models should be revisited once binder information

becomes available for these sections, or for a similar data set.

A basic set of independent variables was developed for each regression model. The set included the log transforms of each of the variables described above and their interactions for the intercept. The same set was also combined with the mid-depth temperature for the slope variables. The variables are listed below:

Intercept Variables:

log(ac)  
log(lat)  
log(defl36)  
log(ac)\*log(lat)  
log(ac)\*log(defl36)  
log(lat)\*log(defl36)

Slope Variables:

T  
T\*log(ac)  
T\*log(lat)  
T\*log(defl36)  
T\*log(ac)\*log(lat)  
T\*log(ac)\*log(defl36)  
T\*log(lat)\*log(defl36)

For each of the basin shape factors, a correlation coefficient was calculated between the dependent variable and each of the above independent variables. The variables from the intercept list and the slope list that had the highest correlation coefficients were used for the initial regression, followed by the calculation of the residuals. A new set of correlation coefficients were calculated between the residuals and the remaining independent variables. The variable with the highest correlation was added to the first two selected variables and the process was repeated. At each regression step, the significance of the independent variables was checked, and if the variable ceased to be significant, it was dropped.

Once the relevant independent variables were selected, the model was checked to see if it provided reasonable results at the extremes of the independent variables. During the course of the analysis, it was noted that some models would experience a slope sign change for thin asphalt, soft subgrade (high defl36), and low latitudes. The models would, in these cases, indicate that the asphalt would get stiffer as the temperature increased. When this behavior was noted, the slope variables would be re-evaluated and the least significant variable, or the slope variable that produced the sign change, was dropped. The behavior was then re-evaluated and, if necessary, the process was repeated. In some cases, the final set of models so derived have a slightly lower R-squared than the best-fitting models, but provide reasonable results over the full range of variables.

### **Basin Shape Models**

The following are the regression equations for all of the basin shape factors:

$$\begin{aligned} \text{AREA} = & 13.0 + 7.77 \log(\text{ac}) \log(\text{defl36}) - 6.78 \log(\theta) \log(\text{defl36}) \\ & + 0.105 T - 0.116 T \log(\text{ac}) \end{aligned} \quad (9)$$

$$\log(F-1) = 0.326 - 0.382 \log(ac) \log(defl36) + 0.327 \log(\theta) \log(defl36) - 0.00447 T + 0.00555 T \log(ac) \quad (10)$$

$$\log(\delta_8) = 3.02 - 1.49 \log(ac) + 0.541 \log(\theta) + 0.394 \log(defl36) - 0.0230 T + 0.0111 T \log(ac) \log(\theta) \quad (11)$$

$$\log(\delta_{12}) = 3.45 - 1.59 \log(ac) + 0.489 \log(\theta) + 0.449 \log(defl36) - 0.0275 T + 0.012 T \log(ac) \log(\theta) \quad (12)$$

$$\log(\delta_{18}) = 4.18 - 1.52 \log(ac) + 0.317 \log(\theta) \log(defl36) - 0.0265 T + 0.0112 T \log(ac) \log(\theta) \quad (13)$$

$$\log(\delta_{24}) = 3.30 - 1.32 \log(ac) + 0.514 \log(\theta) \log(defl36) - 0.00622 T \log(\theta) \log(defl36) + 0.00838 T \log(ac) \log(\theta) \quad (14)$$

$$\log(\delta_{36}) = 3.05 - 1.13 \log(ac) + 0.502 \log(\theta) \log(defl36) - 0.00487 T \log(\theta) \log(defl36) + 0.00677 T \log(ac) \log(\theta) \quad (15)$$

$$\log(\delta_{60}) = 2.67 - 0.770 \log(ac) + 0.650 \log(\delta_{36}) + 0.00290 T \log(ac) \quad (16)$$

$$\log(\text{ratio}_8) = 0.183 + 0.0118 \log(ac) \log(defl36) + 0.00980 T + 0.0696 \log(\theta) - 0.133 \log(ac) - 0.00416 T \log(defl36) \quad (17)$$

$$\log(\text{ratio}_{12}) = 0.200 - 0.117 \log(ac) \log(defl36) + 0.126 \log(\theta) \log(defl36) + 0.00861 T - 0.00183 T \log(\theta) \log(defl36) \quad (18)$$

$$\log(\text{ratio}_{18}) = 0.952 - 0.450 \log(ac) - 0.169 \log(defl36) + 0.327 \log(\theta) + 0.00212 T \log(ac) \quad (19)$$

$$\log(\text{ratio}_{24}) = 1.16 - 0.587 \log(ac) - 0.210 \log(defl36) + 0.481 \log(\theta) + 0.00257 T \log(ac) \quad (20)$$

$$\log(\text{ratio}_{36}) = -0.0912 - 0.367 \log(ac) \log(defl36) + 0.489 \log(defl36) + 0.691 \log(\theta) + 0.00298 T \log(ac) \quad (21)$$

$$\log(\text{ratio}_{60}) = 0.0726 - 0.336 \log(ac) \log(defl36) + 0.334 \log(defl36) + 0.872 \log(\theta) + 0.00246 T \log(ac) \quad (22)$$

where:

- ac = Total thickness of the HMA, mm
- $\theta$  = Latitude of the pavement section
- defl36 = Deflection (normalized to 40.5 kN) at 915 mm from the center of the load plate,  $\mu\text{m}$
- T = Temperature at the mid-depth of the HMA,  $^{\circ}\text{C}$

The regression R-squared and standard error of estimate values for the above equations are in table 7.



**Table 7. Regression and validation statistics.**

| Model Name     | Reg. Statistics |       | Validation Statistics |         |        |
|----------------|-----------------|-------|-----------------------|---------|--------|
|                | R <sup>2</sup>  | SEE   | F-test                | t-stat  | T-dist |
| <b>AREA</b>    | 0.8109          | 1.508 | 0.00026               | 0.0660  | 94.74% |
| <b>logF1</b>   | 0.8127          | 0.075 | 0.00025               | -0.0923 | 92.64% |
| <b>delta8</b>  | 0.7591          | 0.150 | 0.00000               | -0.1931 | 84.69% |
| <b>delta12</b> | 0.7716          | 0.146 | 0.00000               | -0.0895 | 92.87% |
| <b>delta18</b> | 0.7600          | 0.143 | 0.00000               | -0.0523 | 95.83% |
| <b>delta24</b> | 0.7439          | 0.141 | 0.00000               | -0.0921 | 92.66% |
| <b>delta36</b> | 0.7198          | 0.135 | 0.00000               | -0.0490 | 96.09% |
| <b>delta60</b> | 0.6356          | 0.138 | 0.00000               | -0.0245 | 98.04% |
| <b>ratio8</b>  | 0.6841          | 0.026 | 0.00000               | -0.1684 | 86.63% |
| <b>ratio12</b> | 0.7824          | 0.034 | 0.00003               | -0.0005 | 99.96% |
| <b>ratio18</b> | 0.8181          | 0.047 | 0.00042               | 0.0449  | 96.42% |
| <b>ratio24</b> | 0.7980          | 0.064 | 0.00009               | -0.0427 | 96.59% |
| <b>ratio36</b> | 0.7209          | 0.096 | 0.00000               | 0.0166  | 98.68% |
| <b>ratio60</b> | 0.5513          | 0.136 | 0.00000               | 0.1926  | 84.73% |

## MODEL VALIDATION

Each of the models were checked against the validation data set. The results of the validation checks are contained in the right three columns of table 7. These checks were made by comparing the dependent variable from the validation set value to the predicted dependent values calculated by the regression models. The F-test gives the probability that the variation of the validation set dependent variables are different from the predicted values. In all cases, the variations of the two data sets can be considered the same. The t-statistic calculation is used to compare the mean of the dependent variable in the validation set to values predicted by the models when applied to the validation data. The standard error of the difference in the means was calculated. The ratio of the difference in the means and the standard error of estimate of the difference between the means is the t-statistic. In order to reject the regression equation at the 95-percent confidence level, the t-statistic must be larger than 1.96, or the t-distribution value in the right column would have to be less than 5 percent. The validation results indicate that, for each of the equations, the predicted values are considered to be of the same population as the measured values.

As an independent check on the model with the largest t-statistic (delta8), a regression was run with the same model form. The resulting intercept and x coefficients were checked to see if they stayed within the upper and lower 95th percentile bounds of the regression. The coefficients were comfortably within the limits.

## Comparison of Round 1 and Round 2 Data

Models were developed for all deflection basin shape factors from Round 1 data only. At the time that the work was completed, Round 2 testing was completed and the data were available. It was decided to use the data from Round 2 to validate the models. As discussed earlier, the backcalculated asphalt moduli

were found to be significantly different for the Round 1 and Round 2 data sets. The validation check found that three of the models – ratio24, ratio36, and ratio60 – were found to be different at the 95-percent confidence level. The delta18, delta24, delta36, and delta60 models were found to be different at the 90-percent level, but not at the 95-percent level.

Because significant differences between the two data sets were found and the analysis indicated that the differences were due to the site characteristics rather than the models themselves, the two data sets were combined and new models were developed.

**Table 8. Illustration of Round 1 and Round 2 differences using AREA regression statistics.**

| <i>Regression Statistics AREA Factor for Round 1 Data</i> |                     |                       |                    |                |                              |              |
|---|---------------------|-----------------------|--------------------|----------------|------------------------------|--------------|
| Multiple R  | 0.92781             |                       |                    |                |                              |              |
| R-Squared   | 0.86083             |                       |                    |                |                              |              |
| Adjusted R-Squared  | 0.86042             |                       |                    |                |                              |              |
| Standard Error  | 1.30502             |                       |                    |                |                              |              |
| Observations  | 1395                |                       |                    |                |                              |              |
| <i>Analysis of Variance</i>                               | <i>df</i>           | <i>Sum of Squares</i> | <i>Mean Square</i> | <i>F</i>       | <i>Significance F</i>        |              |
| Regression  | 4                   | 14642.07777           | 3660.51944         | 2149.35726     | 0                            |              |
| Residual  | 1390                | 2367.27608            | 1.70308            |                |                              |              |
| Total   | 1394                | 17009.35385           |                    |                |                              |              |
|   | <i>Coefficients</i> | <i>Standard Error</i> | <i>t-Statistic</i> | <i>p-Value</i> | <i>95% Confidence Limits</i> |              |
|   |                     |                       |                    |                | <i>Lower</i>                 | <i>Upper</i> |
| Intercept   | 12.18402            | 0.38799               | 31.40261           | 0.00000        | 11.42291                     | 12.94514     |
| log(ac)*log(defl36)                                       | 9.09498             | 0.15488               | 58.72337           | 0.00000        | 8.79116                      | 9.39880      |
| log(θ)*log(defl36)  | -8.20765            | 0.19325               | -42.47178          | 0.00000        | -8.58674                     | -7.82856     |
| T   | 0.16584             | 0.02168               | 7.64819            | 0.00000        | 0.12331                      | 0.20838      |
| T*log(ac)   | -0.14082            | 0.01042               | -13.51548          | 0.00000        | -0.16126                     | -0.12038     |
| <i>Regression Statistics AREA Factor for Round 2 Data</i> |                     |                       |                    |                |                              |              |
| Multiple R  | 0.91917             |                       |                    |                |                              |              |
| R-Squared   | 0.84487             |                       |                    |                |                              |              |
| Adjusted R-Squared  | 0.84413             |                       |                    |                |                              |              |
| Standard Error  | 1.36466             |                       |                    |                |                              |              |
| Observations  | 842                 |                       |                    |                |                              |              |
| <i>Analysis of Variance</i>                               | <i>df</i>           | <i>Sum of Squares</i> | <i>Mean Square</i> | <i>F</i>       | <i>Significance F</i>        |              |
| Regression  | 4                   | 8489.47470            | 2122.36867         | 1139.64779     | 0                            |              |
| Residual  | 837                 | 1558.74701            | 1.86230            |                |                              |              |
| Total   | 841                 | 10048.22170           |                    |                |                              |              |
|   | <i>Coefficients</i> | <i>Standard Error</i> | <i>t-Statistic</i> | <i>p-Value</i> | <i>95% Confidence Limits</i> |              |
|   |                     |                       |                    |                | <i>Lower</i>                 | <i>Upper</i> |
| Intercept   | 16.06119            | 0.50422               | 31.85345           | 0.00000        | 15.07150                     | 17.05087     |
| log(ac)*log(defl36)                                       | 7.58435             | 0.29024               | 26.13088           | 0.00000        | 7.01466                      | 8.15405      |
| log(θ)*log(defl36)  | -7.65894            | 0.42211               | -18.14434          | 0.00000        | -8.48746                     | -6.83042     |
| T   | 0.06455             | 0.05616               | 1.14930            | 0.25076        | -0.04569                     | 0.17478      |
| T*log(ac)   | -0.11044            | 0.02535               | -4.35630           | 0.00001        | -0.16021                     | -0.06068     |

Rather than use the original models developed with the Round 1 data, the difference between Round 1 and Round 2 will be described by separating the residuals for the AREA prediction for Rounds 1 and 2. The average residual and the sum of the residuals, by definition, are zero for the entire regression set.

Calculating the average residuals for the Round 1 and Round 2 data results in 0.47 and -0.77, respectively, for a difference of 1.24. The standard error of estimate of the difference between the averages is 0.061. Dividing 1.24 by 0.061 results in a t-statistic of 20.25, indicating that the Round 1 and Round 2 sites are significantly different.

To further illustrate the amount of difference between the two rounds, the AREA model form used in equation 9 was applied to Round 1 and Round 2 data separately. The results of the regressions are shown in table 8. The differences are most apparent by comparing the coefficients. The coefficients from the regression run on Round 1 are not within the upper and lower limits of the coefficients for the Round 2 data set.

## **TEMPERATURE ADJUSTMENTS**

Each of the models that were developed as equations 9 through 22 can be used to calculate factors for adjusting the deflection basin shape factor for temperature. The approach is much the same as described for the backcalculated asphalt modulus model: determining the value of the slope of the model and applying that slope value to the difference in temperature. For all of the models based on the logarithmic transform of the basin shape factor, the resulting value is a multiplying factor, and for AREA, it is an additive factor.

### **Temperature Adjustment for Deflection Under the Load Plate**

Many of the earlier developed deflection analysis routines are based on the center sensor deflections only (deflection under the load plate). The center sensor deflections are very sensitive to the temperature of the asphalt. This sensitivity is the reason for the extensive work done by Southgate to develop a means of estimating internal asphalt pavement temperatures.

The use of the Benkelman beam in the 1950s and 1960s led to the development of methods to adjust the deflection measured at any temperature to the deflection that would be expected to be measured at some standard temperature, such as 20°C, or 70°F and 80°F (21.1°C and 26.7°C). A typical set of temperature adjustment curves is shown in figure 5.6, Part III of the *American Association of State Highway and Transportation Officials (AASHTO) Guide for Design of Pavement Structures*.

Attempts to develop a deflection versus temperature relationship proved to be the most difficult of any of the temperature-dependent models. During the analysis of the Round 1 data, regressions were run, station by station, of the defl0 deflection and the mid-depth temperature. A quadratic model provided the best fit of the data sets. The results were good; however, we expect that there are small seasonal influences that also affect the center sensor deflection. The examination of the seasonal deflection response was outside the scope of this analysis. It may be possible that there is a correlation between temperature and the seasonal effect; therefore, an analysis based strictly on deflection and temperature may result in coefficients that include seasonal significance. Also, the sensitivity of the deflection to temperature is expected to be a function of the thickness of the asphalt. Figure 24 shows that the first- and second-order coefficients are not sensitive to the asphalt thickness. Figure 25, however, shows that the constant does relate to asphalt thickness.

This behavior shows that the development of a temperature adjustment procedure on the basis of these regression results would not have a strong relationship to the asphalt thickness.

The asphalt thickness influence on the center sensor deflection adjustment process is more evident in the delta deflection relationships. The results of the delta deflection analysis show a significant relationship between the slope and the thickness of the asphalt. Therefore, the adjustment of the deflection under the load plate using the delta deflection relationships is the recommended method. The delta24 equation can be used for sections with an asphalt thickness of 100 mm or less; the delta36 equation can be used for sections from 100 mm to 200 mm in thickness; and the delta60 equation can be used for sections greater than 200 mm thick. The adjustment process is demonstrated using the delta36 relationship.

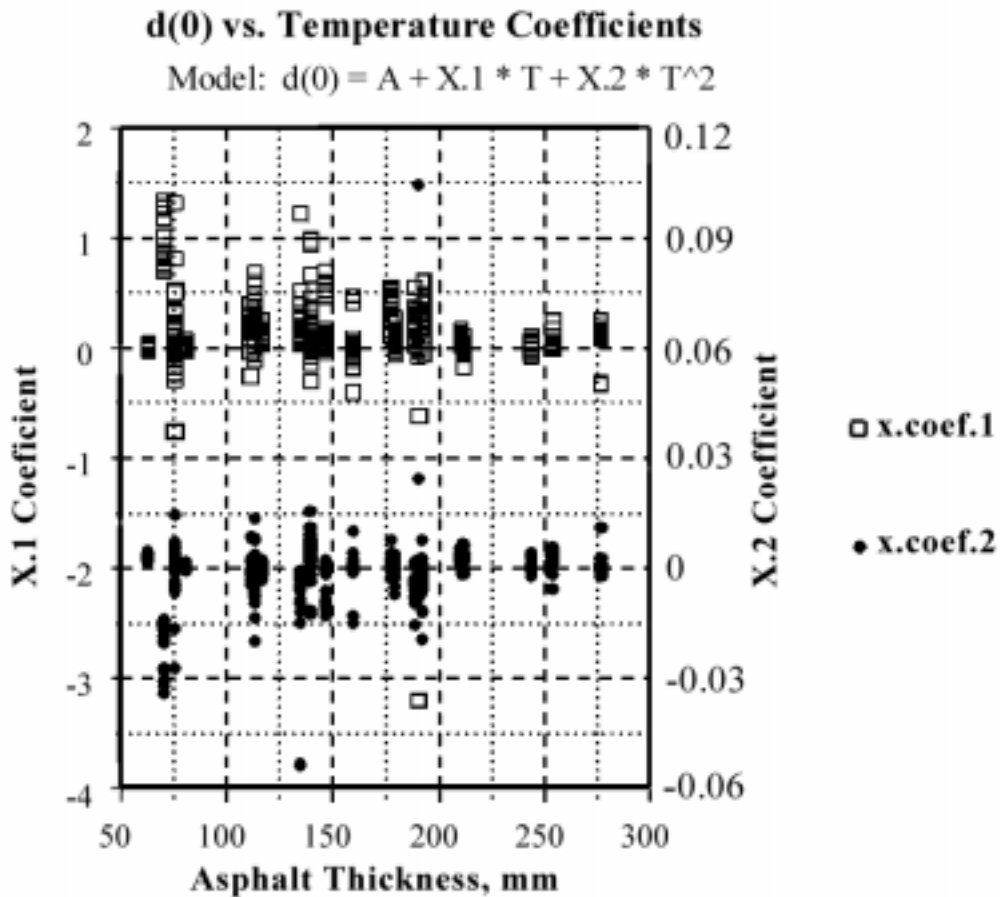
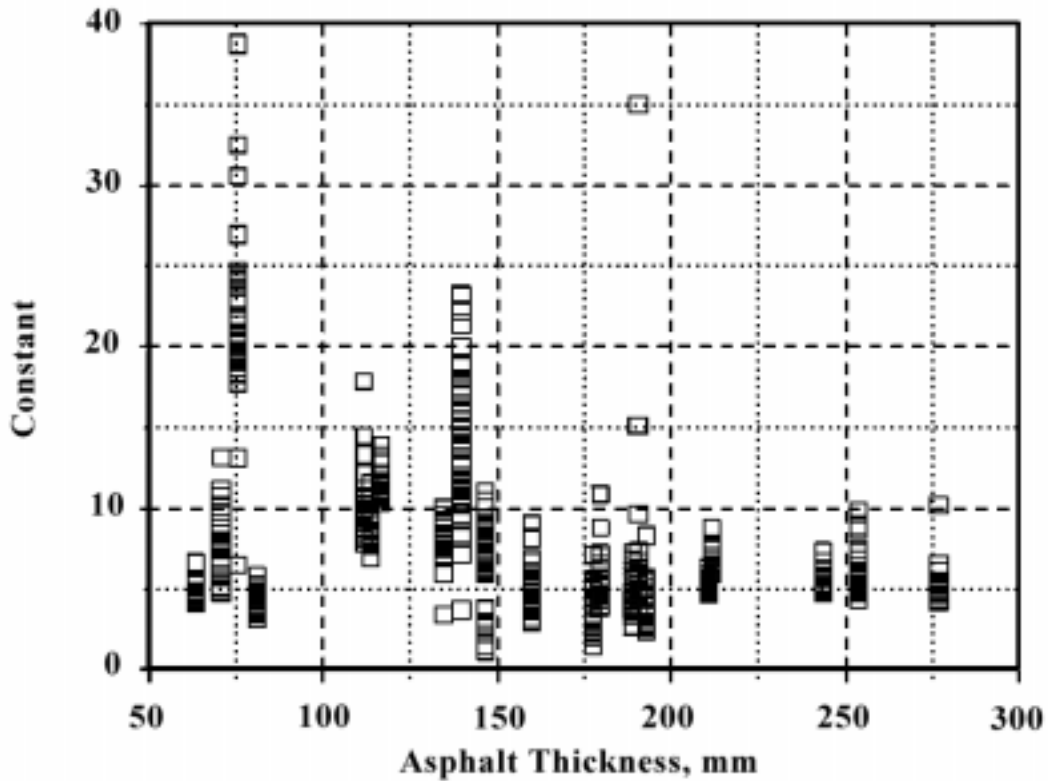


Figure 24. Temperature vesus deflection coefficients.

## d(0) vs. Temperature Coefficients

$$\text{Model: } d(0) = A + X.1 * T + X.2 * T^2$$



**Figure 25. Intercept of temperature versus deflection regressions.**

### *defl0 Temperature Adjustment Factors*

Equation 15 is used to calculate the delta36 value, which is added to the defl36 value required by the equation, resulting in a defl0 value. This calculation is done for the temperature of the asphalt at mid-depth at the time of test and for a reference temperature, such as 20°C. The deflection adjustment factor is the ratio of the two calculated deflections. Figure 27 shows the adjustment factors for several asphalt thicknesses if the deflections are to be adjusted to the deflections expected for a 20°C pavement. This method of calculating deflection adjustment factors accounts for the strength of the subgrade and for the different asphalt behaviors that have been correlated to the site latitude.

Equation 23 shows the process used to calculate the adjustment factor.

$$TAF = \frac{defl36 + \text{delta}36_{\text{Ref. Temp.}}}{defl36 + \text{delta}36_{\text{Meas. Temp.}}} \quad (23)$$

The adjustment factors shown in figure 27 are similar to the adjustment curves shown in the AASHTO Design Guide. New factors or curves can be calculated for different-strength subgrades, as indicated by defl36, or in the stiffness of the binder as implied by the latitude.

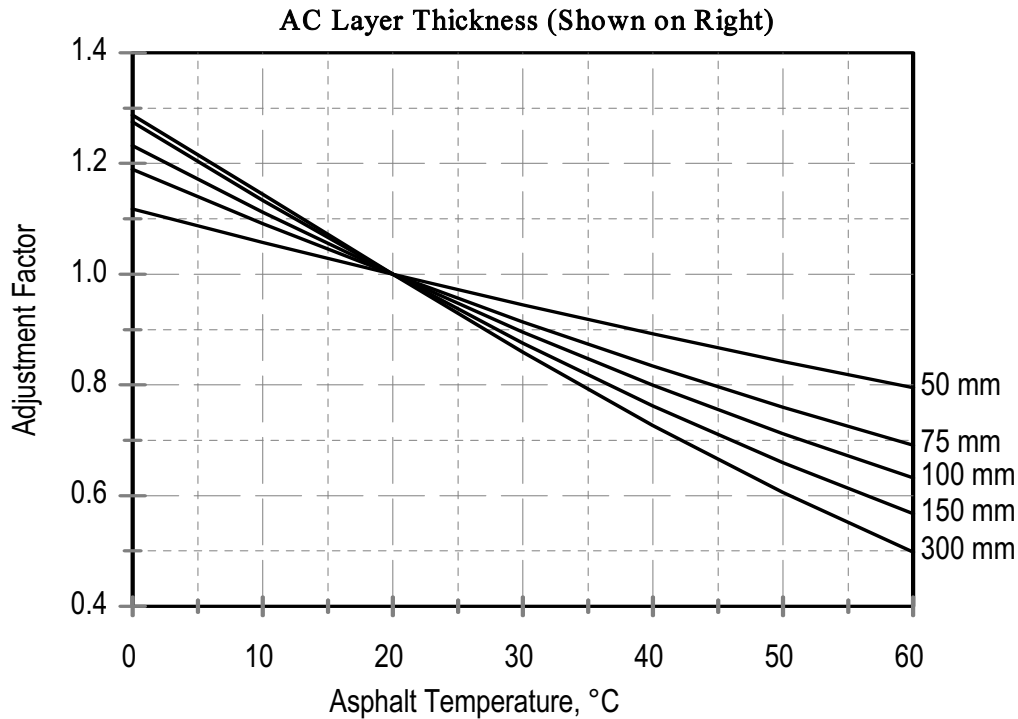


Figure 26. FWD temperature adjustment factors for defl36 = 100 μm and 40° latitude.

#### Temperature Adjustments for Basin Shape Factors

Adjustment factors for all of the deflection basin shape factors may be derived from equations 9 through 22. The defl36, latitude, and asphalt thickness values are fixed at the values for the pavement being evaluated. The equation is solved for the temperature of interest (reference temperature,  $T_{Ref}$ ) and for the temperature of the pavement at the time of test (measured temperature,  $T_{Meas}$ ). For the equations that are based on the log transform of the dependent variable, the results are converted back in order to use the variables in their natural values. The temperature adjustment factor is the ratio of the two values ( $f(T_{Ref})/f(T_{Meas})$ ).

The basin shape factor temperature adjustment factor is calculated as follows:

$$BAF = \frac{\text{Basin Factor}_{T_{Ref}}}{\text{Basin Factor}_{T_{Meas}}} \quad (24)$$

where:

BAF = Basin Adjustment Factor  
 Basin Factor<sub>T<sub>Ref</sub></sub> = Calculated at the Reference Temperature  
 Basin Factor<sub>T<sub>Meas</sub></sub> = Calculated at the Measured Temperature

If an agency selected one specific reference temperature that all deflection basin shape factors were adjusted to, a family of curves could be created using a spreadsheet. Several families should be developed to correspond to the range of subgrade stiffness typically encountered. For computer analysis, the equations can easily be programmed to calculate the adjustment factor for the specific condition.





## **CHAPTER 7. CONCLUSIONS AND RECOMMENDATIONS**

### **CONCLUSIONS**

The FHWA LTPP program's SMP has resulted in the largest and most diverse set of data relevant to pavement temperature and deflection behavior. The data demonstrated that there are very significant relationships between temperature and asphalt pavement deflection and that prediction models for these relationships could be established. Sites cover a wide geographical area, ranging from Canada to the southern United States. However, there were no sites west of the Cascades – a region that has a significantly different climate than the SMP sites at similar latitudes.

The data have demonstrated that the use of infrared surface temperature sensors, in conjunction with deflection testing, provides a very effective way of estimating the temperature within the asphalt pavement. The data set is dominated by readings from early morning to mid-afternoon, limiting the usefulness of the prediction models to normal daytime working hours. It was found that the deflection equipment shaded the pavement surface for up to 6 min before the surface temperature was measured for the LTPP testing. Routine tests conducted by agencies do not result in significant shading times. It was found that the rate of surface cooling, once the surface was shaded, was significant in those first 6 min. Shading rates were developed with limited measurements and the surface temperature data were adjusted to estimate the temperature with 30 s of shading.

Deflections and deflection basin shape factors are very dependent on asphalt temperature, thickness of the asphalt, and the strength of the underlying base and subgrade. The analysis showed that these deflection factors also correlated with the latitude of the site. There were no data available regarding the asphalt binder characteristics or mix characteristics that could be related to stiffness. It was concluded, however, that latitude was a crude predictor of asphalt stiffness based on the typical binders used in the north versus the binders used in the south.

The backcalculated moduli values on newer sections that were in good condition showed very good relationships to the temperature of the asphalt. For older and thinner pavement sections that had surface distress, the relationships were not as good. The same behavior was noted for the backcalculation process. Better results came from sections in good condition and poorer results came from sections in poor condition. Poor backcalculation results generally indicate that the pavement section is in poor structural condition, even in cases where the overall deflections are low.

### **RECOMMENDATIONS**

It is recommended that the BELLS3 model developed and presented in this report be adopted and used for routine testing and that the temperature adjustment processes described in chapter 6 be used as needed for LTPP analysis and for routine analysis.

#### **Temperature Prediction With the BELLS Models**

It is recommended that data be gathered that are more representative of routine testing and for equipment that is not covered, and for evening and nighttime. The data should be combined with the LTPP data and be used to verify or improve the BELLS models for routine testing conditions and for testing outside of the 8:00 a.m. to 4:00 p.m. time frame.

It is recommended that asphalt binder characteristics and asphalt mix characteristics be determined for each of the asphalt SMP sites. The deflection data from the SMP studies should be re-analyzed once the asphalt data are available to establish the relationship between binder and mix stiffness and pavement deflections at various temperatures. It is anticipated that this information will have strong correlations to the regression residuals in the current models and can replace the latitude variable currently used to characterize stiffness. The development of these relationships may result in significant improvements in temperature adjustment procedures and may significantly improve the precision of deflection-based diagnostic methods. If it is not possible to characterize the binder and mix characteristics on the older sections, additional sections should be considered where the characteristics can be determined. Several of the SMP sites that are at newly constructed Specific Pavement Studies (SPS) experiment sites may have binder and mix stiffness data. Additional sections should be selected to supplement the existing sections and to include the full range of binder and mix characteristics.

# APPENDIX. DRAFT STANDARDS

## Draft Standard Practice for Estimating Asphalt Temperature

### AASHTO DESIGNATION: T-### -99

#### 1. Scope

This standard is intended to provide a method for predicting the temperature within the asphalt layers of an asphalt pavement. Deflection testing commonly involves the measurement of the pavement surface temperature. This standard is based on temperature relationships developed as part of the Federal Highway Administration (FHWA) Long Term Pavement Performance (LTPP) program's Seasonal Monitoring Program (SMP).

#### 2. Referenced Documents

- 2.1 AASHTO Standards:
  - T 256-77 Pavement Deflection Measurements
  - P-###-99 Draft Standard Practice for Applying Temperature Adjustment Factors to Backcalculated Asphalt Moduli, Deflection, and Deflection Basin Characteristics
- 2.2 ASTM Standards:
  - D 4602 Guide for Nondestructive Testing of Pavements Using Cyclic-Loading Dynamic Deflection Equipment
  - D 4694 Test Method for Deflections With a Falling-Weight-Type Impulse Load Device
  - D 4695 Guide for General Pavement Deflection Measurements
- 2.3 Strategic Highway Research Program:
  - Manual for FWD Testing in the Long Term Pavement Performance Study, Operational Field Guidelines, Version 2.0, February 1993*
- 2.4 Federal Highway Administration:
  - Temperature Predictions and Adjustment Factors for Asphalt Pavements*  
(Report No. FHWA-RD-98-085)

#### 3. Terminology

- 3.1 Description of Terms Specific to This Standard:
  - 3.1.1 Depth: The distance below the surface of the top layer of asphalt.

#### 4. Summary of Test Method

- 4.1 The surface temperature of an asphalt pavement is measured, preferably with an infrared temperature-sensing device. The time of day the temperature is measured, the average air temperature of the previous day, and the depth at which the asphalt temperature is to be estimated are required data elements. The data elements are entered into a regression formula that predicts the temperature within the asphalt pavement at depth.

## 5. Significance and Use

- 5.1 Analysis of deflection data from asphalt pavements almost always requires that the deflections or analysis results be adjusted for the effects of temperature. Measuring the temperature at depth requires that a hole be drilled into the pavement. The process is time-consuming, resulting in a limited number of temperature measurements. Current deflection testing equipment is often equipped with surface-temperature sensing devices, such as an infrared thermometer, which measures the surface temperature at every test location. To adequately adjust the deflection or deflection results for the effects of temperature, the temperature at some depth must be known. This test method provides a means of estimating that temperature from the surface temperature, time of day, previous air temperature, and the depth of measurement. Utilization of this method results in a significant time-savings over manually drilling holes into the pavement and results in a significant increase in the volume of temperature data.

## 6. Apparatus

- 6.1 Surface Temperature Measurement Device: The surface temperature measurement device can be an infrared thermometer, a hand-held infrared thermometer mounted on the deflection testing device, or a surface contact thermometer. The temperature measurement device should be calibrated according to manufacturers recommendations.

## 7. Calculation

- 7.1 BELLS Method: The BELLS<sup>(1)2</sup> method was originally presented by Baltzer, Ertman-Larson, Lukanen, and Stubstad at the Fourth International Conference on Bearing Capacity of Roads and Airfields. The model was based on data from a faulty infrared sensor and should not be used. Lukanen, Stubstad, and Briggs<sup>(2)</sup> updated the coefficients using new data. The BELLS model is described by the following formula:

$$T_d = 2.8 + 0.894 * IR + \{\log(d) - 1.5\} \{-0.540 * IR + 0.770 * (5\text{-day}) + 3.763 * \sin(\text{hr}-18)\} + \{\sin(\text{hr}-14)\} \{0.474 + 0.031 * IR\}$$

where:

|       |   |   |
|-------|---|---|
| $T_d$ | = | Pavement temperature at depth d, °C   |
| IR    | = | Infrared surface temperature, °C  |
| log   | = | Base 10 logarithm   |
| d     | = | Depth at which mat temperature is to be predicted, mm   |
| 5-day | = | Average air temperature (°C) for the 5 days before the testing  |
| sin   | = | sine function on a 24-hr clock system, with $2\pi$ radians equal to one 24-hr cycle   |
| hr-18 | = | Time of day on a 24-hr clock system; to use the time-hour function correctly, divide the number of hours (after subtracting the appropriate shift of 14 or 18) by 24, multiply by $2\pi$ , and apply the sine function in radians |

---

<sup>2</sup>The superscript numbers in parentheses refer to the list of references at the end of this test method.

7.2 BELLS2 Method for LTPP Testing: The LTPP testing procedure used for Seasonal Monitoring<sup>(3)</sup> and for General Pavement Studies (GPS) flexible testing<sup>(4)</sup> keep the pavement surface shaded for about 6 min prior to recording the surface temperature. The following model is based on data obtained in the SMP testing program.

$$T_d = 2.78 + 0.912 * IR + \{\log(d) - 1.25\} \{-0.428 * IR + 0.553 * (1\text{-day}) + 2.63 * \sin(\text{hr}_{18} - 15.5)\} + 0.027 * IR * \sin(\text{hr}_{18} - 13.5)$$

where:

|                  |   |   |
|------------------|---|---|
| $T_d$            | = | Pavement temperature at depth d, °C   |
| IR               | = | Infrared surface temperature, °C  |
| log              | = | Base 10 logarithm   |
| d                | = | Depth at which mat temperature is to be predicted, mm   |
| 1-day            | = | Average air temperature (°C) the day before testing   |
| sin              | = | sine function on an 18-hr clock system, with $2\pi$ radians equal to one 18-hr cycle  |
| $\text{hr}_{18}$ | = | Time of day on a 24-hr clock system, but calculated using an 18-hr AC temperature rise-and-fall time cycle, as indicated in 7.2.1 and 7.2.2 |

Note: BELLS2 has been verified at both mid-depth and third-depth temperature points. Almost no difference exists in the regressions derived from the data at either depth, thus they were combined.

7.2.1 When using the  $\sin(\text{hr}_{18} - 15.5)$  (decimal) function, only use times from 11:00 to 05:00 hrs. If the actual time is not within this time range, then calculate the sine as if the time was 11:00 hrs (where the sine = -1). If the time is between midnight and 05:00 hrs, add 24 to the actual (decimal) time. Then calculate as follows: If the time is 13:15, then in decimal form,  $13.25 - 15.50 = -2.25$ ;  $-2.25/18 = -0.125$ ;  $-0.125 \times 2\pi = -0.785$  radians;  $\sin(-0.785) = -0.707$ . [Note that an 18-hr sine function is assumed, with a “flat” negative 1 segment between 05:00 and 11:00 hrs.]

7.2.2 When using the  $\sin(\text{hr}_{18} - 13.5)$  (decimal) function, only use times from 09:00 to 03:00 hrs. If the actual time is not within this time range, then calculate the sine as if the time was 09:00 hrs (where the sine = -1). If the time is between midnight and 03:00 hrs, add 24 to the actual (decimal) time. Then calculate as follows: If the time is 15:08, then in decimal form,  $15.13 - 13.50 = 1.63$ ;  $1.63/18 = 0.091$ ;  $0.091 \times 2\pi = 0.569$  radians;  $\sin(0.569) = 0.539$ . [Note that an 18-hr sine function is assumed, with a “flat” negative 1 segment between 03:00 and 09:00 hrs.]

7.3 BELLS3 Method for Production Testing: Routine testing normally results in surface temperature measurements on pavement surfaces that have been shaded for only a short period of time (less than a minute). The following equation is for approximately 30 s of shade.

$$T_d = 0.95 + 0.892 * IR + \{\log(d) - 1.25\} \{-0.448 * IR + 0.621 * (1\text{-day}) + 1.83 * \sin(\text{hr}_{18} - 15.5)\} + 0.042 * IR * \sin(\text{hr}_{18} - 13.5)$$

where the variables are as defined in 7.2.

## **8. Report**

- 8.1 The type of temperature measurement device, the measurement shading conditions, the time of measurement, the date of measurement, and the depth at which the temperature was calculated should be identified.

## **9. Precision and Bias**

- 9.1 Precision: The precision of the temperature estimation is described by the regression standard error of estimate. For the BELLS method, the regression standard error of estimate is 1.9°C; for the BELLS2 method for LTPP testing, the regression standard error of estimate is 1.8°C for temperatures between 0 and 40°C; and for the BELLS3 method for production testing, the regression standard error of estimate is 1.9°C.
- 9.2 Bias: There was no means of measuring the bias during the development of the prediction equations.<sup>(4)</sup>

## **10. Keywords**

- 10.1 Asphalt temperature, FWD, falling-weight deflectometer, Road Rater, Dynaflect, Benkelman beam, temperature corrections, backcalculation.

## (Nonmandatory Information)

### **X1. EXAMPLE PROGRAM FOR CALCULATING THE PREDICTED ASPHALT TEMPERATURE BY THE BELLS METHOD**

#### **X1.1 Explanation**

X1.1.1 Purpose: The source code given in figure X1.2(1) is presented to illustrate the application of the temperature prediction equations, particularly the application of the sine functions.

X1.1.2 Language: The code is written in BASIC and can be run on a number of BASIC interpreters or compilers, or easily converted to other languages.

#### **X1.2 Source Code Listings**

```
`Program to illustrate the implementation of the BELLS equation.
\*****

CLS

INPUT "Input Surface Temperature "; ir
INPUT "Input Hour of test "; hr
INPUT "Input Minutes past the hour "; min
INPUT "Input the depth for predicting the asphalt temperature "; d
INPUT "Input average air temperature for the last 5 days "; air

td = 2.8 + .894 * ir
logdepth = LOG(d) / LOG(10) - 1.5
firstbracket = -.54 * ir + .77 * air + 3.763 *
              SIN(2 * pi * ((hr + min / 60) - 18) / 24)
secondbracket = SIN(2 * pi * ((hr + min / 60) - 14) / 24) *
              (.474 + .031 * ir)
td = td + logdepth * firstbracket + secondbracket

PRINT "The predicted temperature is "; td

END
```

**Figure X1.2(1). Source code listing for BELLS equation.**

```
'Program to illustrate the implementation of the BELLS2 equation with the
coefficients for LTPP testing (about six minutes of shading)
\*****
```

```
CLS
```

```
INPUT "Input Surface Temperature "; ir
INPUT "Input Hour of test "; hr
INPUT "Input Minutes past the hour "; min
INPUT "Input the depth for predicting the asphalt temperature "; d
INPUT "Input average air temperature for the day before the test date ";
air
```

```
decimal.hrs = hr + min / 60
```

```
IF decimal.hrs > 11 OR decimal.hrs < 5 THEN
  IF decimal.hrs < 5 THEN decimal.hrs = decimal.hrs + 24
  sine15.5 = SIN(2 * pi * (decimal.hrs - 15.5) / 18)
ELSE
  sine15.5 = -1
END IF
```

```
IF decimal.hrs > 9 OR decimal.hrs < 3 THEN
  IF decimal.hrs < 3 THEN decimal.hrs = decimal.hrs + 24
  sine13.5 = SIN(2 * pi * (decimal.hrs - 13.5) / 18)
ELSE
  sine13.5 = -1
END IF
```

```
td = 2.78 + .912 * ir
logdepth = LOG(d) / LOG(10) - 1.25
firstbracket = -.428 * ir + .553 * air + 2.63 * sine15.5
last.term = .027 * ir * sine13.5
td = td + logdepth * firstbracket + last.term
```

```
PRINT "The predicted temperature is "; td
```

```
END
```

**Figure X1.2(2). Source code listing for BELLS2 with coefficients for LTPP testing (approximately 6 min of shading).**



```

`Program to illustrate the implementation of the BELLS3 equation
`for routine testing with approximately 30 seconds of surface shade.
\*****
CLS

INPUT "Input Surface Temperature "; ir
INPUT "Input Hour of test "; hr
INPUT "Input Minutes past the hour "; min
INPUT "Input the depth for predicting the asphalt temperature "; d
INPUT "Input average air temperature for the day before the test date ";
air

decimal.hrs = hr + min / 60

IF decimal.hrs > 11 OR decimal.hrs < 5 THEN
  IF decimal.hrs < 5 THEN decimal.hrs = decimal.hrs + 24
  sine15.5 = SIN(2 * pi * (decimal.hrs - 15.5) / 18)
ELSE
  sine15.5 = -1
END IF

IF decimal.hrs > 9 OR decimal.hrs < 3 THEN
  IF decimal.hrs < 3 THEN decimal.hrs = decimal.hrs + 24
  sine13.5 = SIN(2 * pi * (decimal.hrs - 13.5) / 18)
ELSE
  sine13.5 = -1
END IF

td = 0.95 + .892 * ir
logdepth = LOG(d) / LOG(10) - 1.25
firstbracket = -.448 * ir + 0.621 * air + 1.83 * sine15.5
last.term = .042 * ir * sine13.5
td = td + logdepth * firstbracket + last.term

PRINT "The predicted temperature is "; td

END

```

**Figure X1.2(3). Source code listing for BELLS2 equation for production testing (approximately 30 s of shading).**

## REFERENCES

1. Baltzer, S.; Ertman-Larson, H.J.; Lukanen, E.O.; and Stubstad, R.N. "Prediction of AC Mat Temperature for Routine Load/Deflection Measurements." *Proceedings, The Fourth International Conference on the Bearing Capacity of Roads and Airfields, Volume 1*. Minnesota Department of Transportation, pp. 401-412.
2. Lukanen, E.O.; Stubstad, R.N.; and Briggs, R. *Temperature Predictions and Adjustment Factors for Asphalt Pavements*, Report No. FHWA-RD-98-085. Federal Highway Administration.
3. Federal Highway Administration (1994). *LTPP Seasonal Monitoring Program: Instrumentation Installation and Data Collection Guidelines*. Report No. FHWA-RD-94-110. McLean, VA.
4. Federal Highway Administration (1993). *Manual for FWD Testing in the Long Term Pavement Performance Study, Operational Field Guidelines, Version 2.0*. McLean, VA.

# Draft Standard Practice for Applying Temperature Adjustment Factors to Backcalculated Asphalt Moduli, Deflection, and Deflection Basin Characteristics

## AASHTO DESIGNATION: T-###-99

### 1. Scope

- 1.1 This guide is intended to provide temperature adjustment factors for asphalt pavement characteristics, including backcalculated asphalt modulus, deflection under the center of the load plate, and deflection basin shape factors.

### 2. Referenced Documents

- 2.1 AASHTO Standards:  
T 256-77 Pavement Deflection Measurements  
P-###-## Draft Standard Practice for Estimating Asphalt Temperature
- 2.2 ASTM Standards:  
D 4602 Guide for Nondestructive Testing of Pavements Using Cyclic-Loading Dynamic Deflection Equipment  
D 4694 Test Method for Deflections With a Falling-Weight-Type Impulse Load Device  
D 4695 Guide for General Pavement Deflection Measurements
- 2.3 Federal Highway Administration:  
*Temperature Predictions and Adjustment Factors for Asphalt Pavements*  
(Report No. FHWA-RD-98-085)

### 3. Terminology

- 3.1 Description of Terms Specific to This Standard:
  - 3.1.1 Depth: The distance below the surface of the top layer of asphalt.

### 4. Summary of Practice

- 4.1 This practice provides a means of adjusting backcalculated asphalt moduli, deflections under the center of the load, or deflection basin characteristics to remove the effects of temperature.

### 5. Significance and Use

- 5.1 Analysis of deflection data from asphalt pavements almost always requires that the deflections or analysis results be adjusted for the effects of temperature. This allows pavement engineers to analyze deflection results that were taken when the temperature of the asphalt was not at the typical, or critical, temperature.<sup>(1)3</sup>

---

<sup>3</sup>The superscript numbers in parentheses refer to the list of references at the end of this test method.

5.2 All of the relationships provided in this standard are derived from data from the FHWA LTPP program's SMP.<sup>(2-3)</sup> Therefore, the results are best suited to deflection measurements made with a Model 8000 Dynatest Falling-Weight Deflectometer during normal daytime working hours.

## 6. Procedure

6.1 Backcalculated Asphalt Modulus: The semi-logarithmic format of the equation relating the asphalt modulus to the mid-depth asphalt temperature allows for a simple means of adjusting the backcalculated asphalt modulus for the effects of temperature. The temperature adjustment factor for backcalculated moduli is determined using the following equation:

$$ATAF = 10^{\text{slope} * (T_{Ref} - T_{Meas})} \quad (1)$$

where:

ATAF = Asphalt temperature adjustment factor  
 slope = Slope of the log modulus versus temperature equation  
 (-0.0195 for tests in the wheelpath and -0.021 for mid-lane are recommended)  
 $T_r$  = Reference mid-depth HMA temperature  
 $T_m$  = Mid-depth HMA temperature at the time of measurement

6.2 Delta Deflections (deflection under the center of the load minus the deflection at some distance from the center of the load): The basin shape factor temperature adjustment factor is calculated as follows:

$$BAF = \frac{\text{Basin Factor}_{T_{Ref}}}{\text{Basin Factor}_{T_{Meas}}} \quad (2)$$

where:

BAF = Basin Adjustment Factor  
 Basin Factor $_{T_{Ref}}$  = Calculated AREA at the reference temperature  
 Basin Factor $_{T_{Meas}}$  = Calculated AREA at the measured temperature

The relationships for each of the delta deflection basin shape factors are equations 3 through 8, which have been established for the standard sensor spacing used for the FHWA LTPP program's project.

$$\log(\text{delta}8) = 3.02 - 1.49 \log(\text{ac}) + 0.541 \log(\theta) + 0.394 \log(\text{defl}36) - 0.0230 T + 0.0111 T \log(\text{ac}) \log(\theta) \quad (3)$$

$$\log(\text{delta}12) = 3.45 - 1.59 \log(\text{ac}) + 0.489 \log(\theta) + 0.449 \log(\text{defl}36) - 0.0275 T + 0.012 T \log(\text{ac}) \log(\theta) \quad (4)$$

$$\log(\text{delta}18) = 4.18 - 1.52 \log(\text{ac}) + 0.317 \log(\theta) \log(\text{defl}36) - 0.0265 T + 0.0112 T \log(\text{ac}) \log(\theta) \quad (5)$$

$$\log(\text{delta}24) = 3.30 - 1.32 \log(\text{ac}) + 0.514 \log(\theta) \log(\text{defl}36) - 0.00622 T \log(\theta) \log(\text{defl}36) + 0.00838 T \log(\text{ac}) \log(\theta) \quad (6)$$

$$\log(\text{delta}36) = 3.05 - 1.13 \log(\text{ac}) + 0.502 \log(\theta) \log(\text{defl}36) - 0.00487 T \log(\theta) \log(\text{defl}36) + 0.00677 T \log(\text{ac}) \log(\theta) \quad (7)$$

$$\log(\text{delta}60) = 2.67 - 0.770 \log(\text{ac}) + 0.650 \log(\text{delta}36) + 0.00290 T \log(\text{ac}) \quad (8)$$

where:

|          |   |   |
|----------|---|---|
| ac       | = | Total thickness of the HMA, mm  |
| $\theta$ | = | Latitude of the pavement section  |
| defl36   | = | Deflection (normalized to 40.5 kN) at 915 mm from the center of the load plate, $\mu\text{m}$ |
| T        | = | Temperature at the mid-depth of the HMA, $^{\circ}\text{C}$                                   |

6.3 Deflection Under the Center of the Load: The calculation of temperature adjustment factors for deflection measurement under the center of the load plate make use of the delta deflection relationship in equation 7. The equation is applied as shown in equation 9.

$$TAF = \frac{\text{Defl}36 + \text{Delta}36_{\text{Ref. Temp.}}}{\text{Defl}36 + \text{Delta}36_{\text{Meas. Temp.}}} \quad (9)$$

6.4 Deflection Ratios (deflection under the center of the load divided by the deflection at some distance from the center of the load): The temperature adjustment process consists of determining the ratio for the respective offset, as shown in equation 2, using equations 10 through 15.

$$\log(\text{ratio}8) = 0.183 + 0.0118 \log(\text{ac}) \log(\text{defl}36) + 0.00980 T + 0.0696 \log(\theta) - 0.133 \log(\text{ac}) - 0.00416 T \log(\text{defl}36) \quad (10)$$

$$\log(\text{ratio}12) = 0.200 - 0.117 \log(\text{ac}) \log(\text{defl}36) + 0.126 \log(\theta) \log(\text{defl}36) + 0.00861 T - 0.00183 T \log(\theta) \log(\text{defl}36) \quad (11)$$

$$\log(\text{ratio}18) = 0.952 - 0.450 \log(\text{ac}) - 0.169 \log(\text{defl}36) + 0.327 \log(\theta) + 0.00212 T \log(\text{ac}) \quad (12)$$

$$\log(\text{ratio}24) = 1.16 - 0.587 \log(\text{ac}) - 0.210 \log(\text{defl}36) + 0.481 \log(\theta) + 0.00257 T \log(\text{ac}) \quad (13)$$

$$\log(\text{ratio}36) = -0.0912 - 0.367 \log(\text{ac}) \log(\text{defl}36) + 0.489 \log(\text{defl}36) + 0.691 \log(\theta) + 0.00298 T \log(\text{ac}) \quad (14)$$

$$\log(\text{ratio}60) = 0.0726 - 0.336 \log(\text{ac}) \log(\text{defl}36) + 0.334 \log(\text{defl}36) + 0.872 \log(\theta) + 0.00246 T \log(\text{ac}) \quad (15)$$

6.4 AREA Basin Factor: The temperature adjustment factors for the AREA basin factor are calculated by determining the predicted AREA for the respective temperatures, as shown in equation 2, using equation 16.

$$\text{AREA} = 13.0 + 7.77 \log(\text{ac}) \log(\text{defl36}) - 6.78 \log(\theta) \log(\text{defl36}) + 0.105 T - 0.116 T \log(\text{ac}) \quad (16)$$

- 6.5 F-1 Basin Factor: The temperature adjustment factors for the F-1 basin factor are calculated by determining the predicted F-1 factor for the respective temperatures, as shown in equation 2, using equation 17.

$$\log(\text{F-1}) = 0.326 - 0.382 \log(\text{ac}) \log(\text{defl36}) + 0.327 \log(\theta) \log(\text{defl36}) - 0.00447 T + 0.00555 T \log(\text{ac}) \quad (17)$$

## 7. Precision and Bias

- 7.1 No direct calculation of the precision or bias was made for the temperature adjustment factors. The development of the models used to produce the equations for the temperature adjustment factors is described by Lukanen et al.<sup>(1)</sup> Statistical regression information is available regarding the correlation of the independent variables to the dependent variables, and regarding the standard error of estimate of the resulting regression equations.

## 8. Keywords

- 8.1 Asphalt temperature, FWD, falling-weight deflectometer, Road Rater, Dynaflect, Benkelman beam, temperature corrections, backcalculation.

## REFERENCES

1. Lukanen, E.O.; Stubstad, R.N.; and Briggs, R. *Temperature Predictions and Adjustment Factors for Asphalt Pavements*. Report No. FHWA-RD-98-085. Federal Highway Administration.
2. Federal Highway Administration (1994). *LTPP Seasonal Monitoring Program: Instrumentation Installation and Data Collection Guidelines*. Report No. FHWA-RD-94-110. McLean, VA.
3. Federal Highway Administration (1993). *Manual for FWD Testing in the Long Term Pavement Performance Study, Operational Field Guidelines, Version 2.0*. McLean, VA.

## REFERENCES

1. Federal Highway Administration (1994). *LTPP Seasonal Monitoring Program: Instrumentation Installation and Data Collection Guidelines*. Report No. FHWA-RD-94-110. McLean, VA.
2. Federal Highway Administration, Pavement Performance Division (September 1995). *The Long-Term Pavement Performance Program Roadmap, A Strategic Plan*. McLean, VA.
3. Federal Highway Administration (1993). *Manual for FWD Testing in the Long Term Pavement Performance Study, Operational Field Guidelines, Version 2.0*. McLean, VA.
4. Press, W.H.; Flannery, B.P.; Teukolsky, S.A.; and Vetterling, V.T. (1986). *Numerical Recipes, The Art of Scientific Computing*. Cambridge University Press, Cambridge, London, England, pp. 86-89.
5. Press, W.H.; Flannery, B.P.; Teukolsky, S.A.; and Vetterling, V.T. (1986). *Numerical Recipes, The Art of Scientific Computing*. Cambridge University Press, Cambridge, London, England, pp. 81-83.
6. Baltzer, S.; Ertman-Larson, H.J.; Lukanen, E.O.; and Stubstad, R.N. "Prediction of AC Mat Temperature for Routine Load/Deflection Measurements." *Proceedings, Fourth International Conference on the Bearing Capacity of Roads and Airfields, Volume 1*. Minnesota Department of Transportation, pp. 401-412.
7. Inge, Earl, and Kim, Richard (1995). "Prediction of Effective Asphalt Layer Temperature." *Transportation Research Record No. 1473*. National Academy Press, Washington, D.C., pp. 93-100.